Handbook of Clay Science
Edited by F. Bergaya, B.K.G. Theng and G. Lagaly
Developments in Clay Science, Vol. 1

Chapter 5

COLLOID CLAY SCIENCE

G. LAGALY

Institut für Anorganische Chemie, Universität Kiel, D-24118 Kiel, Germany

Clay minerals are distinguished from other colloidal materials by the highly anisometric and often irregular particle shape, the broad particle size distribution, the different types of charges (permanent charges on the faces, pH-dependent charges at the edges), the heterogeneity of the layer charges, the pronounced cation exchange capacity (CEC), the disarticulation (in case of smectites), the flexibility of the layers, and the different modes of aggregation (see Chapter 1) (van Olphen, 1977; Lagaly, 1993, 2005; Jasmund and Lagaly, 1993; Lagaly et al., 1997).

5.1. CLAY MINERAL PARTICLES

5.1.1. Particle and Aggregate Structure

Clay mineral particles, in particular those of smectites, are never crystals in the strict sense (Brindley and Brown, 1980; Moore and Reynolds, 1997; Plançon, 2001). Many crystallographers are dismayed at the particles clay scientists often call 'crystals'. In fact, a smectite 'crystal' is more equivalent to an assemblage of silicate layers than to a true crystal (Fig. 5.1). Montmorillonite particles seen in the electron microscope never have the regular shape of real crystals but look like paper torn into irregular pieces. Instructive pictures of smectite particles were published by Vali and Köster (1986). The core of the particles is surrounded by disordered and bent silicate layers with frayed edges. Layers or thin particles of a few layers protrude from the packets and enclose wedge-shape pores. The particles reveal many points of weak contacts between the stacks of the layers. At these 'breaking points' the particles may easily disintegrate during interlayer reactions, or as a result of mechanical forces that influence rheological behaviour.

In particles of Ca^{2+}-smectite only a few layers form coherent domains in which all silicate layers have the same distance, for instance, corresponding to two layers of water. These domains are separated by zones composed of silicate layers with different distances because of the presence of one, three, four, or even more water

DOI: 10.1016/S1572-4352(05)01005-6

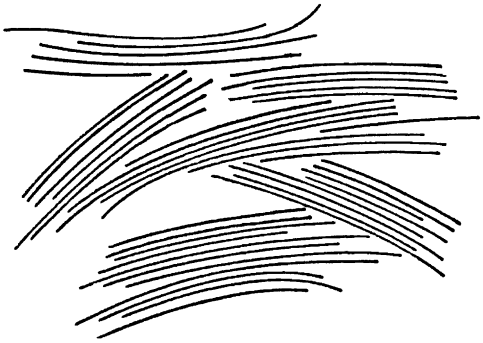

Fig. 5.1. A schematic view of montmorillonite particles. From Lagaly and Malberg (1990).

layers. This structure could clearly be observed by TEM inspection (Chenu and Jaunet, 1990). A few of the units composed of coherent domains and zones of differently spaced silicate layers are aggregated with almost parallel orientation. These particles are arranged in a network with pores of different sizes, thus constituting the whole aggregate (following the nomenclature given in Chapter 1). The pore structure is very complex with lenticular pores between parallel oriented layers together with pores within the network of particles and between the aggregates (see electron micrographs in (Touret et al., 1990)). The texture of synthetic hectorites was recently derived from small-angle X-ray scattering (SAXS) (Koschel et al., 2000; Gille et al., 2002). It seems possible to estimate the volumes of the different types of pores from the kinetics of water uptake (Touret et al., 1990). Nomenclature for the different levels of organisation is still lacking; a simplified one is suggested in Chapter 1.

The electrostatic attractions between the layers and the interlayer cations increase the stacking order in more highly charged 2:1 clay minerals. The domains with equally spaced layers become thicker and the influence of the defects on the shape and position of the (001) reflections decreases. Defects of unequally spaced silicate layers due to different degrees of hydration (probably a consequence of charge inhomogeneity) are still observable by delicate analysis of the X-ray reflection profiles of Na^+-beidellite with water monolayers (Ben Brahim et al., 1986). The different types of layer stacking in vermiculites were reviewed by Suquet and Pézérat (1987). Generally micas are considered as true crystals, and many polymorphs were described (see Chapter 2).

5.1.2. *Layer and Edge Charges*

In the general formula for 2:1 clay minerals, the average charge of the silicate layers is indicated by $(x+y)$ per formula unit. The unit cell of the clay mineral lattice contains two formula units $(Si,Al)_4O_{10}$ and has the dimensions a and b in the plane

of the layer. The surface charge density (σ_0), expressed as C/m^2, is given by

$$\sigma_0 = 1.602 \times 10^{-19}(x + y)/ab$$

where 1.602×10^{-19} C is the elementary charge of one electron.

Typical surface charge densities are listed in Table 5.1. The average layer charge of montmorillonites varies between 0.2 and 0.4 eq/formula unit $(Si,Al)_4O_{10}$, but most montmorillonites have layer charges around 0.3 eq/formula unit corresponding to a surface charge density of 0.10 C/m^2 (Jasmund and Lagaly, 1993; Lagaly, 1993, 2005). On the basis of the high layer charge densities one calculates high surface potentials for isolated particles, e.g., ~200 mV, at a salt concentration of 10^{-3} mol/L and a surface charge density of 0.10 C/m^2 (Verwey and Overbeek, 1948; van Olphen, 1977; Lagaly et al., 1997).

Sign and density of the charges at the crystal edges depend on the pH of the dispersion. Some clay scientists still use the term 'broken bonds' that colloid scientists never used. The charging arises from adsorption or dissociation of protons as in the case of oxides (Fig. 5.2). In an acidic medium an excess of protons creates positive edge charges, the density of which decreases with rising pH. Negative charges are produced by the dissociation of silanol and aluminol groups (Tournassat et al., 2003a, 2003b). On the acidity of the silanol and aluminol groups see Wanner et al. (1994), Janek and Lagaly (2001), and Jozefaciuk (2002).

The interesting question concerns the condition that leads to virtually uncharged edges. When alkylammonium ions were exchanged at pH 6.5, the total amount of ions bound by Wyoming montmorillonite was 1.07 meq/g silicate (Lagaly, 1993, 2005). As the interlayer CEC was 0.78 meq/g silicate, the remaining 0.29 meq alkylammonium ions (= 27% of the total CEC) were bound at the edges. A very similar

Table 5.1. Layer charge ($x + y$), surface charge density σ_0 and equivalent area* A_c of clay minerals

Mineral	$M^{\dagger}$	$(x+y)$(charges/formula unit)	σ_0(Cm^{-2})	ab(nm^2)	A_c (nm^2/charge)
Biotite	455	1	0.326	0.492	0.246
Muscovite	390	1	0.343	0.467	0.234
Vermiculites	390	0.8	0.259	0.495	0.309
		0.6	0.194	0.495	0.412
Beidellite	360	0.5	0.172	0.466	0.466
Montmorillonites	362	0.4	0.137	0.466	0.583
		0.3	0.103	0.466	0.777
		0.2	0.069	0.466	1.165
Hectorite	380	0.23	0.076	0.482	1.048

*The equivalent area is the area per monovalent interlayer cation : $A_c = ab/2(x + y)$.
†Mean molecular mass of the formula unit (Si_4O_{10} $(OH)_2$) without interlayer cations and water calculated for typical compositions (Jasmund and Lagaly, 1993).

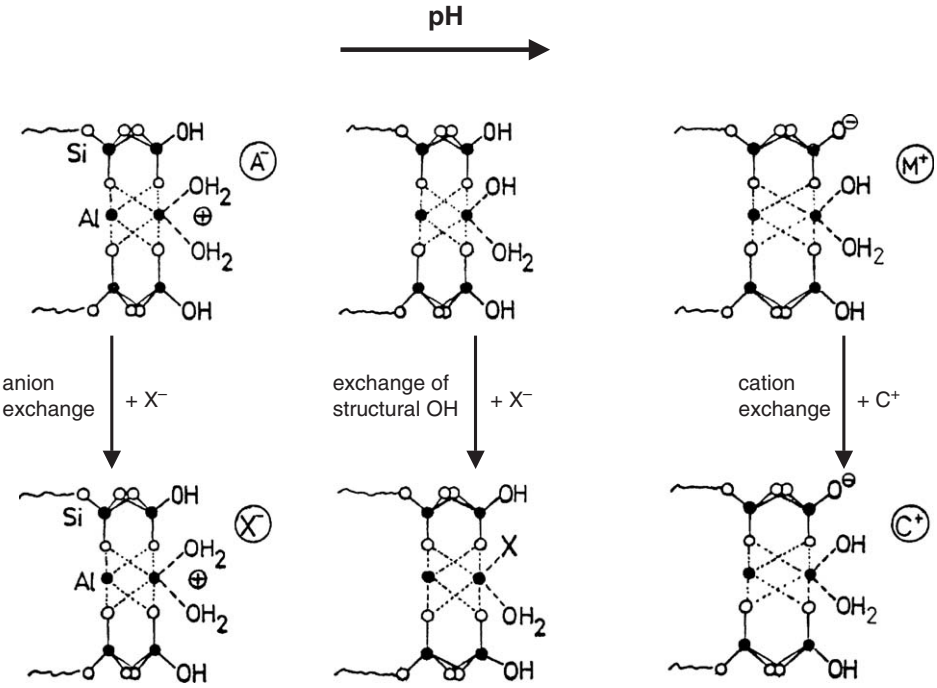

Fig. 5.2. The pH-dependent ion and ligand exchange reactions at the edges of the clay mineral layers, shown for 2:1 clay minerals. From Lagaly (1993).

result was obtained by surface charge measurements using a particle charge detector. This simple instrument indicates the point at which all charges of a colloidal particle are compensated by macro-ions, or in our case by alkylammonium ions. The amount of alkylammonium ions required to uncharge the particles, increased rapidly with pH because in an acidic medium protons compete with alkylammonium ions even in the interlayer space. At pH 6–8, a plateau was reached and, in agreement with the analytical data, a dose of 1.03 meq alkylammonium ions/g montmorillonite uncharged the particles of montmorillonite. The increase at higher pH was caused by the presence of alkylamine molecules, which were strongly adsorbed by the alkylammonium montmorillonite.

The total amount of alkylammonium ions bound by 2:1 clay minerals is often slightly higher than the total CEC determined by other methods (Bain and Smith, 1987; Jasmund and Lagaly, 1993). This is a consequence of the charge regulation at the edges. Adsorption of surface active agents on oxidic surfaces increases the surface charge density by adsorption (anionic surfactants) or desorption (cationic surfactants) of protons (Böhmer and Koopal, 1992; Schmidt and Lagaly, 1999). Thus, adsorption of alkylammonium ions in excess of the CEC is accompanied by

desorption of protons from surface OH groups. The analytical data clearly reveal that, at pH 6.5, a considerable amount of alkylammonium ions are bound at the edges.

The flow behaviour of Na^+-montmorillonite dispersions in water or in dilute NaCl solutions shows characteristic changes with pH (Section 5.6.1). The shear stress decreases steeply at pH > 4 (see Fig. 5.26). This reduction of viscosity is generally attributed to the destruction of the card-house when the amount of positive edge charges becomes too small to stabilise the card-house by edge(+)/face(−) contacts (Brandenburg and Lagaly, 1988; Lagaly, 1989). Thus, rheological measurements indicate an apparent point of zero charge (p.z.c.) of the edges at pH somewhat above 5. The titration experiments of Wanner et al. (1994) revealed the point of zero net proton charge (p.z.n.p.c.) at pH 6.1 for montmorillonite (from bentonite MX-80, American Colloid Co.). Electrokinetic measurements led to strikingly different values, between pH ~3.5 and 8.5, probably near pH ~7 (Section 5.2.4). The p.z.c. at the edges of colloidal pyrophyllite particles ($x + y \sim 0$) was found at pH 4.2 by titrations at various indifferent electrolyte concentrations (Keren and Sparks, 1995).

Exchangeable cations balancing negative charges due to isomorphous substitution within the kaolinite particles are located at the external surface, generally on the basal surfaces or near the edges. Weiss and Russow (1963) deduced from several independent measurements (exchange of tetraalkylammonium ions, TEM observation after adsorption of positively charged colloidal silver iodide particles, adsorption of dyes, exchange of radioactive $^{63}Ni^{2+}$ ions, fluoride decomposition at pH ~7) that only the external tetrahedral basal planes show isomorphous substitutions that are balanced by exchangeable cations. Not all kaolinite particles are characterised by different external basal planes. Particles with two identical surfaces were found as the consequence of layer inversion within the particles.

In comparing model cation exchange curves with experimental data, Bolland et al. (1980) derived charge densities between 1 and 1.3×10^{-10} eq/cm^2 corresponding to 0.10–0.12 C/m^2, and concluded that kaolinite particles possessed permanent charges. They noted that the negative surface charges on the kaolinites could be mistakenly attributed to a pH-dependent, oxide-like charge (Ferris and Jepson, 1975) if the dissolution of Al^{3+} species and formation of gel-like coatings during the titration experiments are not considered.

In common with other clay minerals, kaolinite particles possess variable charges. Apparently, permanent charges cannot be assessed from potentiometric titration experiments alone (Herrington et al., 1992; Ganor et al., 2003; Tournassat et al., 2003a, 2003b). Schroth and Sposito (1997) determined the permanent structural charge density (σ_0) by measuring the surface excess of Cs^+ ions, which are highly selective to permanent charge sites. The net proton surface charge density (σ_H) was measured as a function of pH by potentiometric titrations. The values of σ_0 for the Georgia kaolinites KGa-1 (well-crystallised; Washington County) and KGa-2 (poorly crystallised; Warren County), both from the Clay Minerals Society, were given as −6.3 and

−13.6 mmol/kg. The specific surface areas were given as 10.0 and 23.5 m^2/g (van Olphen and Fripiat, 1979). Assuming a homogeneous distribution of the charges, one calculates a permanent surface charge density of 0.06 C/m^2 for both kaolinites. Thus, the density of the permanent charges corresponds to low-charged smectites.

Because of their importance to colloidal behaviour, the p.z.c. are mentioned (Schroth and Sposito, 1997). The point of zero net charge (p.z.n.c.) was found at pH ~3.6 for both kaolinites, whereas the p.z.n.p.c. were at pH 5.0 (KGa-1) and 5.4 (KGa-2). The authors also observed that the p.z.n.p.c. changed with time due to dissolution effects. Siffert and Kim (1992) deduced an isoelectric point (i.e.p.) of the edges of kaolinite particles (Brittany, France) at pH 4.9. Dollimore and Horridge (1973) derived the point of zero edge charge (≡p.z.n.p.c) at pH 5.8 from flocculation experiments with polyacrylamide. Studying the coagulation kinetics of kaolinite at different pH in the presence of humic acid, Kretzschmar et al. (1998) also found the point of zero edge charge at pH 5.8 (see this paper for further references).

5.2. CLAY MINERALS IN WATER

5.2.1. Hydrates of 2:1 Clay Minerals

The 2:1 clay minerals form hydrates with one, two, three, or four pseudo-layers of water molecules between the silicate layers. The state of hydration changes with the water vapour pressure, the water content, and in salt solutions with the type and concentration of salts, and is dependent on the layer charge and the interlayer cation density. Typical basal spacings are: 1.18–1.24 nm (water pseudo-monolayer), 1.45–1.55 nm (water pseudo-bilayer), and 1.9–2.0 nm (four water pseudo-layers). The term 'water layer' is often used instead of 'pseudo-layer', even if the 'layer' is not always close-packed (see Chapter 13.2). The number of water pseudo-layers is simply derived from the layer separation and the thickness of a water layer in close-packed water molecules (about 0.25 nm).

The dotted fields in Fig. 5.3 comprise the spacings of a large collection of smectites and vermiculites. Na^+-smectites change from a state indicated by a basal spacing $\rightarrow \infty$ into hydrates with four, and at higher salt concentration two layers of water (Slade et al., 1991); vermiculites persist in the two-layer hydrate over the whole range of concentrations. Potassium ions in higher concentrations restrict the interlayer expansion of smectites to water monolayers. The hydration of vermiculites is virtually impeded by KCl solutions at concentrations above 0.01 M. In the presence of calcium ions the four-layer hydrate of smectites and the two-layer hydrate of vermiculites persist over a wide range of concentrations.

The variation of the basal spacings with salt concentration (Fig. 5.3) is of great interest to colloid scientists. To explain the reversibility of salt coagulation for many colloidal dispersions, Frens and Overbeek (1972) and Overbeek (1977) introduced the concept of the 'distance of closest approach'. They postulated that the particles

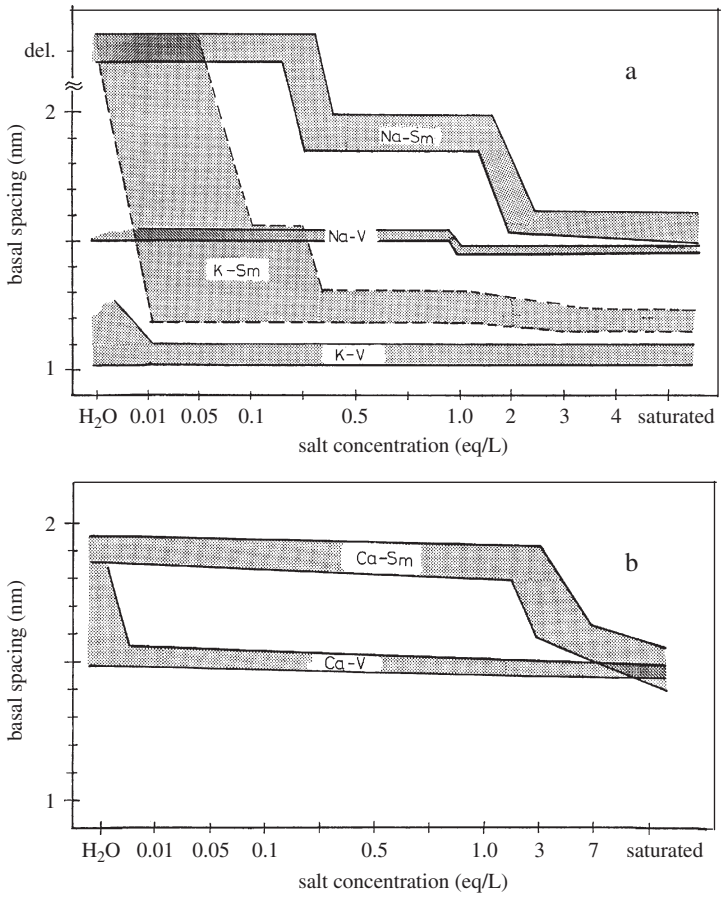

Fig. 5.3. Basal spacing of 2:1 clay minerals as a function of salt concentration. Na–Sm, Na^+–smectites and NaCl; K–Sm, K^+-smectites and KCl; Ca–Sm, Ca^{2+}-smectites and $CaCl_2$; Na–V, Na^+-vermiculites and NaCl; K–V, K^+-vermiculites and KCl; and Ca–V, Ca^{2+}-vermiculites and $CaCl_2$, del = delamination. From Lagaly and Fahn (1983).

are not in direct contact at the onset of coagulation but remain separated by a certain distance. Through a number of calculations, a value of 0.4 nm corresponding to two water layers was derived for the most probable minimum separation. That a distance of closest approach really exists is clearly seen by the behaviour of Na^+- and Ca^{2+}-smectites as well as Na^+- and Ca^{2+}-vermiculites in NaCl and $CaCl_2$ solution. Even far above the critical coagulation concentrations and up to concentrations as high as 5 M NaCl, the silicate layers remain separated by two pseudo-water layers. The water layers are displaced from between the surfaces only when the exchangeable cations, such as K^+, are attracted to the surface by specific interactions. The 'fixation' of K^+ ions (and Cs^+ and Rb^+ ions) is well known to clay scientists and is

explained by the reduced hydration energy and a better geometric fit of the potassium ions into the surface oxygen hexagons in comparison to Na^+ ions (see for instance Pons et al., 1982).

5.2.2. Structure of the Hydrates

The hydrated 2:1 clay minerals may be considered as quasi-crystalline structures (Sposito, 1992; Sposito and Grasso, 1999) because of a certain amount of structural order. The interlayer cations reside near the middle plane of the interlayer space (Weiss et al., 1964; Suquet et al., 1975; Hougardy et al., 1976; Di Leo and Cuadros, 2003). The silicate layers of more highly charged silicates (saponites, vermiculites) assume ordered or semi-ordered layer stacking sequences (Suquet and Pézérat, 1987). More recently, Beyer and Graf von Reichenbach (2002) published an extended revision of the interlayer structure of one- and two-layer hydrates of Na^+-vermiculite. In smectites, the superposition of the layers is generally random (turbostratic structure) but specimens with a certain periodic structure (e.g., beidellites) are also found (Glaeser et al., 1967; Besson et al., 1974). The layers of Wyoming montmorillonite with initially random superposition become more and more regularly stacked after wetting and drying cycles in the presence of potassium ions (Mamy and Gaultier, 1975).

The organisation, mobility, and dynamics of interlayer water molecules were studied in great detail by Güven (1992a), and in particular by Hougardy et al. (1976), Poinsignon et al., (1978), Giese and Fripiat (1979), and Fripiat et al. (1982, 1984). Generally, a part of the water molecules forms hydration shells around the interlayer cationş while the other water molecules fill the space between the hydration shells (Johnston et al., 1992; Swenson et al., 2001) and are in a state probably similar to that around structure-breaking ions. There is no doubt that the properties of interlayer water are different from those of bulk water (Delville and Laszlo, 1989; Bergman et al., 2000; Swenson et al., 2001, 2002). For example, interlayer water is more acidic than bulk water (Mortland and Raman, 1968; Touillaux et al., 1968; Hougardy et al., 1976; Cady and Pinnavaia, 1978; Fripiat et al., 1982, 1984; Delville and Laszlo, 1989; Johnston et al., 1992) (see Chapter 3).

Grandjean and Laszlo (1989) deduced from deuterium NMR studies of montmorillonite-water dispersions that the water molecules are strongly polarised and are simultaneously bound to a negative centre by a hydrogen bridge and to an interlayer cation by electrostatic forces. As a consequence, the acidity of interlayer water molecules is increased. In Na^+-montmorillonite the water molecules reorient predominantly around the hydrogen bond, whereas they reorient around the metal-oxygen axis in the presence of calcium ions.

The influence of the external surface force fields on the water structure around and between the particles is important. Fripiat et al. (1982, 1984) could not detect long-range forces acting on the water molecules outside of the particles, neither at the thermodynamic scale (heat of immersion measurements) nor at the microdynamic

range (NMR measurements). The number of water layers influenced by the surface forces is 3–4, i.e. a water film of ~1 nm thickness. In contrast, Mulla and Low (1983) concluded that the molecular dynamics of vicinal water as seen by IR spectroscopy is affected by the particle surface to an appreciable distance of about 4 nm.

Another question concerns the basicity of the oxygen atoms, i.e. their ability to bind protons (see Chapter 3.3.). Tetrahedral substitution of Al^{3+} for Si^{4+} increases the basic strength of the siloxane groups. The reason is the influence of aluminium atoms on the d_π-p_π bonds to oxygen. As a consequence, three types of water have to be distinguished: (i) the water hydrating the interlayer cations; (ii) an ordered layer of water at the flat oxygen plane; and (iii) less ordered water molecules between regions (i) and (ii). The structure of (ii) depends on the basicity of the siloxane groups. In the absence of tetrahedral substitution, the siloxane groups are really hydrophobic (which is also known from the silica surface) and the water molecules are closely linked one to another by hydrogen bonds. With increasing tetrahedral substitution the hydrophilic character of the oxygen plane increases and the interaction between the water molecules and the surface oxygen atoms increases (Yariv, 1992; Garfinkel-Shweky and Yariv, 1997). Adsorption studies of binary liquids also reveal the hydrophilic/hydrophobic character (see Chapter 7.3).

Molecular dynamics simulations of the montmorillonite hydrates mainly confirm the experimental results on the position of the interlayer cations and the interlayer water structure. Interlayer Li^+ ions partly form inner-sphere surface complexes (i.e. the Li^+ ions are directly co-ordinated to the surface oxygen atoms). Expansion of the interlayer space is accompanied by the conversion of outer-sphere surface complexes into diffuse double-layer species as a result of the strong Li^+–water interactions. However, some of the Li^+ ions persist as inner-sphere surface complexes although they can readily exchange with Li^+ ions in the diffuse double-layer (Chang et al., 1997). Na^+ and K^+ ions also have a significant co-ordination with surface oxygen atoms and exist in inner-and outer-sphere surface complexes (Delville and Laszlo, 1989; Chang et al., 1995, 1998; Skipper et al., 1995). Increasing tetrahedral substitution shows a trend of direct binding between Na^+ and surface oxygen atoms and a corresponding dissimilarity with the co-ordination structure in bulk solution. The co-ordination structure of water molecules around K^+ ions as expected for this water-structure breaking cation (Lagaly et al., 1997) is not nearly so well defined as it is for Li^+ and Na^+ ions. Magnesium cations on montmorillonite reside at the midplane of the interlayer space. Non-solvating water molecules move freely on planes above and below the midplane. In the case of beidellites, the motion of water molecules is more hindered because of the presence of negative charge sites close to the surface (Greathouse et al., 2000). The co-ordination number of calcium ions in the interlayer space is a subject of ongoing debate. Monte Carlo simulations by Greathouse and Storm (2002) indicated an eight-fold water hydration shell. Surface energy studies by contact angle measurements also indicated that divalent cations are shielded from the silicate surface by water molecules whereas monovalent cations can be in direct contact with the surface oxygen atoms (Norris et al., 1993).

Results of simulation studies on the dynamics of water molecules and cations in the interlayer space cannot be directly compared with experimental values, e.g., obtained from tracer measurements. The experimental diffusion coefficients are distinctly lower than the calculated ones, especially in the case of caesium ions (Marry et al., 2002), not only because of the different timescale (nanoseconds in the simulation techniques) but also because of the influence of the macroscopic structure of the clay mineral particles.

5.2.3. *Colloidal Dispersions*

An outstanding property of dispersed montmorillonite particles is delamination into individual silicate layers or thin packets of them when the exchangeable cations are alkali cations, preferentially Li^+ and Na^+, and the salt concentration is sufficiently small (<0.2 mol/L for Na^+ ions) (Fig. 5.4) (Norrish, 1954; Norrish and Rausell-Colom, 1963; Cebula et al., 1980; Schramm and Kwak, 1982a; Nadeau, 1985; Avery and Ramsay, 1986; Sposito, 1992; Jasmund and Lagaly, 1993; Lagaly, 1993, 2005; Sposito and Grasso, 1999). The thickness and width of the individual layers and thin particles or packets of layers, produced by the disarticulation of a large variety of smectites and I/S mixed-layer particles were determined by TEM and X-ray techniques (Nadeau, 1985; Środoń et al., 2000; Dudek et al., 2002) (see Section 5.3.5). The interlayer cations are in the diffuse double layers around the silicate layers and thin particles. The presence of these units that do not interact strongly and flow independently was proved by light and small-angle neutron scattering (Schramm and Kwak, 1982a, 1982b; Avery and Ramsay, 1986). This state is sometimes called 'osmotic swelling' by clay scientists (not by colloid scientists!).

The average interparticle distance (obtained from small-angle scattering) responds to the addition of sodium salts in an almost linear decrease with $2/\sqrt{c}$ (c = salt concentration) until, at $c \approx 0.2$ mol/L, particle rearrangement occurs and the basal spacing abruptly decreases from about 4 to 2 nm (Norrish, 1954; Odom, 1984; Kraehenbuehl et al., 1987) (see Chapter 13.2).

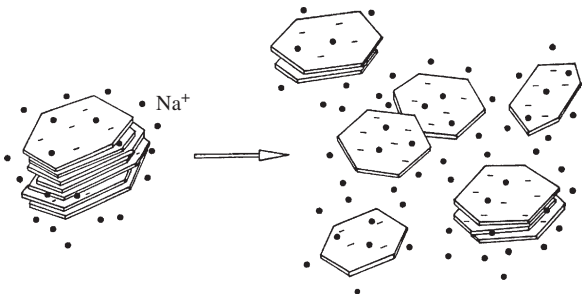

Fig. 5.4. Disarticulation (delamination) of alkali smectite particles in aqueous dispersions. From Jasmund and Lagaly (1993).

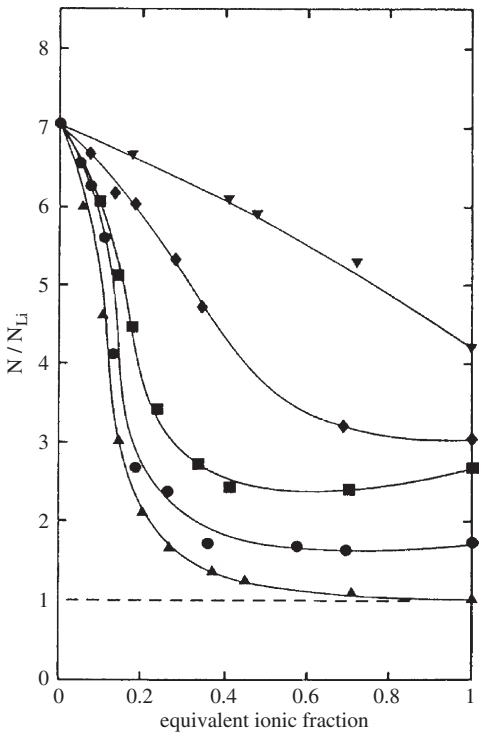

Fig. 5.5. Relative number of layers per particle, N/N_{Li} ($N_{Li} = 1$) as a function of surface coverage when the Ca^{2+} ions are exchanged by Li^+ (▲), Na^+ (●), K^+ (■), Cs^+ (♦), and Mg^{2+} (▼) ions (Schramm and Kwak, 1982a). From (Jasmund and Lagaly, 1993).

With cations other than Li^+ and Na^+ the distances separating individual layers are no longer equal but vary around a mean value. Particles[1] are formed by a columnar-like superposition of a few silicate layers at equal distances. The distances between these particles are larger than within these units. Fig. 5.5 shows the relative number N/N_{Li} of layers per particle ($N_{Li} = 1$ for Li^+ as the exchangeable cation) when the Ca^{2+} ions are progressively replaced by alkali and Mg^{2+} ions (Schramm and Kwak, 1982a, 1982b). In the presence of Ca^{2+} ions the particles contain about seven silicate layers. Even small amounts ($\leqslant 0.2$ equivalent fractions) of alkali metal ions reduce the size of the particles to one to three layers.

From SANS measurements Cebula et al. (1980) inferred that a considerable part of the layers is aggregated to units consisting of two silicate layers (potassium montmorillonite) or three silicate layers (caesium montmorillonite) interleaved with bimolecular water layers.

[1]In the literature, particles with large separations between the silicate layers are often called 'tactoids'.

Delamination of smectite particles into thinner particles or single silicate layers is an important process during soda-activation of bentonites. However, optimal delamination is only attained when the exchangeable cations are Na^+ (or Li^+) and all multivalent cations are removed. Ancillary minerals, in particular carbonates, have also to be removed or decomposed because they act as reservoirs of multivalent cations. Amorphous silica and organic materials can also reduce or even impede delamination. Thus, optimal delamination is only achieved when the bentonites are purified and fractionated (see Section 5.3.1). The technical soda-activation process does not proceed to complete delamination. Rather, the adjustment (often instinctively) of a certain degree of delamination is helpful in optimising the properties of a bentonite dispersion for a particular application.

5.2.4. Electrokinetic Properties

The electrokinetic mobility of colloidal particles is related to their movement in an electrical field (Hunter, 1993; Lyklema, 1995; Lagaly et al., 1997). The potential at the shearing plane is referred to as the 'zeta potential', and is usually derived from the mobility by the Henry or Helmholtz–Smoluchowski equation. However, the relation between the mobility and the zeta potential is much more complicated because of relaxation and retardation effects and the influence of surface conduction. Surface conduction arises from counterions that are not immobile below the shear plane but migrate in directions tangential to the surface in the electrical field[2], reducing the mobility of the particles (O'Brien and White, 1978; Mangelsdorf and White, 1990; Hunter, 1993; Rowlands and O'Brien, 1995; Lyklema, 1995; Lagaly et al., 1997). If the moving particles are aggregates and contain pores, the effect of liquid transport in the pores must be considered (Miller et al., 1992).

The non-spherical shape of clay mineral particles provides a further complication because no mathematical formulations could be derived for the relation between mobility and zeta potential. In an acidic medium the presence of positive edge charges complicates the electrokinetic behaviour. The zeta potential of clay mineral particles (calculated from mobility data by the Helmholtz-Smoluchowski equation, as often reported in the literature) indicates nothing more than the sign of the external charge of the particles, and only provides a value proportional to the electrophoretic mobility. Thus, the reporting of mobility rather than zeta potential values is strongly recommended.

The electrophoretic properties of clay mineral particles received much attention (Thomas et al., 1999, and references therein; Li et al., 2003). Typical mobility data[3] are in the range of -2 to -3×10^{-8} [m^2/sV] and no i.e.p. is observed in the pH range of 2–12 (except for chlorite with an i.e.p. at pH ~5). Similarly, kaolinite particles do

[2]This phenomenon is sometimes called 'anomalous' surface conduction but this term should be avoided.

[3]Mobility has no sign. Nevertheless, signs are used to indicate the sign of the shear plane potential.

not show positive mobility even at pH approaching zero (Siffert and Kim, 1992; Galassi et al., 2001). Due to the spillover effect (see Section 5.4.1) which reduces the influence of the positive edge charges, the aspect ratio (diameter/thickness ratio) of the particles must be considered. Face/face aggregation of the silicate layers (thicker particles) can reduce mobility because of the stronger influence of the positive edge charges in acidic medium whereas a higher extent of delamination will increase the mobility. This effect was clearly observed for dispersed saponites (Thomas et al., 1999).

The mobility of smectite particles is almost constant over a wide pH range around the neutral point (Benna et al., 1999; Thomas et al., 1999; Li et al., 2003). Only very highly charged saponites show a strong pH-dependent mobility because of the strong influence of the positive edge charges and increased aggregation (Thomas et al., 1999). The independence of the mobility over a wide pH range was modelled by Tombácz et al. (1990) (see Section 5.4.10) and Avena and de Pauli (1998). Despite the pH-dependent Na^+/H^+ exchange, the amount of screened structural charge, i.e. the amount of cations below the shear plane, seems to remain constant at this pH range. Indifferent electrolytes with the same valence as the exchangeable cation induce only little, if any, variation of mobility, while divalent cations reduce the mobility more than monovalent cations. Trivalent cations can cause charge reversal (see Section 5.4.8).

The electrophoretic mobility (in a moderately acidic medium) is not much influenced by the layer charge (Thomas et al., 1999). This is because a high layer charge promotes Stern-layer adsorption, and the zeta potential does not increase in direct response to the layer charge. We should also mention that the surface charge density is not proportional to the surface potential but to the hyperbolic sine of the potential (van Olphen, 1977; Hunter, 1993; Lyklema, 1995; Lagaly et al., 1997). As the tetrahedral charge also increases Stern-layer adsorption, the mobility of saponites is smaller than that of montmorillonites of similar charge (Thomas et al., 1999).

Since many factors determine the mobility of clay mineral particles, the p.z.n.p.c. of the edges can only be deduced from mobility data with a certain arbitrariness. Thus, Thomas et al. (1999) concluded that the charge of the edges is negative at $pH \geqslant 3.5$. On the other hand, Benna et al. (1999) suggested that pH ~7 is a more probable value, while Avena and de Pauli (1998) reported $pH \geqslant 8.5$.

In very diluted dispersions (5 mg/L) imogolite fibres showed a mobility that decreased from $+3 \times 10^{-8}\,m^2/s\,V$ at pH ~5 to $-1.5 \times 10^{-8}\,m^2/s\,V$ at pH ~10. In dispersions of 100 mg/L, the mobility decreased from pH 4 to 7 but became zero at $pH > 7$. Dispersed imogolite easily flocculates under alkaline conditions, and the zero mobility value indicates formation of large immobile aggregates (Karube et al., 1992).

Electrokinetic measurements are required to detect charge reversal of colloidal particles by adsorption of multivalent cations or organic cations, such as alkylammonium ions and organic dye cations (Pashley 1985; Hunter and James, 1992; Schramm et al., 1997; Penner and Lagaly, 2000).

The interaction of clay mineral particles with polymers influences the mobility in a subtle way. Adsorption of neutral macromolecules often shifts the position of the shear plane so that the mobility changes despite constant charge densities (Theng, 1979). As an example, poly(vinylpyrrolidone), PVP, with a molecular weight of ~400,000 decreased the mobility of Li^+ montmorillonite particles more strongly than low molecular weight PVP. The high molecular weight PVP is adsorbed in loops that shift the shear plane away from the particle surface in direction to the solution, i.e. to smaller potentials. PVP with a molecular weight of 5000 is mainly adsorbed in trains, and the influence of the shear plane position is distinctly smaller (Séquaris et al., 2002).

Adsorption of polycations usually causes charge reversal when a certain amount is adsorbed. However, the amount of polymer charges at the i.e.p. is often distinctly below the CEC of the clay mineral because accumulation of the positive charges at the external surfaces is decisive. Soft particles where a hard core is surrounded by an envelope of macro-ions show a highly complex relation between the mobility and the properties and charges of the polyelectrolyte envelope (Ohshima, 1995; Lagaly et al., 1997).

Dynamic mobility measurements using electroacoustic instruments became more and more common in colloid science, even if the theoretical background is still in development (Hunter, 1998). This method shows the important advantage that concentrated dispersions, often needed in applications, can directly be measured whereas all other electrophoretic measurements require highly dilute dispersions.

Electroacoustic investigation of kaolinite and montmorillonite dispersions revealed the presence of a high surface conductance that complicates the interpretation of the dynamic mobility spectrum (O'Brien and Rowlands, 1993; Rowlands and O'Brien, 1995; Rasmusson et al., 1997).

5.3. PREPARATION OF COLLOIDAL DISPERSIONS

5.3.1. Fractionation of Clay Dispersions

Clay minerals with a certain degree of purity can be separated from raw clay samples by sedimentation techniques. The first step consists of removal of iron oxides and organic materials. These materials not only affect the properties of colloidal dispersions but also prevent optimal peptisation of clay particles and successful fractionation by sedimentation. To prepare colloidal dispersions it is important to remove carbonates and silica (see Chapter 4). Carbonates can release calcium or magnesium ions into solution, reducing the degree of peptisation. Amorphous silica can act as a cementing agent between the particles.

In contrast to their counterparts from soils, kaolins and bentonites from geologic deposits contain only small amounts of organic materials. However, since they can

contain appreciable amounts of iron oxides, purification is needed to obtain colloidal dispersions with an optimal degree of delamination.

A decisive step in preparing a stable clay dispersion is the replacement of divalent exchangeable cations by Na^+ (or Li^+) ions. Following the procedure described by Stul and van Leemput (1982) and Tributh and Lagaly (1986), the final dispersion obtained by dialysis and adjusted to pH 7.5 is stable, containing particles in an optimal degree of dispersion. Addition of deflocculating agents such as phosphates and polyphosphates is not required to attain the colloidal distribution (Lagaly, 1993).

The stable dispersion of clay minerals in homoionic form is fractionated by gravity sedimentation or, for particle sizes of $<2\,\mu m$, by centrifugation. To reduce particle/particle interaction during sedimentation, the volume fraction of the particles should be in the range of $1-2\times10^{-3}$ (about 5 g clay/1000 mL water). The pH should not decrease below 6.5. Note that the pH of water in contact with the atmosphere is usually <6.

Fractionation by sedimentation belongs to the established industrial separation procedures and is used at a technical scale for kaolin processing. It is the most important procedure to obtain relatively pure clay minerals in the laboratory.

The particle size of the fractions is expressed in Stokes equivalent spherical diameters[4]. The particles of a dispersion settle with a constant velocity v, which is determined by the gravitation force $mg = \rho Vg$ minus the buoyancy $\rho_0 Vg$ and the Stokes' friction force $3\pi\eta v$d:

$$V(\rho - \rho_0)g = 3\pi\eta v d \tag{1}$$

$V(=\pi d^3/6)$ is the particle volume; ρ is the particle density; ρ_0 is the density of the solvent; g is the gravitational acceleration ($=9.81\,m/s^2$); η is the solvent viscosity; and d is the particle diameter. The settling velocity v ($=h/t$) of a particle is therefore:

$$v = \frac{h}{t} = \frac{(\rho - \rho_0)g}{18\eta} d^2 \tag{2}$$

The time (t) needed for a particle to settle within a given distance (h) is given by

$$t = \frac{18\eta}{(\rho - \rho_0)g} \frac{h}{d^2} \tag{3}$$

A quartz particle (density $2.65\times10^3\,kg/m^3$) with a diameter of 20 μm needs 3 min 58 s to settle in water at 25 °C within a distance of 0.1 m. Particles with 10, 2, and 1 μm need 15 min 51 s, 6 h 36 min, and 26 h 25 min. Since viscosity increases with decreasing temperature, the corresponding sedimentation times at 20 °C are distinctly longer: 4 min 38 s (20 μm), 18 min 33 s (10 μm), 7 h 44 min (2 μm), and 30 h

[4]The conditions of the validity of Stokes' law were fully discussed by von Hahn (1928).

55 min (1 μm) (the density of water at 20 and 25 °C is 998.00 and 997.05 kg/m^3, respectively, while the viscosity is 1.002×10^{-3} and 0.8904×10^{-3} kg/ms, respectively).

Fractionation of particles with diameters <1 μm would require very long sedimentation times. For 0.2 μm particles one calculates $t = 660$ h 33 min at 25 °C and $h = 0.1$ m. For still smaller particles the Brownian movement hinders sedimentation. Fractionation then requires the stronger centrifugal fields. In this case the gravitational acceleration, g, has to be replaced by the acceleration $4\pi^2\omega^2 r$ where ω is rotations per second, and r is distance of the particle from the rotational axis (Fig. 5.6).

As acceleration depends on r, the sedimentation velocity $\mathrm{d}h/\mathrm{d}t$ also depends on r. The time $\mathrm{d}t$ for a particle to move through a distance $\mathrm{d}h$ at the position r is given by

$$\mathrm{d}t = \frac{18\eta}{(\rho - \rho_0)4\pi^2\omega^2 r}\frac{\mathrm{d}h}{d^2} \tag{4}$$

Integration gives the time for the particles to move from r_0 to $r = r_0 + h$ (Fig. 5.6):

$$t = \frac{18\eta}{(\rho - \rho_0)4\pi^2\omega^2 d^2}\int_{r_0}^{r}\frac{\mathrm{d}r}{r} = \frac{18\eta}{(\rho - \rho_0)4\pi^2\omega^2 d^2}\ln\frac{r}{r_0} \tag{5}$$

By way of illustration, Table 5.2 gives the sedimentation times for quartz. The separation of increasingly smaller particles requires higher centrifugal forces, i.e. an enhancement of the rotation velocity. Separation of the <0.2 μm fraction needs a running time of 17 min, while that of the <0.02 μm fraction requires 4 h.

The choice of particle density provides a certain problem because not only the densities of the species among the different clay mineral groups vary but the density of the species within a group can also vary due to differences in chemical composition and hydration state. The variation is small for kaolinites (2600–2680 kg/m^3), and somewhat larger for muscovite (2760–3000 kg/m^3) and biotite (2700–3100 kg/m^3) (Grim, 1968). Dry illites may have a density of about 2650 kg/m^3 but due to the

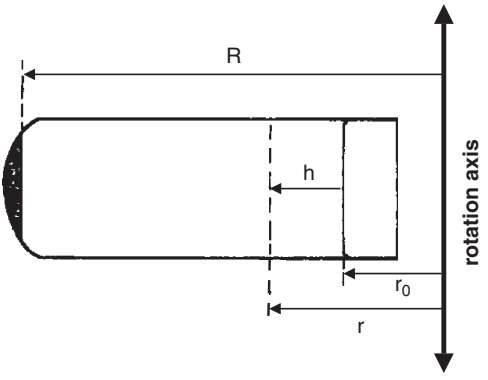

Fig. 5.6. Fractionation by centrifugation.

Table 5.2. Sedimentation in the centrifugal field; for r_0, r, h see Fig. 5.6. Quartz particles (density 2650 kg/m^3) in water (density ~1000 kg/m^3) at 20 °C

r_0*(m)	r(m)	h(m)	Rotations/min	Diameter (μm)	Sedimentation time		
					hours	min	s
0.104	0.124	0.02	1000	0.6	–	8	7
0.112	0.132	0.02	2000	0.2	–	17	4
0.120	0.140	0.02	4000	0.06	–	44	28
0.128	0.148	0.02	5000	0.02	4	1	11

*The increasing values of r_0 are related to the decreasing volume of the dispersion after removal of about 10 mL of the dispersion after each step for particle size analysis (see Section 5.3.5).

relative small particle sizes, adsorbed water decreases the density of the particles in the dispersion.

Smectites are an extreme case. Dehydrated montmorillonites may have densities between 2500 kg/m^3 at low and 2700 kg/m^3 at high iron contents (Grim, 1968). Zerwer and Santamarina (1994) reported the density (in kg/m^3) for pyrometamorphosed bentonite of 2600 (room temperature), 2670 (200 °C), 2680 (400 °C), and 2730 (600 °C). During dispersion the particles delaminate. The thin particles or single silicate layers are surrounded by a few water layers that move with the settling particles. It is very likely that at least two layers of water remain attached to the particles. Assuming an average mass of 750 g/mol unit cell with a basal plane surface area of 0.465 nm^2, and bimolecular water layers (density ~1000 kg/m^3) attached to the basal plane surfaces, one estimates a density for a hydrated single layer of 2250 kg/m^3. This value is recommended for calculating the sedimentation times of dispersed montmorillonite particles.

The density of I/S mixed-layer particles will also be somewhat lower than 2650 kg/m^3 but the real value depends on the size of the fundamental particles (see Section 5.3.3) formed in the dispersion.

Grim (1968) reported densities of montmorillonites, illites, and kaolinites when the particles were equilibrated at relative humidity between 0 and 1. However, the small values at high humidity are certainly not the real densities of the dispersed particles but are caused by condensation of water in the pores of the aggregated particles.

Usually, the density of quartz (2650 kg/m^3) is used in calculating sedimentation times of clay dispersions. For bentonites a density of 2250 kg/m^3 may be more appropriate.

The different densities are not a serious obstacle in separating size fractions. It must be remembered that the diameters related to the sedimentation times are not real particle dimensions but are the diameters of the Stokes' equivalent spheres.

For fractionation (Atterberg procedure) the dispersion of the purified clays can be directly used without dialysis because of the enormous dilution during the procedure.

The dispersion is transferred to one or more cylindrical vessels and well dispersed. After a calculated sedimentation time, the upper part with a depth h (= sedimentation distance) is withdrawn by careful suction or siphoning. For instance, when $h = 0.2$ m and $t = 52$ h 50 min, this part of the dispersion only contains particles $\leqslant 1$ μm. However, the lower part of the dispersion and the sediment still contain $\leqslant 1$ μm particles. The withdrawn dispersion volume has to be replaced by water. After intense mixing the same volume of the dispersion is again removed after the same time period. This procedure is repeated until all $\leqslant 1$ μm particles are separated, i.e. the upper part of the dispersion after the selected sedimentation time remains completely clear and free of particles. The next step is the separation of the next larger fraction, which may be the fraction 1–2 μm using the sedimentation time for 2 μm particles.

The choice of the size fractions was often discussed. A modified Atterberg scale is recommended (Tributh and Lagaly, 1986): > 63, 63–20, 29–6.3, 6.3–2, 2–0.6, 0.6–0.2, and < 0.2 μm. (This is fractionation in a logarithmic scale because the logarithm decreases by 0.5 in every step).

An important condition for a clear separation is a sufficiently low particle concentration that allows the particles to settle independently (granular or free sedimentation). Clay mineral dispersions often show a combination of free and structural sedimentation when the particle concentration is too high. In this case not all particles settle and form a sediment (see Section 5.6.3).

5.3.2. *Dispersions of Kaolins*

The width of kaolinite particles varies from about 0.1 to 20 μm (Jepson, 1984). The content of ancillary minerals (feldspars, quartz, mica, smectites) in kaolins varies with particle size. Pure kaolinite can often be obtained from kaolins by selecting the appropriate particle size fractions. In fractions < 0.1 μm, smectites are enriched; in fractions > 1 μm, quartz, feldspars, and micas become abundant (Jepson, 1984). However, the variation of the composition with particle size depends on the deposit, and pure kaolinite cannot be obtained in any case by fractionation.

When the hydrogen bonds and the dipole interactions that hold together the silicate layers of kaolinite particles are weakened by intercalation of suitable organic molecules, the particles can be separated into thinner ones under the action of mechanical forces. This reaction was used by Chinese ceramists to improve the quality of porcelain (Weiss, 1963). Colloidal dispersions of kaolinite can be prepared when kaolinite is treated with DMSO and ammonium fluoride (Lahav, 1990; Chekin, 1992). The fluoride ions replace some OH^- groups and reduce the number of hydrogen bonds and the bonding energy between the layers (Costanzo et al., 1984).

5.3.3. *Dispersions of Smectites and Vermiculites*

Smectite particles may be as large as 2 μm and as small as 0.1 μm, with average sizes of about 0.5 μm (Grim and Güven, 1978; Odom, 1984). The morphology of

individual particles ranges from platy to lath-shape; some are even fibrous but mostly the particles are of irregular shape. Aggregates may be compact, foliated, or reticulated (Keller, 1985; Keller et al., 1986).

The unique fractionation procedure for smectites distinguishes smectites from all other clay minerals. Pre-treatment reactions and saturation with Na^+ ions enhance delamination, i.e., the particles disarticulate into individual silicate layers during sedimentation. Those particles with equivalent diameters measured by sedimentation are artefacts, and not the same particles that are originally present in the bentonite. Nevertheless, fractionation is a sensitive tool for detecting differences between bentonites of different origin. A bentonite consisting of particles with varied thickness and plate width may be fractionated by sedimentation at conditions where all particles are delaminated. The mass content of the different particle-size fractions is then representative of the number of silicate layers with a given diameter (mean equivalent spherical diameter) that were originally aggregated into thicker particles. Naturally, nothing can be said about the thickness of the original particles. Thus, the particle size distribution obtained by fractionation represents the plate width distribution in the parent bentonite. A bentonite that produces fractions of very fine particles must contain particles of small diameters. In fact, bentonites of various deposits differ mainly in the particle size distribution below 2 μm. Again, it should be noted that the diameter derived from the sedimentation process is the diameter of the Stokes' equivalent sphere and not any real particle diameter.

As many montmorillonites are formed by alteration and weathering processes, particles of different size may not have the same layer charge. However, the mean layer charge of the particles of various fractions often changes only slightly (Lagaly, 1994). For instance, the layer charge of Wyoming montmorillonite only increased from 0.27 charges/formula unit (<0.06 μm fraction) to 0.28 charges/formula unit (2–63 μm fraction). The Bavarian montmorillonite (bentonite from Niederschönbuch) showed similar changes: 0.27 charges/formula unit for <0.06 μm particles and 0.29 charges/formula unit for 2–63 μm particles. However, distinct changes of the charge distribution curves were observed. During peptisation and fractionation, the particles are completely disarticulated. Afterwards the layers are re-aggregated by coagulation, and the sequence of the differently charged layers (as a consequence of charge heterogeneity) is not the same as in the parent material (see Section 5.4.2). Dialysis can also change the charge distribution to some extent, not only because of the disaggregation/re-aggregation mechanism but also because of the increased risk of chemical attack on the thin silicate layers (Lagaly, 1994).

As a consequence of the disarticulation of smectite particles into individual silicate layers, I/S mixed-layer particles can disintegrate at the low-charged interlayer space. The type of fundamental particles obtained depends on the charge distribution, i.e. the variation of the cation density from interlayer space to interlayer space (Fig. 5.7). The particles break up only at interlayer spaces with cation densities typical of smectites.

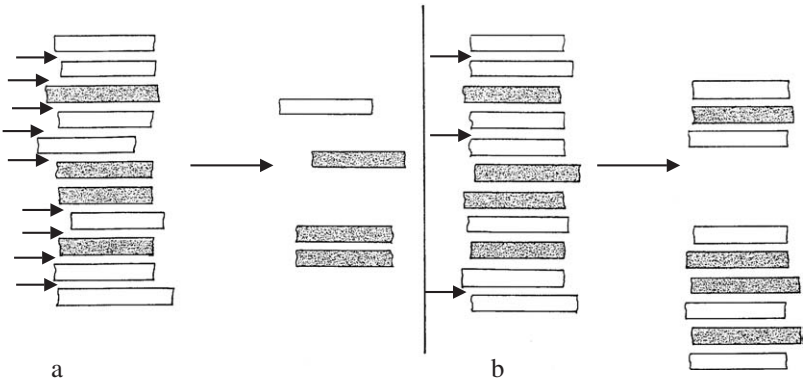

Fig. 5.7. Delamination of I/S mixed-layer particles. Different types of fundamental particles form depending on the variation of the interlayer cation density, i.e. the charge distribution. (a) Low mean layer charge: the particles split (arrows) between the low-charged layers and the low and more highly charged layers (dotted) but not between the highly charged layers. (b) Higher mean layer charge: the particles split only between the low-charged layers.

The way in which the I/S mixed-layer particles delaminate has technical consequences because many common clays contain I/S materials. The different types of particles produced by the break-up of the mixed-layer particles of soda-activated clays determine the flow behaviour of these dispersed clays (Lagaly, 1989).

Submicron vermiculite particles could be prepared from macroscopic vermiculite flakes by ultrasound treatment (Pérez-Maqueda et al., 2001; Wiewiora et al., 2003).

5.3.4. H^+-Saturated Smectites

It is sometimes desirable to prepare dispersions of H^+-saturated smectites. Leaching of smectites with acids results in a high degree of H^+ saturation and is accompanied by a severe chemical decomposition of the layers. Since the Al^{3+} ions (also Mg^{2+} and other divalent ions) released during decomposition are preferentially adsorbed, the structure progressively transforms into the Al^{3+} form (Janek et al., 1997; Janek and Lagaly, 2001). The dispersion is stable for a certain time (Schwertmann, 1969) but as decomposition progresses, the Al^{3+} ions released from the structure cause coagulation. Barshad (1969) recommended passing a Na^+-smectite dispersion (1–2%) rapidly (200 mL within 1–5 min) through a series of three exchange resin columns arranged in the order: H^+ resin $\rightarrow HO^-$ resin $\rightarrow H^+$ resin. By this means, a H^+-saturated, highly peptised smectite dispersion is obtained that remains stable for some time.

5.3.5. Determination of Particle Size and Shape in Colloidal Clay Dispersions

It is difficult to evaluate the size and shape of dispersed particles. The oldest method for assessing the size of dispersed clay mineral particles is the sedimentation

procedure, giving particle size in terms of Stokes' equivalent diameters (Section 5.3.1). The application of the pipette method (von Hahn, 1928; Andreasen, 1931, 1935) in the gravitational and centrifugal field was optimised by Tributh and Lagaly (1986). During sedimentation of dispersed particles a certain volume of the dispersion is removed by a pipette at a given height after calculated time intervals. The mass of the particles in this volume is determined by weighing after slow evaporation of the water. It is important that the volume ratio particles/water does not exceed 2×10^{-3} to ensure free sedimentation of the particles (Section 5.6.3). This ratio should not be $< 10^{-3}$ to have enough material for weighing. Thus, about 5 g clay ($< 2\,\mu m$) are recommended for 1000 mL water.

The specific surface area of the dispersed particles in contact with water can be directly determined by the co-ion exclusion (Chan et al., 1984). As very small concentration changes have to be measured, the method yields reliable values only for dispersed smectites.

XRD is a common technique to determine the size of crystalline colloidal particles. The technique is based on the peak profile analysis of periodic structures, i.e. the effect of interstratification has to be excluded. A simple but useful method to derive the size of coherent scattering domains is based on the Scherrer equation. The Bertaut-Warren-Averbach (BWA) method is the most universal method. It allows the mean size, the size distribution, and the effect of strain (fluctuations of *d*-values) to be evaluated (Dudek et al., 2002). SAXS was employed to determine the specific surface area and fractal dimensions of soil particles (Borkovec et al., 1993).

The different methods of particle-size determination in colloidal dispersions (sedimentation, turbidity measurements, static and dynamic light scattering, streaming methods, flow field flow fractionation (Allen, 1997)) are based on the assumption of spherical particles. In all cases the information obtained is the mean equivalent spherical diameter and never the real dimension. When different methods are applied, different size-dependent properties are measured. Because of the non-spherical shape of the clay mineral particles, the application of different characterisation methods is a prerequisite to obtain information on the size and shape of colloidal particles. To compare different investigation methods, one has to consider that different methods give different average values, e.g., microscopic methods give the number-weighted particle diameter, and dynamic light scattering (photon correlation spectroscopy, PCS) the intensity-weighted diameter (Lagaly et al., 1997). Plaschke et al. (2001) investigated smectite particles from a low-mineralised groundwater by AFM, PCS, flow field flow fractionation (FFFF), and laser-induced breakdown detection (LIBD). AFM revealed particles (aspect ratio ~0.1) with a broad distribution and a number-weighted average diameter of 73 nm. LIBD indicated an average value of 63 nm. The maximum of the number size distribution was found by FFFF at 70 nm. PCS gave an intensity-weighted average hydrodynamic diameter of 235 nm corresponding to the maximum of the number-weighted distribution at 138 nm. Mackinnon et al. (1993) found reasonable agreement between size determination of kaolinite particles by sedimentation, electron microscopy, image

analysis, and laser scattering when the particle sizes were calculated from the scattering data by the Mie theory.

The relation between the real dimensions of rods and discs and the measured equivalent spherical diameter depends on the type of measurement (Jennings and Parslow, 1988; Lagaly et al., 1997). As shown by Jennings and co-workers (Oakley and Jennings, 1982; Jennings and Parslow, 1988; Jennings, 1993; Hinds et al., 1996) and Slepetys and Cleland (1993), the ratio diameter/length (for rods) or diameter/thickness (aspect ratio of discs) can be estimated from the equivalent diameters measured by two different methods, giving distinctly different equivalent diameters. For example, when kaolinite dispersions were analysed by rotary diffusion (electro-optic and magneto-optic experiments) or light scattering as against sedimentation (Jennings, 1993; Slepetys and Cleland, 1993).

Microscopic observations (TEM, SEM, ESEM, AFM, etc.) are useful for investigating clay minerals as they directly provide shape and geometric dimensions within the inherent instrumental uncertainties. However, the transfer of particles from the dispersion to the sample holder of the electron microscope can strongly change the appearance of the particles and their size. In many cases the microscope methods may not be statistically satisfactory (Dudek et al., 2002). The modern technique of jet-freezing allows particles in colloidal dispersions, and also the structure of emulsions and microemulsions to be determined (Lagaly et al., 1997). Reliable information about the state of montmorillonite particles in dispersion and formation of band-type and card-house structures was obtained (Vali and Bachmann, 1988; Benna et al., 2001a, 2001b).

5.4. COAGULATION OF COLLOIDAL CLAY MINERAL DISPERSIONS AND MECHANISMS OF COAGULATION

5.4.1. Coagulation by Inorganic Salts

Since the colloidal state of dispersed clay minerals is decisive in many practical applications, the coagulation of kaolinite and montmorillonite dispersions was investigated for many decades (Jenny and Reitemeier, 1935; Kahn, 1958). Unlike other colloidal dispersions, well-dispersed clay minerals (kaolinites, smectites, illites, palygorskite) in the sodium form may be coagulated by very low concentrations of inorganic salts. The critical coagulation concentration, c_K, of sodium chloride varies between 3 and 20 mmol/L. The data assembled in Table 5.3 also reveal the modest influence of different types of montmorillonites, even illites, beidellites and Laponites in that all give similar c_K values. For palygorskite see Section 5.4.2.

The very strong influence of the valence of the counterions is typical of electrostatically stabilised dispersions. The 0.025% Na^+-montmorillonite dispersions were coagulated by 5 mmol/L sodium chloride, 0.4 mmol/L calcium chloride, and 0.08 mmol/L aluminium chloride (Table 5.4) (Penner and Lagaly, 2000). Oster

et al. (1980) reported a c_K of 0.125 mmol/L $CaCl_2$ for 0.1% dispersions of Na^+-montmorillonite (Wyoming) and illite (Fithian, Montana). As expected, K^+ ions were strong coagulants for illites. Hesterberg and Page (1990b) reported c_K values of $KClO_4$ for 0.05% dispersions of K^+ illite: $c_K = 2.5$ mmol/L (pH= 6); 3 mmol/L (pH= 6.6); 8 mmol/L (pH= 7.2); 11 mmol/L (pH= 9.3); and 14 mmol/L (pH= 10). NaCl coagulated Na^+-illite dispersions at concentrations between 6.5 and 48 mmol/L at pH 6–10 (Table 5.3).

As a function of pH, the c_K value of Na^+-montmorillonite showed a plateau between pH 4 and pH 6–7, and increased at higher pH (Perkins et al., 1974; Swartzen-Allen and Matijević, 1976; Keren et al., 1988; Goldberg and Forster, 1990). The dispersion coagulated spontaneously at pH < 3.5 and was destabilised by the base necessary to raise the pH above 10.5. The c_K value of Laponite increased linearly with pH. A step-wise increase was also found for Na^+-kaolinite and $NaNO_3$.

Dynamic light scattering was indicated that the kaolinite (KGa-2) dispersions show fast coagulation kinetics (stability factor $W = 1$) below pH 5.8 (point of zero edge charge), regardless of the ionic strength (10^{-3}–1 mol/L $NaClO_4$). Above pH ~5.8 the dispersions were charge-stabilised and the coagulation rate strongly depended on pH and ionic strength (Kretzschmar et al., 1998).

The c_K value increased with solid content (Williams and Drover, 1967). The 0.5% dispersions of Na^+-montmorillonite (Wyoming) were coagulated by 20 mmol/L sodium chloride, 3 mmol/L calcium chloride, and 1.5 mmol/L aluminium chloride (test-tube tests) (Table 5.4) (Penner and Lagaly, 2000; Lagaly and Ziesmer, 2003).

The values of c_K also depended on the type of anion (Table 5.5). Nitrate instead of chloride increased c_K from 5 to 16 mmol/L and sodium sulphate to 18 mmol/L (0.025% dispersion). The influence of certain phosphates can be extremely strong (Lagaly, 1989; Manfredini et al., 1990; Penner and Lagaly, 2001). Thus, Na_2HPO_4 and NaH_2PO_4 coagulated the 0.025% dispersion at 1100 and 460 mmol/L, respectively. Sodium diphosphate ($Na_4P_2O_7$) up to its solubility limit (~130 mmol/L) did not coagulate the dispersion. In contrast, sodium phosphate (Na_3PO_4) showed the very low coagulation concentration of 25 mmol/L because the dispersion was highly alkaline (pH 11.5–12) at the point of coagulation. NaOH also coagulated at 20 mmol/L. In contrast to the influence of chlorides and nitrates, the c_K of NaH_2PO_4 and NaH_2PO_4 decreased with increasing solid content (Table 5.5).

The effect of phosphate was also seen when the montmorillonite dispersion was coagulated with NaCl in the presence of sodium diphosphate. Even an addition of 0.1 mmol/L $Na_4P_2O_7$ increased the c_K of NaCl from 5 to 195 mmol/L (Permien and Lagaly, 1994c). Larger quantities of this phosphate raised the c_K to about 300 mmol/L NaCl (Table 5.6). This effect was also observed for a 0.1% pyrophyllite dispersion at pH 5.3 which was coagulated by 0.4 mmol/L sodium nitrate but 100 mmol/L of this salt was required in the presence of 0.16 mmol/L sodium hexametaphosphate $Na_6P_6O_{18}$.

The critical coagulation concentration of 5–10 mmol/L Na^+ ions for Na^+-clay mineral dispersions is extremely low compared with the usual values between 25 and

Table 5.3. Reliable critical coagulation concentrations c_K of sodium chloride for clay mineral dispersions

Origin	c_K(mmol/L)	Conditions of coagulation*	Reference
Kaolinites			
Benson deposite, Troy, USA	7–12	$\leqslant 1\%$, $<10\,\mu m$, pH = 7.1	Hsi and Clifton (1962)
Not identified	16–40	0.025%, pH = 4−10	Swartzen-Allen and Matijević (1976)
Montmorillonites			
Wyoming, USA	3.5	0.025–0.8%	Kahn (1958)
Upton, Wyoming	13	0.025%, $<0.1\,\mu m$, pH = 6−7	Frey and Lagaly (1979b)
	10–15	0.025%, 0.1–2 μm, pH = 6−7	
Upton, Wyoming	12	0.1%, $<2\,\mu m$,	Oster et al. (1980)
Upton, Wyoming	10, 13, 31, 44	0.1%, $<2\,\mu m$, pH = 5, 7.5, 8.5, 9.8	Keren et al. (1988)
Crook County, Wyoming	10–33	0.1%, $<0.2\,\mu m$; pH = 6.3−9	Hetzel and Doner (1993)
Crook County, Wyoming	13.3; 50	0.1%, $<2\,\mu m$, pH = 7.6, 10.7	Neaman and Singer (1999)
Otay, California, USA	7–13	0.1%, $<0.2\,\mu m$, pH = 6−9.3	Hetzel and Doner (1993)
Chambers, Arizona, USA	1–10	0.025%, pH = 4−10	Swartzen-Allen and Matijević (1976)
Cheto, Arizona	15, 24, 29, 32	0.07%, $<2\,\mu m$, pH = 6.4, 6.7, 8, 9	Goldberg and Forster (1990)
Cyprus	8–12	0.025%, 0.1–2 μm, pH = 6−7	Frey and Lagaly (1979b)
Cerro Bandera, Argentina	8	0.09%, pH = 7.4	Helmy and Ferreiro (1974)
Beidellites			
Unterrupsroth, Germany	7	0.025%, $<0.1\,\mu m$, pH = 6−7	Frey and Lagaly (1979)
	5–7	0.025%, 0.1–2 μm, pH = 6−7	
Silver City, Idaho, USA	4–5, 28–52	0.1%, $<0.2\,\mu m$, pH = 6.1−7.2; 8.3–9.3	Hetzel and Doner (1993)

(*continued on next page*)

Table 5.3. (*Continued*)

Origin	c_K(mmol/L)	Conditions of coagulation*	Reference
Laponites			
Laponite CP.	10	2% (!), pH = 8.5 (?)	Neumann and Sansom (1971)
	2–20	0.2%, pH = 7−12	Perkins et al. (1974)
Illites			
Fithian, Illinois, USA	55	0.1%, <2 μm	Oster et al. (1980)
Silver Hill, Montana, USA	5.5, 6.5, 29, 36, 48, 57.5†	0.05%, <0.2 μm, pH = 5.8, 6, 7.5, 9, 10, 10.6	Hesterberg and Page (1990a, 1990b)
Palygorskites			
Mt. Grainger (Australia)	2.5, 25	0.1%, <2 μm, pH = 6.7; 10.6	Neaman and Singer (1999)
Mt. Flinders (Australia)	0.2, 25	0.1%, <2 μm, pH = 7.3, 10.9	Neaman and Singer (1999)
Yucatan (Mexico)	1, 25	0.1%, <2 μm, pH = 7.1, 10.6	Neaman and Singer (1999)
Florida (USA)	2.5, 25	0.1%, <2 μm, pH = 7.4, 10.6	Neaman and Singer (1999)

*Solid content of the dispersion, size fraction, pH.
†Coagulation with $NaClO_4$.

Table 5.4. C_K of Na^+, Ca^{2+}, and Al^{3+} chloride for Na^+-montmorillonite dispersions (0.025, 0.5, 1.0% w/w solid content) at pH ~6.5 (Na^+, Ca^{2+}) (test-tube tests). Montmorillonite from Wyoming (M 40A) (Penner and Lagaly, 2000)

Exchangeable cation	c_K(mmol/L)		
	0.025%	0.5%	1%
Na^+	5	15	20
Ca^{2+}	0.4	2	3
Al^{3+}	0.08	1	1.5

Table 5.5. C_K of sodium salts for 0.025 and 2% dispersions of Na^+-montmorillonite (Wyoming M 40A) (Penner and Lagaly, 2001)

	c_K(mmol/L)		pH		c_K(mmol/L)		pH
	0.025%	2%			0.025%	2%	
NaCl	5	30	6.5	Na_2HPO_4	1100	80	9
$NaNO_3$	16	12	6.5	NaH_2PO_4	460	40	~5
Na_2SO_4	18	35	6.5	Na_3PO_4	25	35†	11.5
$NaHSO_4$	4	4	~5	$Na_4P_2O_7$	–*	–*	10
				NaOH	20	30*	11.5, 12

*No coagulation up to the solubility limit of ~130 mmol/L.
†0.5% dispersion.

500 mmol/L (Verwey and Overbeek, 1948; Matijević, 1973; Overbeek, 1982; Lagaly et al., 1997). Decades ago, this observation was explained by the interaction of positive edge charges with negative basal surface charges producing T-type contacts and card-house type aggregation (Hofmann, 1961, 1962, 1964; van Olphen, 1977). However, pH $\approx$6.5 is near or, more likely, above the p.z.c. of the edges, i.e. positive edge charges are no longer present or their number is very small.

An additional effect increases the negative field at the edges (Secor and Radke, 1985; Chou Chang and Sposito, 1994, 1996; Sposito and Grasso, 1999): The edge thickness of montmorillonite particles is small relative to the Debye-Hückel length at the critical salt concentration. The negative double layer extending from the basal plane surfaces spills over into the edge region. Even for an edge charge density of $+0.1\,C/m^2$ (which is very high!) and a face charge density of $-0.1\,C/m^2$ (typical of montmorillonite), the influence of the negative face charges is still significant at sodium salt concentrations $\leqslant 10^{-3}$ M (Secor and Radke, 1985). Coagulation therefore occurs between edges (–) and faces (–) (Fig. 5.8). The importance of the edge surface in the coagulation process also follows from the coagulation experiments of Keren and Sparks (1995) with colloidal pyrophyllite particles.

Table 5.6. C_K of NaCl in the presence of phosphates: 1. Na^+-montmorillonite dispersion (Wyoming) and sodium polyphosphates $(NaPO_3)_n$ (Oster et al., 1980); 2. Na^+-beidellite (Unterrupsroth, Germany, fraction 0.1–2 µm, 0.025% dispersion) and sodium diphosphate $Na_4P_2O_7$ (Frey and Lagaly, 1979b)

Phosphate	Phosphate concentration (mmol/L)	c_K mmol/L	pH
	Na^+-montmorillonite		
$(NaPO_3)_n$	0	12	
	0.01	20	
	0.1	80	
	1	120	
	Na^+-beidellite		
$Na_4P_2O_7$	0	6	6
	1.25*	230	6
	5	250	8.3
	10	270	9
	12.5	280	9.3
	25	310	9.7

*Na^+-montmorillonite dispersion at 0.1 mmol/L $Na_4P_2O_7$: c_K = 195 mmol/L NaCl (Permien and Lagaly, 1994c).

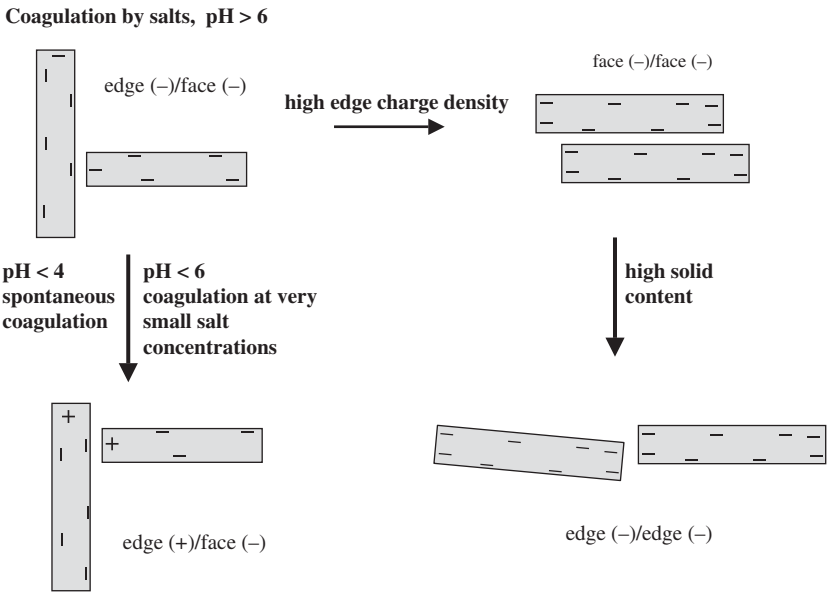

Fig. 5.8. The different modes of coagulation of clay mineral particles. From Lagaly and Ziesmer (2003).

As the negative edge charge density is very small, coagulation requires low sodium salt concentrations. Pierre (1992) calculated the electrostatic repulsion between an edge (–) and a face (–) on the basis of the DLVO theory. Assuming that the value of the charge density at the edges and the faces is identical, this repulsion is distinctly smaller than between faces. Because of the edge(–)/face(–) coagulation in dilute dispersions, the c_K values of Laponite, montmorillonites, beidellites, and illites are very similar (Table 5.3). The increased Stern-layer adsorption at high layer charges reduces the potential of the diffuse layer. As a result, both the electrostatic repulsion and the colloid stability are not distinctly enhanced.

Kaolinites have a surface charge density (see Section 5.1.2) that is comparable to that of montmorillonites (Table 5.1), and hence similar coagulation concentrations are expected.

As explained by the DLVO theory (Verwey and Overbeek, 1948; Overbeek, 1977, 1980, 1982), the critical coagulation concentration of Ca^{2+} (0.4 mmol/L) and Al^{3+} counterions (0.08 mmol/L), is distinctly smaller than that of Na^+ ions. The relationship between the c_K values is

$$c_K(Na^+) \approx 12c_K(Ca^{2+}) \approx 63c_K(Al^{3+})$$

while the DLVO theory predicts:

$$c_K(Me^+) = (4 - 64)c_K(Me^{2+}) = (9 - 729)c_K(Me^{3+})$$

where Me denotes a metal ion. The range of the predicted c_K values is related to different diffuse layer potentials. The smaller value corresponds to potentials $\leqslant 50$ mV, the larger value to $\geqslant 150$ mV. The observed ratios are near the values for lower potentials and indicate the pronounced effect of Stern-layer adsorption of the di- and trivalent cations on clay mineral surfaces (Chan et al., 1984; Goldberg, 1992; Quirk and Marčelja, 1997; Permien and Lagaly, 1994a, 1994b; Sridharan and Satayamurty, 1996). The aggregation of clay mineral layers in the presence of multivalent cations is enhanced by ion-ion correlation forces (Kjellander et al., 1988; Kjellander, 1996).

The strong Stern-layer adsorption is also indicated by the increase in c_K values with solid content (Tables 5.4 and 5.5). When the salts solely regulate the thickness of the diffuse ionic layer, c_K is independent of the solid content of the dispersion. However, c_K increases with solid content when the counterions are adsorbed at the surface, as they are in the Stern layer (Stumm et al., 1970; de Rooy et al., 1980).

The slightly increased coagulation concentration of $NaNO_3$ in comparison with NaCl may be due to the water structure breaking effect of nitrate ions. As a result, the hydration of the cation increases, and its adsorption in the Stern layer decreases. Coagulation then requires a slightly higher salt concentration. This effect was also observed in coagulation experiments with latex dispersions (Zimehl and Lagaly, 1986; Lagaly et al., 1997).

The 'liquefying' property[5] of phosphates is related to two effects. Phosphate anions are strongly adsorbed on oxide surfaces, and also on the edges of the silicate layers. They replace structural OH groups by ligand exchange (Muljadi et al., 1966; Parfitt, 1978; Jasmund and Lagaly, 1993; Lagaly 1993, 2005). By acting as multivalent anions phosphate increases the negative edge charge density, and hence the salt stability. As the electrostatic repulsive force is strongly dependent on the surface potential as long as this value is low (Verwey and Overbeek, 1948; Lagaly, 1986; Lagaly et al., 1997) a weak increase of the edge charge density by phosphate adsorption can strongly increase the repulsive force and the c_K value.

The second effect is the transition of edge(–)/face(–) coagulation into face(–)/face(–) coagulation (Fig. 5.8). When the increased salt concentration required for edge(–)/face(–) coagulation approximates the salt concentration for face(–)/face(–) aggregation, the dispersion coagulates face-to-face because the area between two faces is larger than between an edge and a face. Keren and co-workers (Keren et al., 1988; Heller and Keren, 2001) suggested that face/face aggregation between two layers or particles might be initiated at surface regions with lower than average charge density because of layer charge heterogeneity.

Transition from edge(–)/face(–) to face(–)/face(–) coagulation, in particular at somewhat higher particle concentration, is promoted by the following effect. As discussed by Tateyama et al. (1988), edge(–)/face(–) attraction depends on the angle between the two particles and particle thickness. This potential is very small for delaminated montmorillonite because the layers are only 1 nm thick. Attraction becomes strong enough only for an almost perpendicular orientation of the two particles. Such contacts are only formed at low particle concentrations. At higher concentrations, the strong repulsion between the faces disrupts the edge/face contacts more easily and the attraction must be enhanced to reach the face/face coagulation condition.

A striking effect is the pronounced decrease in the critical coagulation concentration of sodium hydrogen phosphates at higher montmorillonite contents (Table 5.5). In dispersions with high clay mineral contents and a high negative edge charge density of the particles, the strong repulsion between the faces forces the particles into adopting a certain parallel orientation (Section 5.6.1), promoting edge(–)/edge(–) coagulation (Fig. 5.8) (Pierre, 1992, 1996). This is less likely to occur in dilute dispersions. Coagulation is then initiated when the interaction between the edges(–) becomes attractive. This process may include a certain overlapping of silicate layers forming band-type fragments. This type of coagulation requires lower concentrations than those initiated by face(–)/face (–) coagulation.

[5]Liquefaction describes the decrease in the viscosity of dispersions by certain agents, e.g., of kaolin dispersions by phosphate addition (Lagaly, 1989; Manfredini et al., 1990; Penner and Lagaly, 2001), which is very important for ceramic masses and paper coating. Phosphates also decrease the viscosity of bentonite dispersions although an increase in viscosity was observed under certain conditions (Penner and Lagaly, 2001).

In comparison with sodium hydrogen phosphates (Na_2HPO_4, NaH_2PO_4) and sodium diphosphate ($Na_4P_2O_7$), sodium phosphate (Na_3PO_4) shows a very weak liquefying effect. The critical Na^+ concentration is $3 \times 25 = 75$ meq Na^+/L and therefore higher than for NaCl, $NaNO_3$, and NaOH, but distinctly lower than for sodium hydrogen phosphates. This is because the high pH (11.5) reduces the adsorption of phosphate by ligand exchange (Muljadi et al., 1966; Parfitt, 1978). Model calculations for the homologous anion arsenate showed a distinct adsorption maximum at pH ~7 (Manning and Goldberg, 1996). The increase in negative edge charge density as a result of the high pH and modest adsorption of phosphate raises the c_K value for edge(–)/face(–) coagulation but the increase is not sufficiently high to initiate face(–)/face(–) coagulation.

A modest liquefying effect is also observed with sulphate anions. The critical Na^+ concentration is 36 mmol Na^+/L for Na_2SO_4 which is somewhat higher than for sodium chloride and sodium nitrate. Wendelbo and Rosenqvist (1987) suggested that sulphate in soils from rain or industrial effluents could promote the dispersion of clays in soils.

5.4.2. Coagulation of Mixed Clay Mineral Dispersions

An interesting question concerns the coagulation of dispersions containing two different clay minerals. Goldberg and Glaubig (1987) measured the critical coagulation concentration of NaCl for mixtures of Na^+-montmorillonite and Na^+-kaolinite, and of $CaCl_2$ for mixtures of the corresponding Ca^{2+}-clay minerals (Table 5.7a). The addition of only 25% (w/w) montmorillonite to the kaolinite dispersion caused the c_K value of the mixed dispersion to approach that of the pure montmorillonite dispersion. The flocs contained both clay minerals with the kaolinite particles probably being incorporated into the montmorillonite particles (cf. footnote 1). These particles were coagulated when the salt concentration approximated the critical coagulation concentration for the montmorillonite dispersion. The stronger coagulation power of calcium cations impeded this effect. Thus, even small amounts of montmorillonite can deflocculate kaolinite dispersions at low salt concentrations. This effect was long known (Schofield and Samson, 1954) and explained by the attachment of the thinner and smaller montmorillonite layers to the positive edges of the large kaolinite particles.

Mixing palygorskite needles with montmorillonite presents an example of coagulation of dispersions containing particles with different shapes. Dispersions of palygorskite at neutral pH were coagulated by very low concentrations of NaCl (0.2 and 2.5 mmol/L) depending on the origin of the samples (Table 5.7b). The c_K values of the four samples increased strongly with pH and reached 25 mmol/L at pH 10–11(Neaman and Singer, 1999).

Because of the low rate of isomorphous substitution in palygorskite, the negative surface charge density is small and the dispersions are sensitive to salt addition. The pronounced anisometric shape of the particles may also contribute to the low critical

Table 5.7a. C_K of mixed dispersions of Na^+-montmorillonite and Na^+-kaolinite (Goldberg and Glaubig, 1987)

% (w/w) montmorillonite	c_K(mmol/L NaCl)	pH
0	<0.2	5.8
10	2.3	5.7
25	11.4	5.9
50	13.2	6.2
100	14.0	6.4

Table 5.7b. C_K of mixed dispersions of montmorillonite and palygorskite at neutral pH. Palygorskite: *A* Mount Flinders (Australia), *B* Yucatan (Mexico), *C* Florida (USA), *D* Mount Grainger (Australia) (Neaman and Singer, 1999)

% (w/w) montmorillonite	c_K (mmol/L NaCl)			
	A	B	C	D
0	0.2	1.0	2.5	2.5
10	1.0	2.5	5.0	5.0
20	2.5	5.0	5.0	5.0
40	5.0	7.5	7.5	13.3
50	5.0	13.3	9.2	13.3
60	13.3	13.3	13.3	13.3
100	13.3	13.3	13.3	13.3

coagulation concentration. The variation in c_K values for different samples is likely to relate to different charge densities. The stronger increase of c_K with pH in comparison with montmorillonite is a consequence of the different surface structure.

In combination with montmorillonite, the c_K values show the same trend as for kaolinite/montmorillonite dispersions, i.e. they approach the values for the montmorillonite dispersion. The higher repulsion between montmorillonite particles probably impedes aggregation of the palygorskite needles.

A particular case is the coagulation of dispersions containing two smectites. When a dispersion of delaminated low- and high-charge smectites is coagulated by the addition of sodium chloride, the particles can aggregate in different ways (Fig. 5.9). When selective coagulation occurs, one type of particles is formed first, and hence the coagulate consists of a mixture of particles that contain the same layers as the starting particles (but may differ in size). When low- and high-charge layers aggregate within individual particles, mixed-layer particles grow with random, regular, or zonal (segregation) layer sequences. The problem is to analyse the coagulate and find which type of aggregation is predominant. The analysis is further complicated as the charge density within the individual particles of the parent smectites varies to some

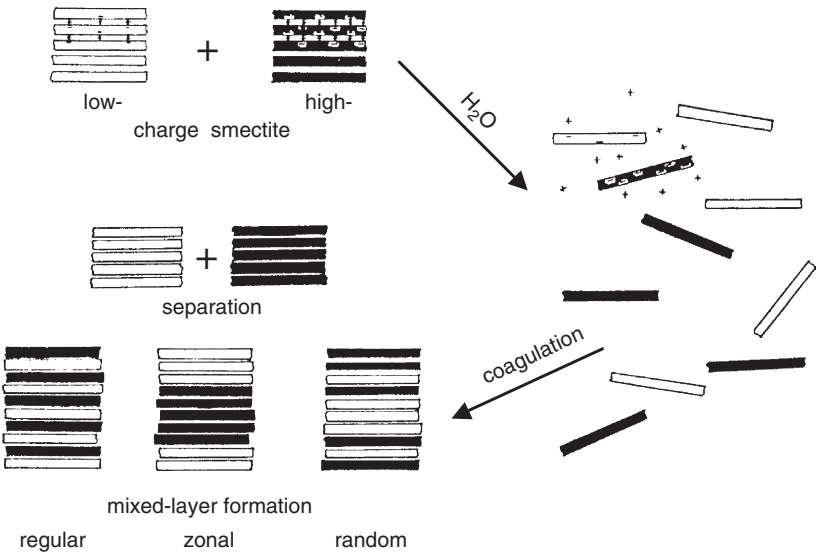

Fig. 5.9. Disarticulation of two Na^+-smectites in water; formation of a mixed colloidal dispersion and re-aggregation by coagulation (surface charges and interlayer cations not entirely shown). From Frey and Lagaly (1979b).

extent (charge heterogeneity). Only the alkylammonium method allows a clear distinction to be made between selective coagulation and random or regular mixed-layer formation (Frey and Lagaly, 1979a, 1979b; Lagaly, 1981, 1994).

Two differently charged smectites were used: a montmorillonite (Upton, Wyoming) with a mean surface charge density σ_0 of 0.096 C/m^2 (mean interlayer cation density $\bar{\xi} = 0.192$ C/m^2), and a beidellite (Unterrupsroth, Germany) with σ_0 of 0.13 C/m^2 ($\bar{\xi} = 0.26$ C/m^2). The cation density in the interlayer space of the montmorillonite varied from 0.17 to 0.25 C/m^2 and of the beidellite from 0.20 to 0.35 C/m^2 (Fig. 5.10).

The homoionic Na^+-smectites were dispersed in 0.01 M sodium diphosphate solution at pH > 7 to give dispersions with a mass content of 250 mg/L. Equal volumes of these colloidal dispersions were mixed and coagulated under different experimental conditions. Aggregation type was determined by particle size. Larger particles (0.1–2 μm fraction) were selectively coagulated. Two different experimental conditions were used to separate beidellite from montmorillonite: (i) slow coagulation by adding NaCl solution gradually to raise the Na^+ concentration to 0.28 M at pH 9. The coagulate consisted mostly of beidellite-like particles while the remaining dispersion contained montmorillonite; (ii) rapid coagulation by fast addition of NaCl to give a final concentration of 0.5 M NaCl. The coagulate contained a mixture of low- and high-charge particles. As discussed in Section 5.4.1, the beidellite coagulated at a lower salt concentration. The particles composed of low- or

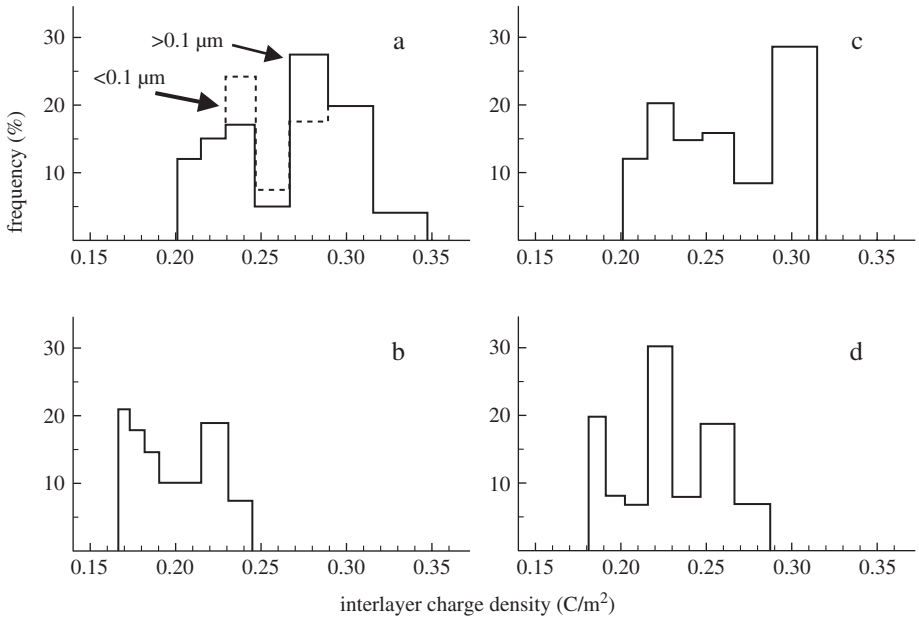

Fig. 5.10. Formation of mixed-layer particles by coagulation of dispersions containing two smectites. (a) Pure beidellite (Unterrupsroth, Germany; particle size fraction $<0.1\,\mu m$ and $0.1–2\,\mu m$). (b) Pure montmorillonite (Wyoming, USA; particle size fraction $<2\,\mu m$). (c) Coagulated material from the mixed colloidal dispersion, particle size fraction $0.1–2\,\mu m$. (d) Coagulated material from the mixed colloidal dispersion, particle size fraction $<0.1\,\mu m$. From Frey and G. Lagaly (1979b).

high- charge layers were not identical with the particles of the starting materials. The charge distribution curve of the high-charge particles (Fig. 5.10c) was substantially different from that of the starting beidellite particles (Fig. 5.10a).

When the particles were smaller than $0.1\,\mu m$, the coagulate consisted of mixed-layer particles. The charge distribution curve (Fig. 5.10d) clearly showed a succession of low- and high-charge layers within the same particle. The layer sequence was not completely random; swelling tests revealed a certain amount of segregated layers (Frey and Lagaly, 1979a).

The delamination and re-aggregation of I/S mixed-layer particles were thoroughly investigated by Nadeau (1985) and Środoń et al. (2000). At conditions of delamination, only the smectitic interlayer spaces show extensive expansion; the particles break into 'fundamental particles' consisting of one, two, or a few illitic layers (Fig. 5.7, see Section 5.3.3). The physical dimensions of the fundamental particles were determined by TEM. Once the clay minerals had been fully disarticulated, mixed colloidal dispersions could be prepared. Re-aggregation produced I/S mixed-layer particles that were substantially different from the starting materials. Aggregation

may be performed not only by coagulation but also by simple air-, spray-, or freeze-drying. Some possible applications are directed to the design of special heterogeneous catalysts and the preparation of very thin films and coatings (Nadeau, 1987; Lagaly, 1987a).

5.4.3. *Influence of Alcohols*

Addition of methanol, ethanol and propanol decreased the critical coagulation concentration of 0.025% Na^+-montmorillonite dispersion from 8 to 3.6 mmol/L NaCl (with 70% v/v methanol), to 1.2 mmol/L NaCl (with 70% v/v ethanol), and to 0.8 mmol/L NaCl (with 60% v/v propanol) (Permien and Lagaly, 1994c). This effect was even more pronounced in the presence of 0.1 mmol/L sodium diphosphate. The c_K value then decreased from 195 to 7.5 mmol/L NaCl (with 70% methanol), to 2.5 mmol/L NaCl (with 70% ethanol), and to 5 mmol/L NaCl (with 60% propanol).

The adsorption of counterions at the particle surface generally increases when organic solvents are added to the aqueous dispersion. Several examples were reported by de Rooy et al. (1980). Similarly, the c_K of NaCl for Na^+-montmorillonite dispersions decreases after addition of methanol, ethanol, and propanol. The effect is very strong for the phosphate-stabilised dispersions where c_K is reduced from 195 mmol/L NaCl to $\leqslant$7.5 mmol/L NaCl.

5.4.4. *Influence of Surface Active Agents on Salt Coagulation*

It was surprising that small amounts ($<$1 mmol/L) of hexadecylpyridinium chloride (cetylpyridinium chloride, CPC) raised the critical coagulation concentration of NaCl from 8 to 16 mmol/L (Table 5.8). At higher CPC concentrations, the dispersion was coagulated by the surfactant itself. The addition of sodium dodecylsulphate (SDS) increased the c_K value of NaCl even more strongly. In the presence of 100 mmol/L SDS, a salt concentration of 136 mmol/L was required to coagulate the 0.025% dispersion (Permien and Lagaly, 1995).

Adsorption of hexadecyl pyridinium ions presumably modifies the distribution of the Na^+ ions between the Stern layer and the diffuse ionic layer. The hydrophobic chains near the surface also influence the water structure in a certain region (Lagaly et al., 1983), pushing the Na^+ ions away from the surface. The resulting weak increase in the Stern potential enhances c_K from 8 to 16 mmol/L.

The stabilising effect of dodecylsulphate anions is stronger. At pH ~6.5 a few surfactant anions can adsorb at sporadically occurring positive edge sites. These anions can then act as nuclei around which additional surfactant molecules can cluster (Rupprecht and Gu, 1991). As a result, the negative edge charge density and the salt stability increase. It would be interesting to determine the salt stability as a function of sodium dodecylsulphate adsorbed. However, the adsorption of small amounts of anionic surfactants at pH $>$ 4 is difficult to measure because of the pronounced volume exclusion effect for anions (Chan et al., 1984; Chou Chang and Sposito, 1996).

Table 5.8. C_K of NaCl for 0.025% dispersions of Na^+-montmorillonite (Wyoming, M 40) at pH ~6.5 in the presence of cetyl pyridinium chloride (CPC) and sodium dodecylsulphate (SDS) (Permien and Lagaly, 1995)

Surfactant concentration mmol/L	c_K(mmol/L)	
	CPC	SDS
0	8	8
5×10^{-4}	9.5	
10^{-3}	9	10
10^{-2}	7	10
2×10^{-2}	11	
10^{-1}	13	10
2×10^{-1}	16	
1	*	12
10	*	81
100	*	136

*Coagulation by CPC itself.

5.4.5. Stabilisation by Betaines

Betaines as surface-modifying agents

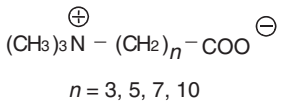

$n = 3, 5, 7, 10$

were synthesised to prepare organic derivatives that delaminate when dispersed in water. The quaternary ammonium groups replace the interlayer cations, whereas the negative charges at the opposite end and their compensating cations initiate the separation of the silicate layers: Colloidal dispersions of single silicate layers with attached betaines are formed (Schmidt and Lagaly, 1999). In contrast to the dispersions of Li^+- and Na^+-montmorillonite with yield values of ~400 mPa the betaine-montmorillonite dispersion showed Newtonian flow, and the viscosity of the dispersion (solid content 1.5% w/w, pH 7) approximated the viscosity of water.

LiCl coagulated the dispersion of Li^+- and betaine-montmorillonite ($n = 3$) at a concentration of 8 mmol/L. The c_K value increased with n to a maximum of 60 mmol/L LiCl at $n = 7$, then decreased slightly at $n = 10$ (Table 5.9). The strong influence of small amounts of diphosphate was again noted: A maximum c_K value of 1320 mmol/L LiCl was reached for $n = 7$.

Surface modification with betaines reduced the stability of the montmorillonite dispersions in water-alcohol solutions. Whereas the colloidal dispersions of Li^+- and

Table 5.9. Critical LiCl concentration for the coagulation of 0.05% dispersions of Li^+- and betaine-montmorillonite (Wyoming M 40) in water and in the presence of 0.1 mmol/L $Na_4P_2O_7$ Schmidt and Lagaly (1999)

Cation	c_K(mmol/L)	
	in water	with phosphate
Li^+	8	570
Betaine		
$n = 3$	8	505
$n = 5$	17	835
$n = 7$	60	1320
$n = 10$	50	1180

betaine-montmorillonite (in the absence of any salt) were stable up to a methanol molar fraction $\chi = 0.7$, dispersions of the long-chain derivatives ($n = 7$, 10) coagulated at $\chi = 0.1$, i.e. were only stable in water. In water/propanol mixtures, Li^+ and betaine montmorillonite ($n = 3$) as well as betaine-montmorillonite ($n = 10$) were stable up to a molar fraction of propanol $\chi = 0.3$, and the samples with $n = 5$, 7 up to $\chi = 0.5$ and 0.4.

Adsorbed betaines show a pronounced stabilisation effect when the negative edge charge density is sufficiently increased by phosphate adsorption (Table 5.9). As the number of betaine molecules corresponds to the CEC (Schmidt and Lagaly, 1999), the total number of negative betaine end groups is identical with the number of layer charges (Fig. 5.11), and the enhanced stability cannot arise from an increased charge density. Nor is it very probable that steric stabilisation occurs because the chains are too short to make this mechanism effective. As the negative charges are shifted away from the particle surface, the electrostatic interaction occurs over a smaller distance than the van der Waals interaction. This would increase salt stability. However, the decisive effect seems to be the formation of lyospheres composed of betaine and water molecules around the particles (Fig. 5.11a) (Ottewill and Walker, 1968). As the lyospheres incorporate large amounts of water, the Hamaker constant of the envelope approximates the value for of the dispersion medium (water), and the van der Waals interaction weakens (Verwey and Overbeek, 1948; Vincent, 1973). The dominance of the electrostatic repulsion then increases the salt stability. For the short chain betaine ($n = 3$), the lyospheres (if ever formed) are too thin to reduce the van der Waals interaction.

In the absence of phosphate a few betaine molecules can bridge between the surface charges and the sporadically occurring positive edge charges (Fig. 5.11b). Since betaines with $n < 7$ are too short to form bridges, the above-mentioned shift of the charges may slightly enhance salt stability.

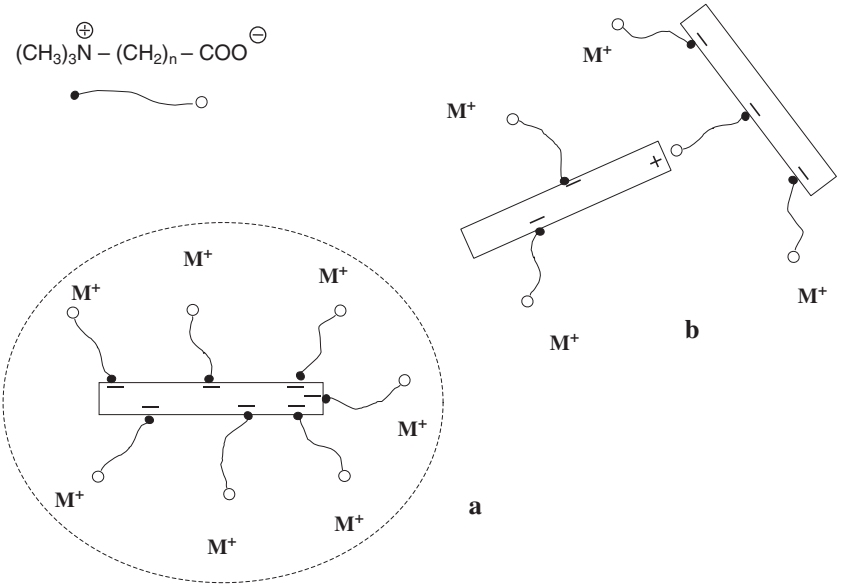

Fig. 5.11. Stabilisation by adsorbed betaine molecules. (a) Lyospheres composed of water and betaine molecules surround the particles. (b) Betaine molecules bridge between surface charges and positive edge charges of neighbouring particles. From Lagaly and Ziesmer (2003).

Replacement of water by organic solvents in the lyospheres can increase the van der Waals attraction, and hence reduce the stability of the (salt-free) dispersions (Machula et al., 1993; Király et al., 1996b). However, the Hamaker constants for water and the alcohols are not very different (water 3.7×10^{-20} J, ethanol 4.2×10^{-20} J) (Israelachvili, 1994), and this effect will only be weak. Thus, the decisive effect of alcohol addition is the compression of the diffuse double layer (de Rooy et al., 1980) causing the betaine-montmorillonite complex to coagulate at a critical alcohol concentration.

5.4.6. Coagulation by Organic Cations

Tetramethylammonium chloride coagulated a Na^+-montmorillonite (Wyoming) dispersion at the same concentration (5 mmol/L) as NaCl (Penner and Lagaly, 2000). Monovalent long-chain cations such as

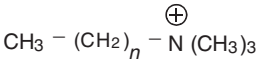

trimethyl alkylammonium ions

trimethyl alkylammonium ions coagulated at very low concentrations, $c_K \leqslant 0.3$ mmol/L (Table 5.10). Restabilisation was observed when larger amounts of surface-active agents (above the CEC) were added.

Very small coagulation concentrations were also observed with large organic cations such as monovalent crystal violet (0.1 mmol/L), divalent methyl green (0.2 mmol/L), and trivalent TTP, tris(trimethylammonium phenyl) methane chloride, (0.05 mmol/L). Dispersions coagulated by crystal violet were restabilised by addition of CV in amounts > 1.5 mmol/g montmorillonite.

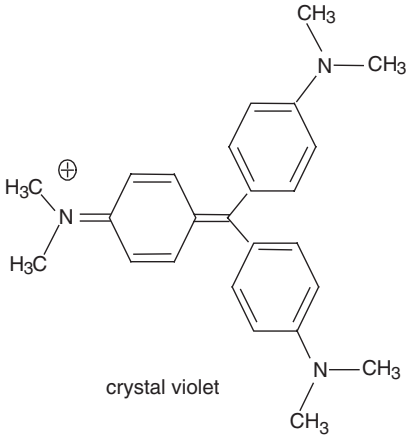

crystal violet

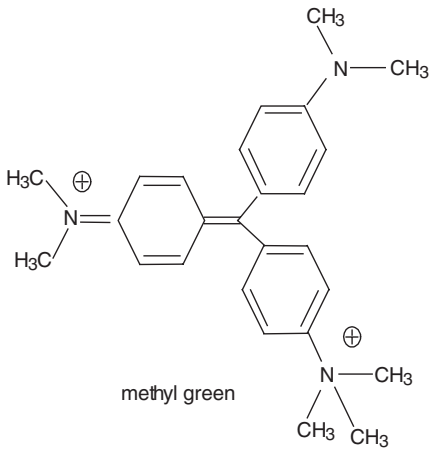

methyl green

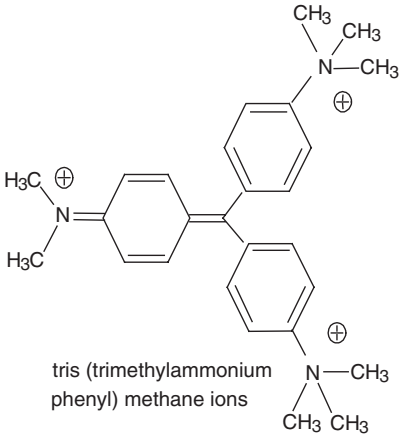

tris (trimethylammonium phenyl) methane ions

Divalent paraquat and diquat cations were also strongly coagulating with c_K values of ~0.1 mmol/L. The divalent long-chain hexyl- and dodecyl-bispyridinium cations showed coagulation concentrations similar to trimethyl alkylammonium (Table 5.10). The valence of the organic cations was not as dominant as for inorganic cations. In all cases the c_K value increased with the montmorillonite content of the dispersion.

Table 5.10. Coagulation of Na^+-montmorillonite dispersions by organic cations. C_K of the 0.025% dispersions by test-tube tests, of the 0.5% (w/w) dispersions from rheological measurements, pH ~6.5. Montmorillonite from Wyoming (Penner and Lagaly, 2000)

Cation	Valency	c_K(mmol/L)	
		0.025%	0.5%
Tetramethylammonium	1	5	5.8
Hexyl trimethylammonium	1	0.3	2
Dodecyl trimethylammonium	1	0.15	0.76
Hexadecyl trimethylammonium	1	0.09	0.35
Methyl bispyridinium	2	0.2	0.85
Hexyl bispyridinium	2	0.2	0.62
Dodecyl bispyridinium	2	0.1	0.18
Crystal violet	1	0.1	0.9
Methyl green	2	0.2	0.9
Tris(trimethylammonium phenyl)methane	3	0.05	0.09
Paraquat	2	0.08	0.4
Diquat	2	0.1	0.45

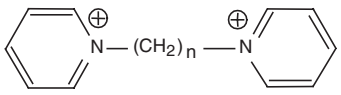

alkyl bispyridinium ions

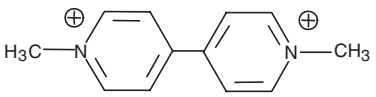

paraquat

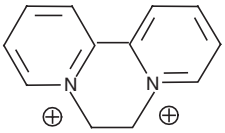

diquat

The reduced salt stability and the dependence of c_K on the solid content as a consequence of the specific adsorption of the counterions (as defined by Lyklema (1984, 1989)) is very pronounced for large organic cations. The c_K of long chain cations generally decreases with chain length (Table 5.10). The adsorption of organic cations can obscure the influence of counterion valence. As evident from Table 5.10, increasing valence does not reduce c_K as it does with inorganic counterions. The adsorption of organic cations is not only regulated by electrostatic forces but is enhanced by van der Waals interactions between the organic cations and the surface.

In addition, the influence of the cations on surface properties, notably the increase in hydrophobicity with increasing chain length (Lagaly et al., 1983) has to be considered. The disturbance of the water structure enhances the adsorption of counterions and decreases the Stern potential and the electrostatic repulsion.

In a case of strong counterion adsorption, the amount of salt at the point of coagulation can approximate the total amount of adsorption sites on the particles ('equivalent coagulation' (de Rooy et al., 1980)). Because of particle formation in montmorillonite dispersions the amount of organic cations is similar in magnitude to the amount of surface charges but not identical with it (Penner and Lagaly, 2000).

It is difficult to explain the smaller c_K of the monovalent crystal violet (CV) compared with the divalent methyl green (MG). A reason may be the different orientation of the cations on the surface. The plane of the CV cations is inclined to the silicate layer, whereas that of the MG cations is parallel to the montmorillonite surface (Rytwo et al., 1995). The van der Waals contact is probably enhanced between the inclined CV cations of two adjacent montmorillonite layers, promoting coagulation. The higher yield value of CV-containing montmorillonite dispersions compared with the corresponding dispersions with MG was explained in a similar way (Penner and Lagaly, 2000).

5.4.7. Coagulation by Acids

Acids like HCl, HNO_3, H_2SO_4, and H_3PO_4 coagulated a 0.025% Na^+-montmorillonite (Wyoming) dispersion (pH ~2) at concentrations similar to the corresponding salts: $c_K(HCl,\ HNO_3) = 5.5$ mmol/L, $c_K(H_2SO_4) = 12.5$ mmol/L, and $c_K(H_3PO_4) = 32$ mmol/L.

In acidic medium (pH < 5) the edges of clay mineral particles are positively charged, promoting coagulation by edge(+)/face(–) contacts and formation of house-of-card aggregates (Fig. 5.8). Because of this heterocoagulation process acidic dispersions are very sensitive to salts. Indeed, Na^+-montmorillonite dispersions coagulate spontaneously at pH < 3.5. The c_K value of NaCl increased from about 1 mmol/L at pH ~3.5 to a plateau of ~2 mmol/L; with the transition into edge(–)/face(–) coagulation at pH ⩾ 6 this value increased to 10 mmol/L (Swartzen-Allen and Matijević, 1976). The pH-dependent colloidal stability was explained on the basis of an ionisation model and the DLVO theory (Tombácz et al., 1990).

Acids, such as HCl and HNO_3, coagulate at 5.5 mmol/L. The concentration for coagulation apparently corresponds to the proton concentration (solution pH ~2.3) at which the positive edge charge density is high enough to initiate edge(+)/face(−) coagulation. In the presence of sulphuric and phosphoric acids the stabilising effect is also evident. When these acids or their anions (e.g., $H_2PO_4^-$, HPO_4^{2-}) are adsorbed at the edges, higher proton concentrations are required to recharge the edges. Therefore, the critical proton concentration increases from 5.5 meq/L for HCl and HNO_3 to 25 meq/L for H_2SO_4 and 32 meq/L for H_3PO_4 (which dissociates only one proton in weakly acidic medium; pK_a values: 2.1; 7.2; 12.7).

The reaction with acids not only consists of protonating the edges. Protons also replace interlayer cations, and initiate a slow decomposition of the silicate layers by liberating octahedral cations (Jasmund and Lagaly, 1993; Janek et al., 1997; Janek and Lagaly, 2001). Since this process is much slower than edge protonation, the reported c_K values of acids may be in the right order of magnitude.

5.4.8. *Influence of Poly(hydroxo metal) Cations*

Trivalent cations are highly effective coagulating agents as expressed by the Hardy–Schulze rule (Section 5.4.1). Several trivalent cations (Al^{3+}, Fe^{3+}, but not La^{3+}) can also induce the dissociation of water molecules in their hydration shell to produce protons (hydronium ions):

$$[Al(H_2O)_6]^{3+} + H_2O \rightarrow [Al(OH)(H_2O)_5]^{2+} + H_3O^+$$

Thus, an aluminium salt solution ($pK_a = 4.8$) is as acidic as a solution of acetic acid ($pK_a = 4.75$). Solutions of iron salts are even more acidic ($pK_a = 2.2$). A pH shift must therefore be considered when these salts are added to dispersions. In relation to their coagulating power the consecutive reactions are more important. The hexaquo aluminium ions are only present at $pH \leqslant 3$. The formation of the hydroxopentaquo complex at higher pH initiates polycondensation and formation of high- charge polynuclear cations (poly(hydroxo aluminium) cations) (Bottero et al., 1980, 1987; Bertram et al., 1985). One of these is the Keggin cation $[Al_{13}O_4(OH)_{24}(H_2O)_{12}]^{7+}$ which plays an important role in the preparation of Al-pillared clay minerals (see Chapter 7.5). Basic aluminium salt solutions ('aluminum chlorohydrate') are widely used in the production of anti-transpirants. They contain chain-like poly(hydroxo aluminium) cations with a low degree of crosslinking, and probably form sheet-like aggregates.

The polycondensation of the hydrated iron ions starts at $pH < 3.5$ (Dousma and de Bruyn, 1976; Khoe and Robins, 1989). In contrast to the chain-like poly(hydroxo aluminium) ions the polynuclear iron species form more complex, sphere-like macro-ions (Bottero et al., 1991; Tchoubar et al., 1991; Hagen, 1992).

The formation of colloidal particles during ageing, even in very acidic solutions, is characteristic of poly(hydroxo metal) complexes and other hydrated multivalent cations, such as Cr^{3+} and Ti^{4+}. For example, hematite (α-Fe_2O_3) and akaganeite (β-FeO(OH)) form at pH ~1. Diaspore (γ-Al_2O_3) forms at pH 2–2.5 (Matijević, 1977). The crystal modification is not only determined by concentration, pH, and temperature but also by the type of anions present.

The potential for interaction between colloidal particles in the presence of polycations is controlled by a number of factors in a very subtle way (Matijević, 1981). As a function of pH and aluminium concentration the phase diagrams reveal fields of destabilisation and restabilisation. On oxidic surfaces poly(hydroxo metal) cations are more strongly adsorbed than monomeric hexaaquo complexes (Matijević, 1977).

Re-charging of negative colloidal particles by multivalent cations was explained by Matijević (1973) on the basis of the adsorption of poly(hydroxo metal) cations. Charge reversal of montmorillonite particles by such Al^{3+} complexes was reported (Penner and Lagaly, 2000). Kaolinite particles were also re-charged by adsorption of Co^{2+}, Cd^{2+}, and Cu^{2+} (Hunter and James, 1992).

An anomalous stability of aqueous boehmite (γ-AlO(OH)) dispersions at high electrolyte concentrations (!) was reported by several authors (van Bruggen et al., 1999 and references therein). This might be because the polymeric cations shift the (apparent) plane of surface charges away from the bare particle surface into the solution. The electrostatic repulsion then operates over a shorter distance between two particles than the van der Waals attraction. When pH is too low, smaller oligomers or even Al^{3+} cations are formed that are not large enough to overcome the van der Waals attraction. When the pH is too high, polycondensation of the hydroxo complexes leads to the formation of individual colloidal particles without providing any stabilisation. Only at a certain range of pH values is the shift of the apparent plane of positive charges large enough for repulsion to overcome the van der Waals attraction.

Frenkel and Shainberg (1980) reported a certain re-stabilisation of montmorillonite dispersions by poly(hydroxo metal) cations, the iron cations being stronger than the aluminium cations. Evidently, the poly(hydroxo metal) complexes of different metal cations can influence dispersion stability in different ways. Polymer morphology is certainly an important factor (Oades, 1984).

5.4.9. Clay Mineral-Oxide Interactions

The interaction between clay minerals and colloidal (hydr)oxides[6] is very important in soil science. Goldberg and Glaubig (1987) observed a reduction of the c_K values of NaCl and $CaCl_2$ for dispersions of Na^+-montmorillonite and sodium kaolinite in the presence of 2 and 10% amorphous aluminium and iron (hydr)oxides.

The colloidal behaviour of clay-oxide dispersions is much more complicated than it appears at first sight. Dispersed oxides usually show a p.z.c. at a particular pH. Below this value the particles are positively charged while above this pH they are negatively charged. The colloid stability of oxide dispersions therefore decreases with increasing pH to a minimum (spontaneous coagulation), then increases again (Fig. 5.12). Below the p.z.c. anions are the counterions, and c_K is strongly dependent on the valence of the anions. At pH above the p.z.c., the valence of the cations determines the critical coagulation concentration. We should stress that the p.z.c of oxides not only depends on the chemical composition but also on the crystal structure and modification and the way the particles were prepared and aged. Also, adsorption of solutes, especially anions, can strongly influence the position of the

[6](Hydr)oxide is used as a general term for hydroxides like $Al(OH)_3$, oxyhydroxides such as FeO(OH), and oxides. Most amorphous samples are oxyhydroxides.

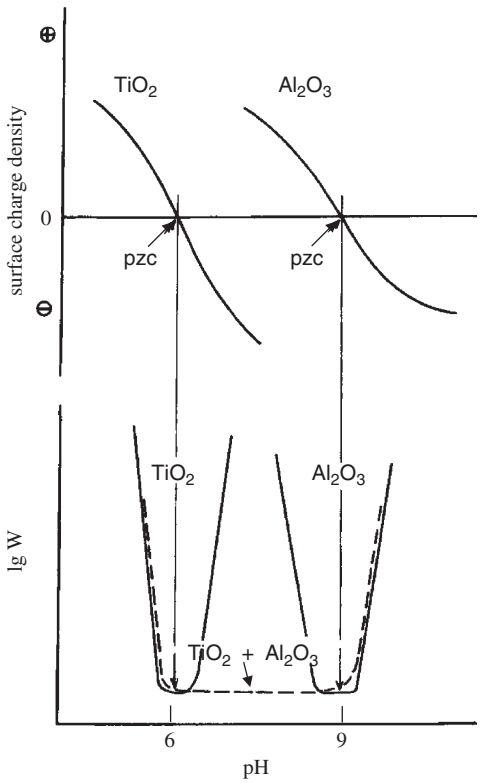

Fig. 5.12. Heterocoagulation between two oxides, e.g. TiO_2 and Al_2O_3. Surface charge density σ of the oxides and stability factor W as a function of pH. The mixture of both oxides should coagulate spontaneously between pH = 6 and pH = 9 (- - - -). Adapted from Healy et al. (1973). From Lagaly et al. (1997).

p.z.c. It is essential in coagulation studies to determine the p.z.c. This is mostly done by measuring the electrokinetic mobility as a function of salt concentration and pH (Lyklema, 1984, 1995).

Assuming a p.z.c. of about 6 of the oxide, heterocoagulation can occur between the positively charged oxide particles and clay mineral particles at pH < 6. When aluminium and iron (hydr)oxides were precipitated in the presence of kaolinite alternating stabilisation and re-stabilisation domains were observed as a function of pH (Arias et al., 1995). The coagulation process and the type of coagulate depend on the mass ratio between the oxide and the clay mineral. A certain amount of the heterocoagulate may be formed spontaneously, but salt addition is needed to coagulate the remaining part of dispersed particles.

At the p.z.c. of the (hydr)oxide, selective coagulation of the (hydr)oxide particles may be observed. Above the p.z.c. the oxide particles and the edges and faces of clay

minerals are negatively charged. If the c_K values of the pure components (oxide and clay mineral) are distinctly different, selective coagulation may occur; if not, the critical coagulation concentration will be intermediate between the c_K values of the components. It is therefore imperative to observe very carefully the coagulation process.

Several additional effects have to be considered in clay-oxide interactions:

(i) since the solubility of the (hydr)oxides is pH-dependent, multivalent cations released into the solution not only act as coagulating species but also adsorb on the surface of clay mineral particles, changing the surface charge density;

(ii) in mixed oxide dispersions the more soluble oxide can cover the other particles forming core shell particles. This behaviour is well known for alumina (p.z.c. ~8.8) and titania (p.z.c. ~6) particles (Healy et al., 1973). When dispersions of Al_2O_3 and TiO_2 were mixed and immediately coagulated, the dispersion became unstable between the p.z.c. values of the components (broken line in Fig. 5.12). When the mixed dispersions were coagulated a few hours later, all particles of the mixed dispersion behaved like alumina particles because of the formation of alumina shells around the TiO_2 particles. In a similar way, the surface structure of clay minerals could be changed by the deposition of aluminium (hydr)oxide species;

(iii) an important factor is the relative size of the different particles. The smaller particles can be coagulated or attached to the surface of the larger particles and change the colloidal behaviour of the larger particles (see also Section 5.4.2). McAtee and Wells (1967) observed the adsorption of gibbsite particles on the edges of kaolinite and the basal surfaces of montmorillonite particles by TEM. Evidently, the gibbsite particles re-charged the montmorillonite particles. Similar observations were reported for iron (hydr)oxides and kaolinite. The influence of surface charge, however, was strongly dependent on the type of hydroxide (Greenland, 1975). Bridging of iron (hydr)oxide aggregates by montmorillonite particles was described by Ferreiro et al. (1995);

(iv) if (hydr)oxides are precipitated in the presence of colloidal particles, complexes between metal ions and OH^- can be formed at the surface of the particles under conditions that did not cause metal hydroxide precipitation in homogeneous solutions (surface precipitation). In dispersions of clay minerals and (hydr)oxides dissolution and surface precipitation can therefore strongly change the surface structure of the clay mineral particles;

(v) an interesting effect is the interaction between particles having surfaces with distinctly different charge densities but of the same sign. In this case the repulsion can change into attraction (Lagaly et al., 1972, 1997; Usui, 1973; Gregory, 1975; McCormack et al., 1995). This effect promotes the mixing of differently charged particles during re-aggregation (Sections 5.4.2 and 5.4.10).

(vi) the properties of a clay-oxide dispersion can be strongly influenced by the way the particles were brought into contact (Yong and Ohtsubo, 1987). Due to edge(+)/face(–) contacts, a 9% Na^+-kaolinite dispersion showed a high value

of yield stress at pH ~3 (Fig. 5.13). When ferrihydrite was added at pH 3, the hydroxide was preferentially adsorbed on the faces of the kaolinite particles and re-charged them (edge(+)/face(+)) so that the yield stress disappeared. With increasing pH, the edges of the kaolinite particles became negative, and edge(−)/face(+) contacts formed a network of particles with a broad maximum of yield stress at pH ~7. The initial re-charging of the ferrihydrite reduced the positive face charge density, causing the network to disintegrate, and the yield stress to approach zero at pH ~10. If the ferrihydrite was added at pH 9.5, all particles were negatively charged, and a yield value was not observed. Decreasing pH increased the positive charge of the ferrihydrite, which then bridged the negative kaolinite particles, and the yield value increased to a sharp and high maximum. The very high positive charge density of the hydroxide at still lower pH promoted adsorption of ferrihydrite on the basal plane surfaces of the kaolinite particles, and the kaolinite(−)/ferrihydrite(+)/kaolinite(−) network collapsed, as indicated by the strong decrease in yield value;

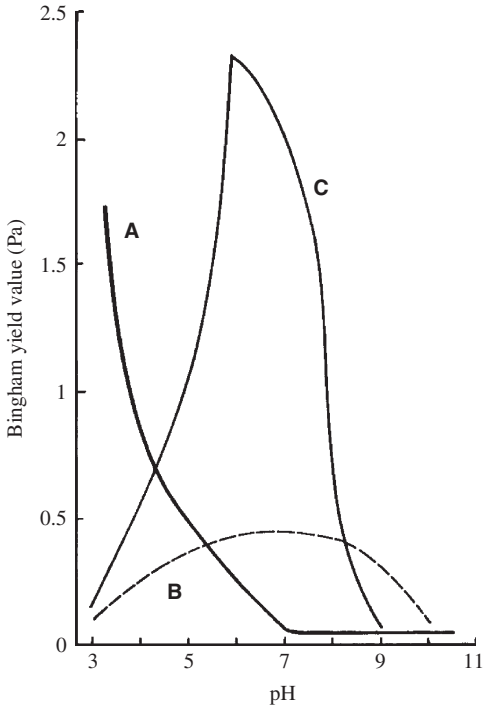

Fig. 5.13. Bingham yield value of a 9% (w/w) Na^+-kaolinite (Georgia) dispersion (A), yield value when a synthetic ferrihydrite (1 g ferrihydrite per 19 g kaolinite) was added at pH = 3 (B) or at pH = 9.5 (C). Adapted from (Yong and Ohtsubo, 1987). From (Jasmund and Lagaly, 1993).

(vii) the presence of (hydr)oxides, especially in amorphous form, can reduce the mechanical swelling of the clay minerals. This may be ascribed to cementation of the clay mineral particles by shells of (hydr)oxides, and penetration of poly(hydroxo metal) ions, such as poly(hydroxo aluminium) and poly(hydroxo iron) ions, between the layers. The permeability can be influenced in two ways. If the particles form larger individual aggregates, the permeability may increase. It decreases when the (hydr)oxides act as cementing agents (Deshpande et al., 1964; El Rayah and Rowell, 1973; Blackmore, 1973; Greenland, 1975; Alperovitch et al., 1985). The conclusion is that the behaviour of such systems depends very much on the very nature of the (hydr)oxides and the way they react with the clay mineral.

5.4.10. Calculation of Interaction Energies

The interaction between dispersed clay mineral particles or individual silicate layers may be described by the DLVO theory (Barclay and Ottewill, 1970; Ottewill, 1977; van Olphen, 1977; Sposito, 1992; Güven, 1992a; Sposito and Grasso, 1999) even though other types of interactions (Sun et al., 1986; Low, 1987; van Oss et al., 1990) and long-range Coulombic attraction (McBride, 1997) may be operative. As the charge density of the faces is determined by isomorphous substitution and defects within the layer, the calculations are carried out on the assumption that the charge density of the faces remains constant when the salt concentration is varied (Usui, 1973; Gregory, 1975; van Olphen, 1977).

A pronounced Stern-layer adsorption is characteristic (Chan et al., 1984; Sridharan and Satayamurty, 1996). The surface potential calculated by the DLVO theory for montmorillonite layers (surface charge density $\sim 0.10\,C/m^2$) would be 308, 206, and 88 mV at NaCl concentrations of 10^{-5}, 10^{-3}, and 10^{-1} mol/L, respectively. Such high surface potentials are not determinative of colloid stability because they lead to a strong Stern-layer adsorption. Chan et al. (1984) derived distinctly smaller values from anion exclusion measurements (Section 5.3.5). The distribution of cations between the Stern layer, the diffuse double layer, and the solution can be calculated by a model developed by Nir et al. (1986, 1994) and Hirsch et al. (1989). An advantage of this model is that complex formation of the counterions in solution can be considered.

For an Opalinus clay Madsen and Müller-Vonmoos (1985) found good agreement between the swelling pressure calculated by the DLVO theory and that measured experimentally. Lubetkin et al. (1984) measured the pressure created by several alkali montmorillonites and beidellites as a function of the distance between the plates (calculated from the mass content of smectite on the assumption that the particles were completely delaminated) (Fig. 5.14a). At separations > 5 nm the repulsive pressure arose solely from electrostatic repulsion. On the basis of diffuse layer interactions, reasonably good agreement between theory and experiment was obtained (Fig. 5.14b). The effect of particle formation (see Section 5.2.3) is clearly seen in Fig. 5.14a. In the

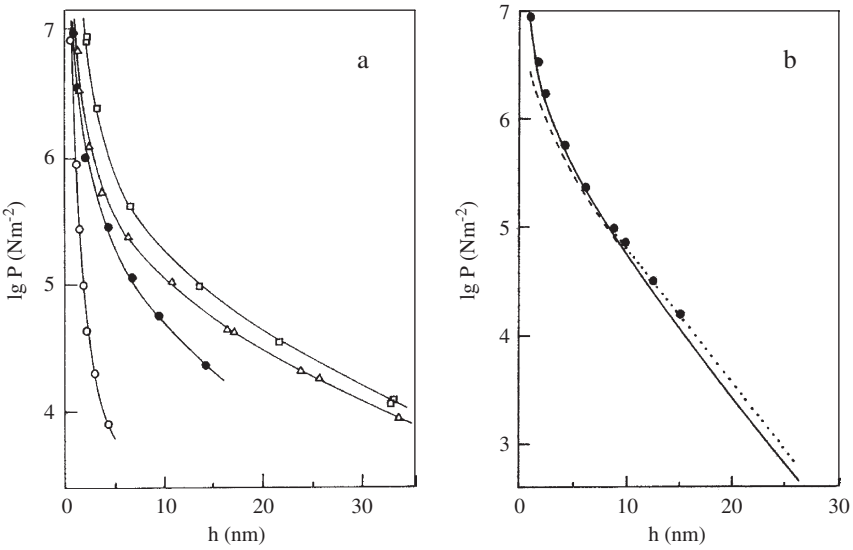

Fig. 5.14. Pressure against plate distance h for Wyoming montmorillonite. (a) In 10^{-4} M salt solutions of various counterions: □, Li^+; △, Na^+; ●, K^+; ○, Cs^+. (b) Experimental data for Li^+ montmorillonite in 10^{-2} M LiCl (●), and calculated curves for the constant potential model (- - -), constant surface charge model (—), and by approximation (….). From Lubetkin et al. (1984).

presence of alkali metal ions, other than Li^+ and Na^+ ions, the distances between the silicate layers are no longer equal. As these distances are smaller within than between particles, the pressure decreases more strongly in the presence of K^+ and Cs^+ ions than when Li^+ and Na^+ ions are present.

Ottewill (1977) noted that the theory should be corrected because a partition of the counterions between the clay dispersion and the external finite reservoir has to be considered due to the finite volume of the dispersion. At separations of about 1 nm there is a discontinuous decrease in basal spacing, indicating transition into the quasi-crystalline structure. It is then no longer reasonable to calculate the interaction forces on the basis of the simple DLVO model. As discussed in Section 5.2.2 the distribution of interlayer cations deviates considerably from that of two interacting double layers. The hydration shells around the interlayer cations resist further compression of the interlayer space (see Israelachvili (1994) for a discussion of hydration forces).

Huerta et al. (1992) considered the effect of counterions and co-ions of unequal size and calculated the swelling pressure by the modified Gouy-Chapman theory for constant surface charge density. The influence of co-ion size was only important at surface charge densities distinctly below 0.10 C/m^2.

By considering H^+-saturated montmorillonite as a solid acid with ionisable surface groups, Tombácz et al. (1990) calculated the density of these groups (sites) and

their intrinsic ionisation constants from potentiometric and conductometric titrations. Two types of ionisable sites with intrinsic ionisation constants $pK_{s1} = 2.6$ and $pK_{s2} = 6.4$ were distinguished. The total number of sites, $N_1 + N_2 = 4.8 \times 10^{17}$ (sites/m^2), was calculated from the CEC of 0.59 meq/g (montmorillonite of Kuzmice). The ratio of weak and strong acid groups was $N_2/N_1 = 0.41$, i.e. 29% of all sites were weak acidic centres. The most acidic sites were the H_3O^+ ions replacing exchangeable Na^+ ions (Janek and Lagaly, 2001). The surface potential as a function of pH was calculated from the charge densities. At 10^{-3} M NaCl and above pH ~4, the surface potential showed a plateau at 185 mV. This value decreased to 70 mV in 10^{-1} M NaCl and to 30 mV in 1 M NaCl, and the plateau extended to pH ≈ 6. On the basis of these surface potentials, the total interaction curves (Hamaker constant $A = 0.5 \times 10^{-20}$ J) were hypothetical at small distances (see remark above), but they clearly showed that the maximum of the total interaction energy disappears at about 0.1 M NaCl (pH= 2), 0.3 M NaCl (pH= 4), and 0.4 M NaCl (pH= 8). These results agree with the experimental data for samples treated with sodium hexametaphosphate (0.1, 0.2–0.25, and 0.35–0.40 M at pH= 2, 4, and 8, respectively (Tombácz et al., 1990)) and diphosphate (0.36–0.44 M at pH= 9, Frey and Lagaly, 1979b).

A quite different (and, for a colloid scientist, strange) view was put forward by Low and co-workers (Sun et al., 1986; Low, 1987; Miller and Low, 1990) on the basis of extensive studies on the clay–water system. They suggested that hydration of the clay mineral surface was the primary cause of swelling. This 'non-specific interaction of water' (undefined term) with the clay surface could not be fully explained. Hydration of the interlayer cations was assumed to be of minor importance. However, Delville and Laszlo (1989) showed that the Poisson-Boltzmann formalism correctly reproduces the relation between interlayer distance and swelling pressure. The driving force is the stabilisation of water molecules within the interlayer force field. In all cases, the Poisson-Boltzmann approximation, modified to incorporate ion/polyion-excluded volume effects, led to a concentration profile in agreement with Monte Carlo calculations. Quirk and Marčelja (1997) examined published data on the extensive swelling of Li^+-montmorillonite as revealed by $d_{(001)}$ spacings over the pressure 0.05–0.9 MPa and $1–10^{-4}$ M LiCl. Both the Poisson–Boltzmann and DLVO double layer theories satisfactorily predict surface separations over the range 1.8–12.0 nm. The DLVO theory with a 0.55 nm-thick Stern layer indicated Stern potentials of −58 to −224 mV (for $1–10^{-4}$ M LiCl) and a constant Gouy plane charge of 0.038 C/m^2 (about 30% of the layer charge). There was no additional pressure contributing to hydration forces (Israelachvili, 1994) for surface separations of about 1.8 nm or larger. (The hydration force was considerable for muscovite, with a surface charge density about three times that of montmorillonite (Pashley and Quirk, 1984)).

In the presence of Ca^{2+} (and other di- and trivalent metal) ions, the particles remain coagulated and cannot be dispersed even in pure water. Fitzsimmons et al. (1970) showed that, just after contact of Na^+-montmorillonite dispersions with calcium-saturated exchange resins, Ca^{2+}-montmorillonite exists as single layers like the

sodium form. With time the individual silicate layers aggregated by overlapping of the edges, forming large, flat sheets (band-type aggregation; Section 5.6.1). The basal spacings (Fig. 5.3) indicate that calcium ions maintain the 'quasi-crystalline' structure. These ions are located in the middle of the interlayer space, restricting the interlayer distance to 1 nm (basal spacing 2 nm), and impeding transition into the structure with diffuse ionic layers.

Kleijn and Oster (1982) were the first to explain the attractive interactions in the presence of calcium ions in terms of the DLVO theory. The cations located between the layers are assumed to be in equilibrium with the bulk solution (see also Dufrêche et al., 2001) so their charge density was slightly different in magnitude from the charge density of the layers. The electrostatic contribution to the Gibbs energy was calculated for constant surface charge density (van Olphen, 1977). The Gibbs energy was positive (peptisation) over a wide range of salt concentrations (c_S) and surface charge densities (σ_0) when the exchangeable cations were monovalent. Na^+-montmorillonite particles were coagulated by salt concentrations slightly above 0.1 M as long as the surface charge density remained below 0.1 C/m^2 (Table 5.1) and by salt concentrations slightly below 0.1 M for $\sigma_0 = 0.1 - 0.15\,C/m^2$. For more highly charged clay minerals (vermiculites, micas) the Gibbs energy was negative even at very low salt concentrations, and formation of colloidal dispersions was not expected. In the presence of divalent cations the colloidal dispersions became unstable at $c_S \leqslant 10^{-3}$ M and $\sigma_0 > 0.07\,C/m^2$.

Kjellander et al. (1988) used an advanced statistical mechanical method to calculate the diffuse double-layer interaction. This model gives strongly attractive double-layer interactions for divalent ions (Fig. 5.15) in contrast to what the simple Poisson-Boltzmann theory predicts. The position of the minimum is in reasonable agreement with basal spacing measurements by XRD. The most important reason for the occurrence of the potential minimum is the attraction due to the ion-ion correlation. In the Gouy-Chapman model of the diffuse ionic layer, this correlation is entirely neglected, i.e. the ion density in the neighbourhood of each ion is assumed to be unaffected by this ion. This neglect of the ion-ion correlation is a reasonable approximation when both the electrolyte concentration and the surface charge density are sufficiently low. However, if either condition is violated, the ion-ion correlation must be taken into account. This would lead to attractive double layer interactions between equally charged particles at short separations (Kjellander, 1996). The correlation influences the interaction by two different mechanisms: (i) by changing the ion concentration in the middle of the interlayer space; and (ii) by contributing to an attractive electrostatic fluctuation force (Kjellander, 1996).

An interesting aspect of the coagulation of clay mineral particles by salts should be mentioned. Frens and Overbeek (1972), Overbeek (1977) and Frens (1978) introduced the 'distance-of-closest-approach' concept to explain the reversibility of coagulation. The existence of such a limiting distance of about two water layers (~0.5 nm) is clearly proved by the behaviour of montmorillonite. Even in concentrated NaCl solutions the basal spacing of Na^+-montmorillonite does not decrease

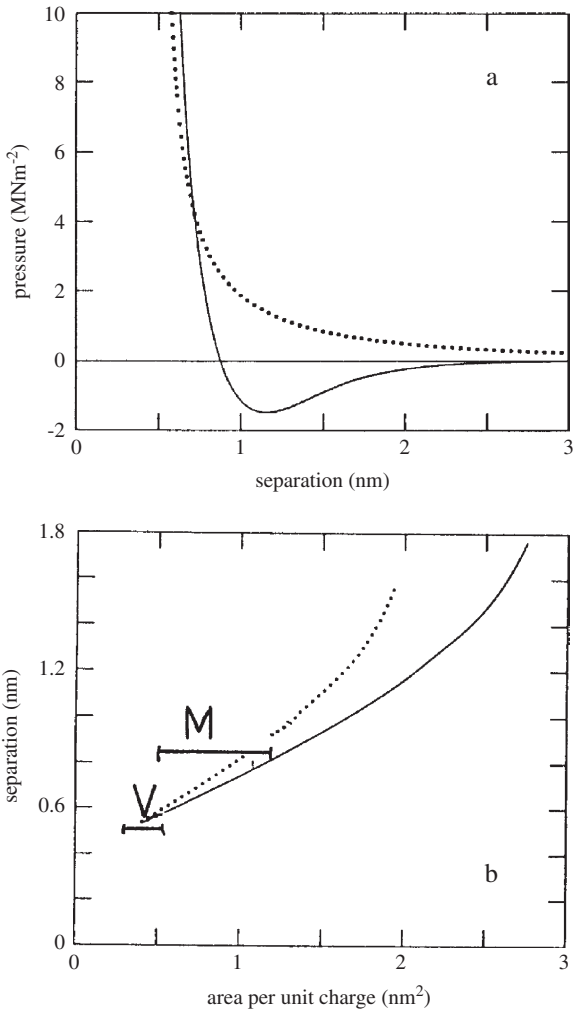

Fig. 5.15. Calculation of the pressure between two silicate layers of Ca^{2+}-montmorillonite and vermiculite. (a) total pressure, calculated for montmorillonite with a surface charge density $\sigma_0 = 0.12\,C/m^2$ (full line); results of the DLVO theory shown as dotted line. (b) Position of the potential minimum as a function of the area per unit charge. Solid line: the total net pressure; dotted line: pressure without van der Waals interaction included. (M), montmorillonites; (V), vermiculites Kjellander et al. (1988). From Jasmund and Lagaly (1993).

below 1.4–1.5 nm, i.e. two layers of water are maintained between the coagulating silicate layers (Fig. 5.3) (Jasmund and Lagaly, 1993; Lagaly, 1993, 2005; Lagaly et al., 1997). This water is only displaced when, in addition to the electrostatic forces, specific interactions, as defined by Lyklema (1984, 1989, 1995), become important.

A well-known example is the collapse of more highly charged silicate layers in the presence of potassium ions (van Olphen, 1977; Jasmund and Lagaly, 1993).

Fig. 5.16 illustrates the coagulation of mixed dispersions of two smectites (Section 5.4.2). Only very small particles were mixed during coagulation. The maximum total interaction energy $V_{t,m}$ is calculated for particles of 10^2 and $10^4\,nm^2$ and surface charge densities of 0.069, 0.096, and $0.12\,C/m^2$. The total interaction curves are obtained by the linear superposition approximation for constant surface charge density (van Olphen, 1977). The curves terminate at a layer separation of 1 nm because at smaller distances DLVO calculations are no longer appropriate. At 0.3 M NaCl, $V_{t,m}$ is about 5 kT/particle for the small particles and $\sigma_0 = 0.069\,C/m^2$, and increases to17 kT/particle for $\sigma_0 = 0.096\,C/m^2$ (Fig. 5.16a). An increase of concentration to 0.38 M NaCl leads to $V_{t,m} \approx 1$ kT/particle for $\sigma_0 = 0.069\,C/m^2$ and 10 kT/particle for $\sigma_0 = 0.096\,C/m^2$. Thus, mixing of both types of layer is highly probable during coagulation. The curves calculated for larger particles (Fig. 5.16b) clearly

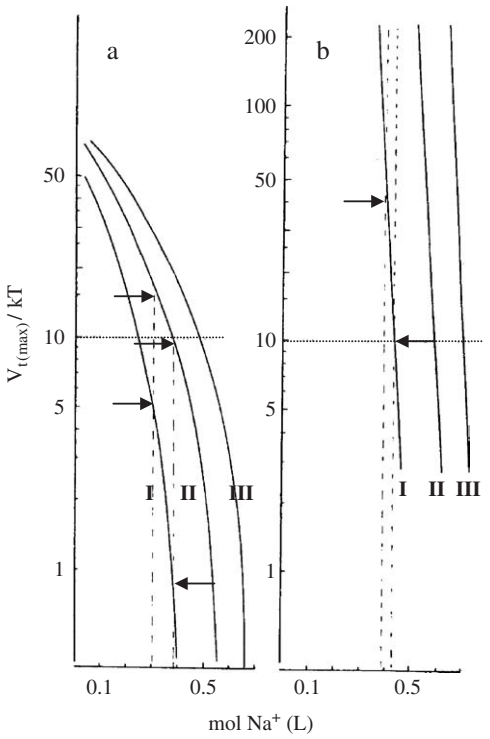

Fig. 5.16. Maximum interaction energy (in kT/plate) as a function of Na^+ concentration for particles $10 \times 10\,nm^2$ (a) and $100 \times 100\,nm^2$ (b) Surface charge densities: I, 0.069; II, 0.096; III, $0.120\,C/m^2$; calculated for constant charge density, Hamaker value $5\ 10^{-20}$ J. From Frey and Lagaly (1979b).

show that at a salt concentration of about 0.4 M only the low-charge layers are coagulated. $V_{t,m}$ of the high-charge layers remains so large as to prevent coagulation.

It is interesting to consider the depth of the secondary minimum. For larger layers with low charge density the depth is about 50 kT/particle, and $\approx$20 kT/particle for the high-charge layers. Thus, aggregation of the low-charge layers is initiated by preliminary demixing in the secondary minimum.

In more sophisticated calculations, the total interaction energies have to be calculated between differently charged plates. This reduces $V_{t,m}$ and makes the mixing of the small particles still more probable (Lagaly et al., 1972; Usui, 1973; Gregory, 1975; Derjaguin et al., 1987). For large particles, the differences of $V_{t,m}$ remain large enough to prevent the layers from mixing during coagulation. The effect of particle size on the simultaneous coagulation of differently charged particles is also evident from the calculations by Pugh and Kitchener (1971).

5.5. FLOCCULATION AND STABILISATION BY POLYMERS

5.5.1. Flocculation and Stabilisation Mechanisms

Macromolecules can flocculate colloidal dispersions by two different mechanisms: bridging between the particles and charge neutralisation (Fig. 5.17) (Theng, 1979; Chaplain et al., 1995; Lagaly et al., 1997).

Bridging requires that the macromolecules can attach to the surface of two approaching particles and that the bridging part of the macromolecules is compatible with the solvent (the solvent has to be a better-than-theta solvent). In aqueous dispersions a certain low salt concentration is often needed to bring the particles in distances that can be spanned by the macromolecules.

Charge neutralisation occurs when the charges on the particle surface and the polymer are opposite in sign. The polyions can then compensate the surface charges (Fig. 5.17b, c). However, site-by-site compensation only occurs at suitable geometrical conditions. A general model is flocculation by patch-charge interactions (Gregory, 1973; Mabire et al., 1984). For example, polycations are adsorbed in patches, giving rise to an excess of positive charges. This excess is compensated by negative charges of patches that are not covered by the polycations. An attractive force operates between one or more cationic patches of one particle and domains of negative surface charges of a neighbouring particle. These contacts can be broken and re-established under shearing forces. The formation of polymer patches on charged colloidal particles was observed by AFM (Akari et al., 1996).

Since flocculation is often irreversible, the amount adsorbed and the properties of the flocs depend on the manner by which the macromolecules were added to the dispersion. The formation of flocs can retard equilibration when adsorption sites within the flocs are difficult to access by the macromolecules (see Section 5.5.3). The amount adsorbed and the type of aggregation are therefore critically sensitive to the

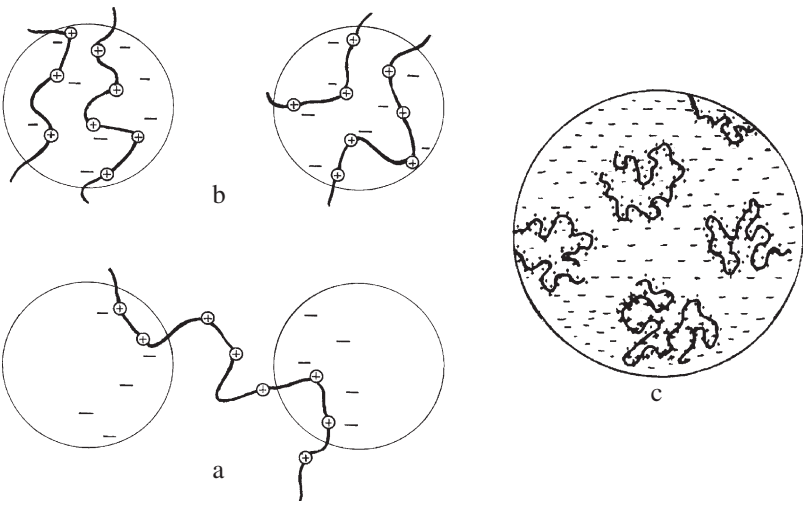

Fig. 5.17. Destabilisation of colloidal dispersions by (a) bridging flocculation, (b) charge neutralisation, and (c) patch-charge interaction. From Lagaly et al. (1997).

details of the mixing and stirring procedure, giving rise to non-reproducible experimental results (Chaplain et al., 1995). The amount adsorbed usually decreases as the solid/liquid ratio increases (Lee et al., 1991). Polymer adsorption and the influence of polymers on dispersion stability are strongly dependent on the true nature of the polymer. For example, polyacrylamides may be neutral (uncharged) polymers, anionic (hydrolysed) products, cationic derivatives, or copolymers (of acrylic acid and acrolein derivatives).

Many polymers flocculate a dispersion at very low concentration but re-stabilise at higher concentration. The latter is an osmotic process, referred to as 'steric stabilisation' (Napper, 1983; Lagaly et al., 1997). When the macromolecules of two approaching particles begin to interpenetrate, the segment density between the particles becomes larger than outside of the interpenetrating domain. Solvent penetrates between the particles, and the particles remain separated (Fig. 5.18). The influence of volume restriction is related to the loss of conformational entropy, and only comes into play at high particle concentrations or near the theta point.

The most important condition for steric stabilisation is that the solvent is a better-than-theta solvent in relation to the macromolecular segments remaining in the solvent. Examples are poly(ethylene oxides), poly(vinyl alcohol), and polyacrylates in water. The polymer must have anchor segments with a high affinity for the particle surface if it is to become attached to the particles. Thus, di-block copolymers are often very suitable.

Steric stabilisation provides a high stability to the dispersion. Destabilisation requires the reduction of the solvency. The particles flocculate when the theta

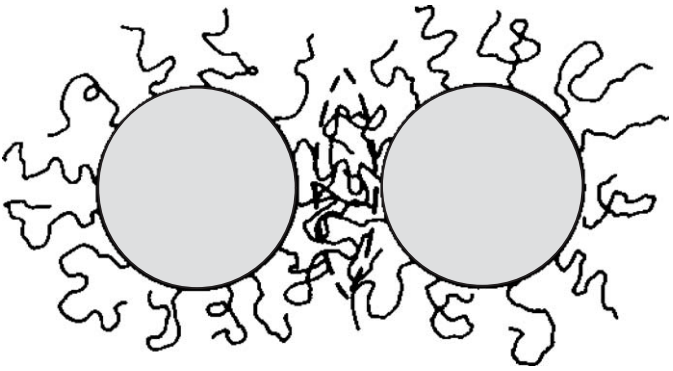

Fig. 5.18. Steric stabilisation as the consequence of the osmotic effect due to the high concentration of segments in the region within the dashed lines. From Overbeek (1982).

condition is reached by the addition of another solvent or a solute. An important advantage is that destabilisation is completely reversible: increasing the solvency or changing the temperature re-stabilise the dispersion. A pronounced influence of temperature is noted in contrast to electrostatically stabilised dispersions. Depending on the thermodynamic functions, the dispersions can be destabilised with increasing but also with decreasing temperature.

A prerequisite for steric stabilisation is the attachment of the macromolecules at the particle surfaces. Macromolecules enriched in the solvent cause destabilisation by the depletion effect (Napper, 1983; Vincent, 1990; Lagaly et al., 1997).

5.5.2. *Flocculation by Polyanions*

Polymers are extensively used as flocculating agents for clay dispersions. In practical applications, polyanions are more effective in flocculating clay dispersions than polycations. Polyanions are attached to the particles at a few sites, and larger parts of the macromolecules remain free in solution to form bridges between neighbouring particles.

Several studies are reported on the adsorption of polyacrylates and polyacrylamides by montmorillonite (Stutzmann and Siffert, 1977; Siffert and Espinasse, 1980; Bottero et al., 1988; Heller and Keren, 2002, 2003) and on kaolinite (Hollander et al., 1981; Pefferkorn et al., 1985, 1987; Nabzar and Pefferkorn, 1985; Stenius et al., 1990; Lee et al., 1991).

Neutral polyacrylamide is adsorbed at the edges and faces of kaolinite particles. The amount adsorbed was independent on salinity (NaCl) and pH between 3.5 and 10, then decreased above pH 10. The adsorption density on the lateral surfaces was distinctly higher than on the basal surface. The adsorption of anionic polyamide[7]

[7]Technical "non-ionic" polyacrylamides also contain about 2–6 mol% carboxyl groups!

also occurred preferentially at the edges. Adsorption decreased strongly with increasing pH (increasing negative charge density of the edges) but increased with NaCl concentration (up to 3.3 mol/L) due to charge screening (Lee et al., 1991).

Adsorption of polyacrylamide on the basal surface of kaolinite occurs mainly on the aluminium hydroxide surface, being driven by van der Waals interactions and an entropy contribution when adsorbed water molecules are displaced by the macromolecules (Lee et al., 1991). At the edges, polyacrylamides are mainly bound by hydrogen bonds between the amide groups and aluminol and silanol groups. Formation of these hydrogen bonds seems to be competitive with hydrogen bond formation between neighbouring aluminol and silanol groups. Hydrogen bonding to silanol groups as anchoring sites is promoted in acidic medium when neighbouring aluminol groups are protonated. Bonding to aluminol groups is favoured in alkaline medium when the neighbouring silanol groups are dissociated. In agreement with this model the adsorption of a statistical copolymer (acrylamide-acrolein) showed a minimum at pH 6–8 (Pefferkorn et al., 1985, 1987). In the case of smectites, amide groups can be protonated by the increased acidity of the interlayer water molecules and then bound by electrostatic forces (Stutzmann and Siffert, 1977).

Polyacrylates and anionic (hydrolysed) polyacrylamides are adsorbed by complex formation between the carboxyl groups of the polyanion and aluminium ions exposed at the edges. Thus, adsorption of polyacrylate by montmorillonite reached a maximum at pH ~7 (Siffert and Espinasse, 1980). A further consequence is that adsorption increased with the degree of hydrolysis (increased number of carboxyl groups) (Stutzmann and Siffert, 1977).

Bottero et al. (1988) studied the effect of polyacrylamide on dispersions of Na^+-montmorillonite. The polyacrylamide did not flocculate montmorillonite particles but influenced the structure of the particles. Similarly, Heller and Keren (2002) observed that in electrolyte-free dispersions only polymers with high molecular weight form a three-dimensional structure of the clay mineral particles. The effectiveness of polyacrylamides in bridging flocculation increased with decreasing degree of hydrolysis.

The addition of polyacrylamide to Na^+-kaolinite dispersions (2% by mass) initiated different types of aggregation (Nabzar et al., 1984). The fraction of flocculated kaolinite first decreased to a minimum, and then increased to a maximum (Fig. 5.19). Polyacrylamide adsorbed at the edges broke up edge(+)/face(−) contacts and increased the dispersibility of the kaolinite particles (B→C in Fig. 5.19). Pronounced adsorption of polyacrylamides on the edges of kaolinite particles was observed by Lee et al. (1991). Bridging of the particles occurred at somewhat higher levels of polyacrylamide addition (C→D), increasing the amount of flocculated kaolinite. At high dosages of polymer, flocculation was reduced by steric stabilisation (D→E). Floc density (determined from the volume and weight of sediment after freeze-drying) was inversely related to the amount flocculated. The presence of a few macromolecules on

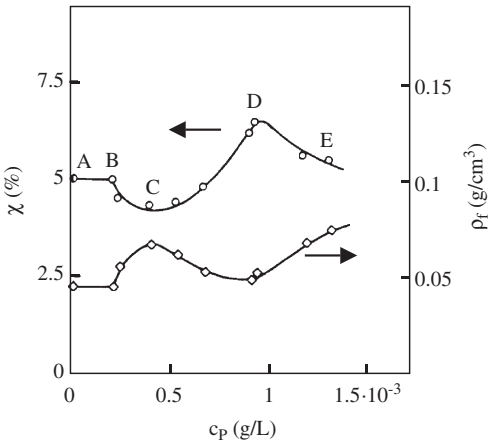

Fig. 5.19. Flocculation of Na^+-kaolinite dispersions (2% by weight) with polyacrylamide ($M = 1.2 \times 10^6$) (concentration c_P) in 10^{-4} M NaCl at pH = 3.7. ○, fraction χ of kaolinite flocculated; ◇, density ρ_f of the flocs (Nabzar et al., 1984). From (Jasmund and Lagaly, 1993).

the edges of the particles prevented formation of extended networks during sedimentation, giving rise to densely packed particles (C in Fig. 5.19). Bridging produced relatively loosely packed flocs (E in Fig. 5.19). The increase in floc density at E indicated that the most loosely packed aggregates were the first to be redispersed by steric stabilisation.

5.5.3. *Flocculation by Polycations*

Polycations are strongly adsorbed by clay mineral particles. Since a large proportion of the segments become attached to the negatively charged surface, bridging between particles does not occur as easily as with polyanions. In many cases flocculation occurs as a consequence of charge neutralisation (Theng, 1979).

Cationic polymers generally flocculate a clay dispersion at a narrow polymer concentration. Even slightly higher polymer concentrations cause re-dispersion. Flocculation, therefore, often requires a sophisticated adjustment of clay, polymer, and salt concentrations as well as pH (Kim et al., 1983). In the domain of re-dispersion the clay mineral-polymer complexes can be flocculated by addition of anionic surfactants but again optimal flocculation is achieved at narrow surfactant concentrations that depend on the amount of polycations added (Magdassi and Rodel, 1996).

Durand-Piana et al. (1987) examined the effect of cationic groups attached to polyacrylamide on the flocculation of Na^+-montmorillonite dispersions. Random copolymers consisting of m units acrylamide (AM) and n units *N*,*N*,*N*-trimethyl

aminoethyl chloride acrylate (CMA) were synthesised:

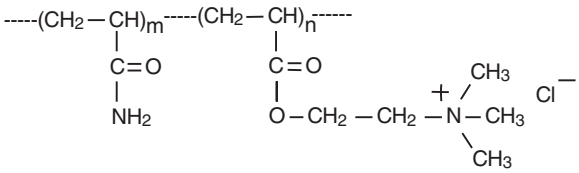

The 'cationicity' $\tau = n/(n+m)$ was varied between 0 and 1. At low cationicity the weakly charged polyelectrolytes caused flocculation by interparticle bridging. The optimal flocculation concentration decreased with increasing molecular mass, and for $\tau \geqslant 0.01$ with increasing cationicity. Above $\tau \approx 0.2$ flocculation apparently occurred by charge neutralisation, and the optimal flocculation concentration became independent of molecular mass (Fig. 5.20). The saturation value of adsorption decreased when the solid content of montmorillonite exceeded 2 g/L. Polymer-induced aggregation of montmorillonite platelets can be so extensive as to limit the number of surface sites available for polymer adsorption.

Parazak et al. (1988) studied the flocculation of dispersed montmorillonite, kaolinite, illite, and silica by three types of polycations: poly(dimethylamine epichlorohydrin), poly(dimethyl diallylammonium chloride), and poly(1,2-dimethyl-5-vinylpyridinium chloride). They interpreted the results in terms of 'hydrophobic interactions' although patch-charge interactions seem more appropriate.

Since the charges on polycations and clay mineral particles are opposite in sign, polycations can penetrate the interlayer space of smectites to a certain extent.

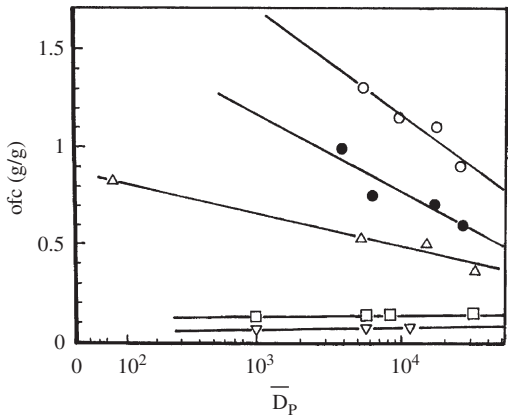

Fig. 5.20. Optimal flocculation concentration (ofc, g/g Na^+-montmorillonite) vs. degree of polymerisation, $\bar{D}_p$, for polycations (see formula) of various cationicities τ: ○, $\tau = 0.01$; ●, $\tau = 0.05$; △, $\tau = 0.13$; □, $\tau = 0.30$; ▽, $\tau = 1.0$ Durand-Piana et al. (1987). From Jasmund and Lagaly (1993).

However, as the number of contacts between polymer and surface increases, interlayer diffusion of the polycation is retarded and eventually ceases. Complete coverage of the interlayer surfaces by polycations may be achieved by a disaggregation-reaggregation process as proposed for the adsorption of lysozyme by Na^+-montmorillonite (Larsson and Siffert, 1983). When a particle with its external faces saturated by polycations collides with another with no polycations on its faces, strong interactions between the polymer-covered face and the bare face can cause an individual layer to peel off either tactoid. This would expose two fresh surfaces for further interaction with polycations. Eventually, all layers are interleaved with polycations, and thick particles are formed (Breen et al., 1996; Billingham et al., 1997; Breen, 1999).

In papermaking, cationic lattices ('polymer microparticles') are used as flocculants to improve retention, drainage, and formation ('retention aids') (Xiao et al., 1999). In the presence of polycations such as cationic polyacrylamides and poly(ethylene imines), the microparticles are flocculated by patch-charge interactions. Being shear-sensitive, these flocs can de-agglomerate under the influence of the high shear forces used in paper machines. Bridging of these particles by montmorillonite particles makes the flocs shear-resistive (Fig. 5.21) (Horn, 2001/2002). However, bridging by montmorillonite is not always effective. In certain two-component microparticle

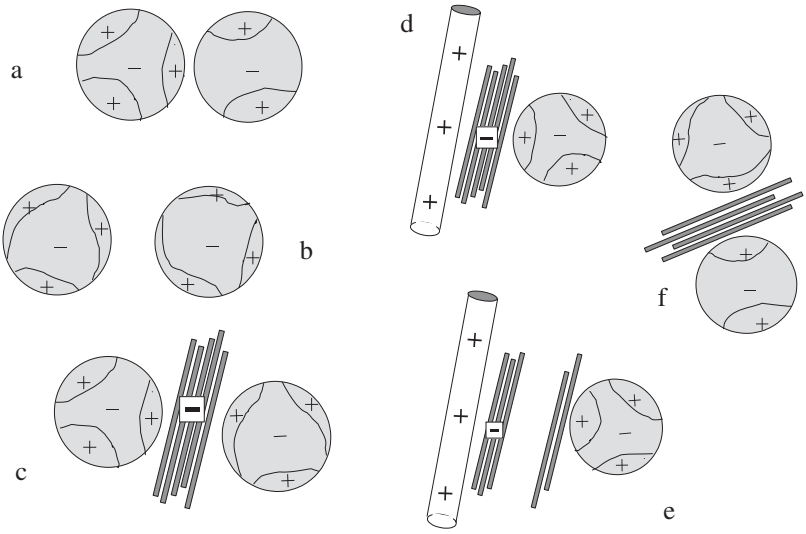

Fig. 5.21. Patchwise coagulation of latex particles and bridging by montmorillonite particles. (a) Flocculation by patch-charge interaction of latex particles covered by polycations, (b) de-agglomeration by shear forces and re-distribution of the adsorbed polycations, (c) bridging of the latex particles by montmorillonite lamellae forming shear-resistive flocculates, (d) attachment of latex particles on the fibres by montmorillonite particles, (e) detachment of the particles by delamination of the clay mineral during shearing, (f) agglomeration of these particles.

retention systems, cationic polyacrylamide and bentonite particles induce the deposition of calcium carbonate particles on the fibre surface. The montmorillonite particles form bridges between the fibre and calcium carbonate particles, both of which are covered with polycations. However, delamination of thicker montmorillonite particles by shearing can lead to detachment and subsequent flocculation of the polyamide-coated carbonate particles (Alince et al., 2001). The shear resistivity of bridging clay mineral particles and particle-fibre agglomerates depends, therefore, on the shear stability of the montmorillonite particles. Thick montmorillonite particles with many breaking points will be less shear-resistive than thin particles consisting of large coherent domains.

5.5.4. Peptisation (Deflocculation) of Clay Dispersions by Macromolecules

As seen in the previous section, optimal flocculation is reached at a distinct polymer concentration. When this concentration is exceeded, restabilisation occurs, and the amount of flocculated clay decreases. Restabilisation is accompanied by an increased salt stability. An instructive example was reported by van Olphen (1977) (Fig. 5.22). Addition of CMC (sodium carboxy methylcellulose) to a Na^+-bentonite dispersion

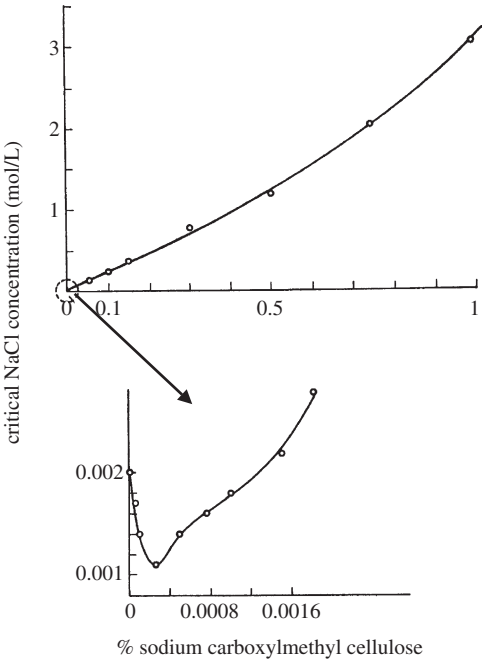

Fig. 5.22. Effect of sodium carboxy methylcellulose on the salt stability of Na^+-bentonite dispersions (van Olphen, 1977). From Jasmund and Lagaly (1993).

first decreased the critical NaCl concentration from 20 to 10 mmol/L at 0.0003% CMC (sensitising action of CMC). The colloidal stability then increased strongly up to 3.1 mol/L at 0.1% CMC. Steric stabilisation is the main cause of the enhanced salt stability.

The effect of polymer addition, shown in Fig. 5.22, is basically different from the action of several other polyanions like natural tannates (Fig. 5.23a). Addition of small amounts of Quebracho tannate, a common additive in drilling muds, caused a steep increase in the critical salt concentration reaching a plateau at 270 meq/L NaCl. The Quebracho polyanion does not exert steric stabilisation but simply acts by recharging the edges. Because tannate is added as the sodium salt, the total amount of Na^+ ions in the dispersion increases to 430 meq/L at the highest dosage of tannate (broken line in Fig. 5.23a). This range of critical cation concentrations is typical of face/face aggregation of clay mineral particles (see Section 5.4.1).

Polyphosphate ions belong to the most important deflocculants in practical applications. In the presence of polyphosphate, the critical coagulation concentration of NaCl increased to a maximum and decreased with further addition of the

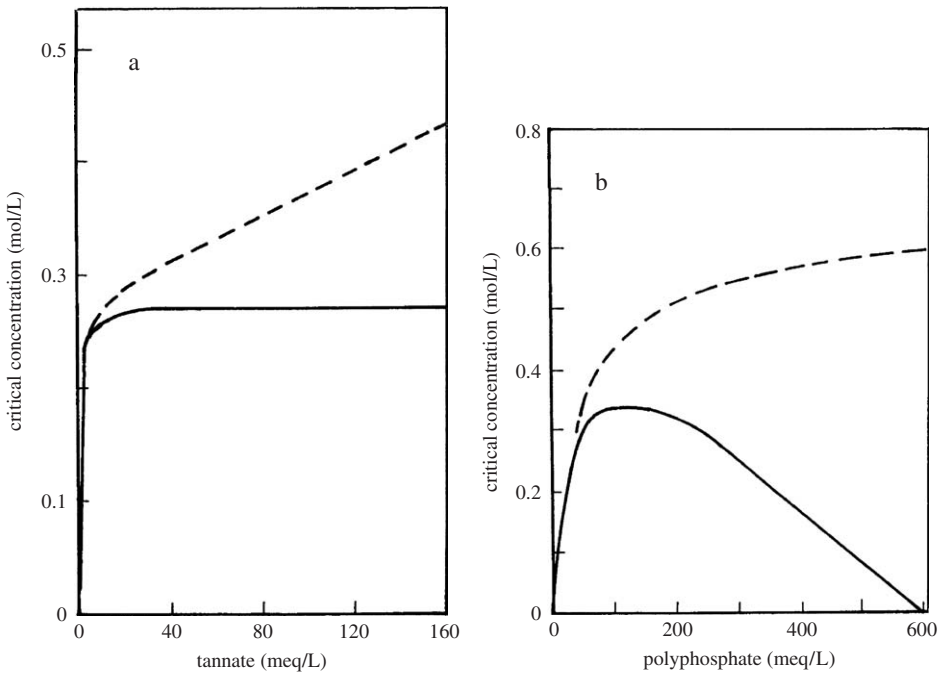

Fig. 5.23. Effect of polyanions on the salt stability of Na^+-bentonite dispersions. Solid line critical NaCl concentration to attain coagulation broken line total Na^+ concentration at the point of coagulation. (a) Quebracho tannate (sodium salt), (b) sodium polyphosphate. From Lagaly (1993).

polyanion (Fig. 5.23b). However, the total concentration of Na^+ ions increased only slightly at higher amounts of polyphosphate ($\geqslant 200$ meq/L) and is, again, typical of face/face aggregation. Polyacrylates are important dispersants for kaolinites in the paper industry. They stabilise dispersions by increasing the absolute value of the (negative) surface potential (Li et al., 2001) and steric stabilisation.

Using dynamic light-scattering, Kretzschmar et al. (1998) showed that under acidic conditions humic acid markedly increased the stability of kaolinite dispersions, primarily by reversing the charge of the edge surface. However, at high-electrolyte concentrations, steric stabilisation by adsorbed humic substances became effective.

5.6. AGGREGATION OF CLAY MINERAL PARTICLES AND GELATION

5.6.1. *Modes of Aggregation*

The most well-known mode of aggregation is the house-of-cards model where the clay mineral particles are held together by edge/face contacts (Fig. 5.24a) (Hofmann, 1961, 1962, 1964). This type of network only forms when the edges are positively charged, or in a slightly alkaline medium above the critical salt concentration. Formation of edge/face contacts below pH ≈ 6 is due to heterocoagulation between the positive edges and the negative faces of the particles or silicate layers.[8] House-of-cards aggregation is characterised by non-Newtonian flow[9] of the dispersions, and the development of yield stresses in acidic medium (Figs. 5.25 and 5.26). Note the yield value at pH 4.5 increased with temperature.

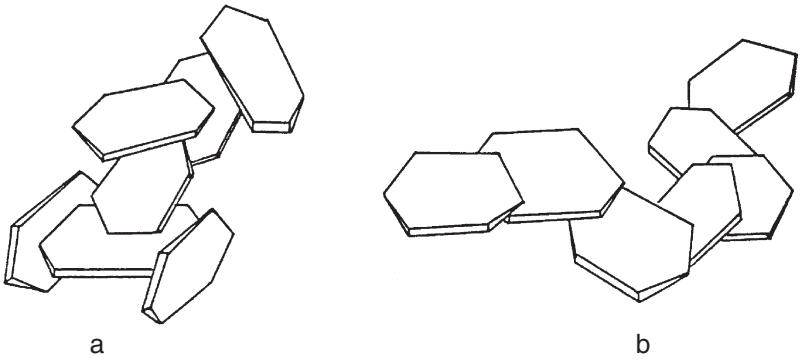

Fig. 5.24. Aggregation of clay mineral layers in (a) card-house and (b) band-type networks by edge/face and face/face contacts.

[8]Card-house type edge(+)/face(−) aggregation was also observed for gibbsite particles, γ-AlO(OH), with isoelectric points at pH ~7 (edges) and pH ~10 (faces) Wierenga et al. (1998).

[9]For a review on the flow behaviour of colloidal dispersions see Güven (1992b).

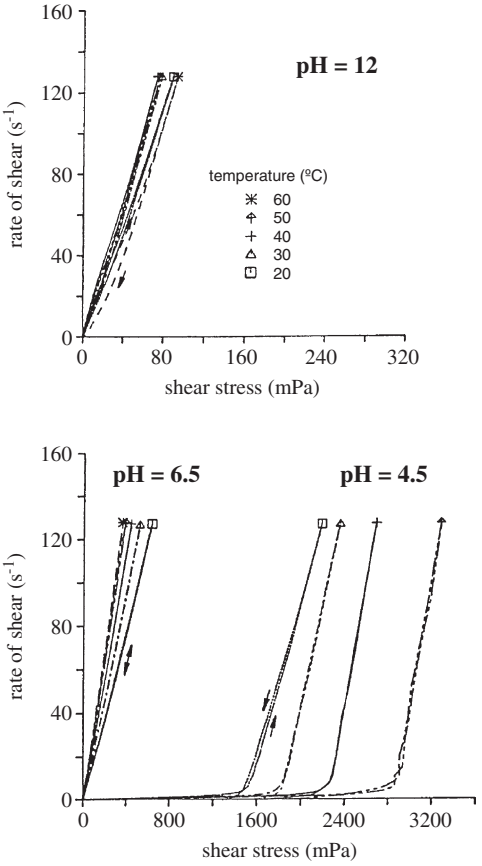

Fig. 5.25. Flow curves (shear rate vs. shear stress) for Na^+-montmorillonite dispersions (Wyoming, 4% by weight) at various pH and different temperatures (pH adjusted by addition of HCl or NaOH).

With increasing pH the network composed of edge/face contacts breaks down and the shear stress τ (at a given rate of shear, $\dot{\gamma}$) of the Na^+-montmorillonite dispersion decreases to a sharp minimum (Fig. 5.26). The increase in shear stress at pH > 5 results from the higher degree of delamination and therefore from the higher number of particles in the dispersion. Raising the pH above 7 by increased addition of NaOH reduces the degree of delamination and the electroviscous effect (see below). As a result, the shear stress again decreases (Permien and Lagaly, 1995).

Weiss and Frank (1961) and Weiss (1962) were the first to stress the importance of face/face contacts and the possible formation of three-dimensional band-type networks ('Bänderstrukturen') (Fig. 5.24b). The band-type network of Ca^{2+}-kaolinite

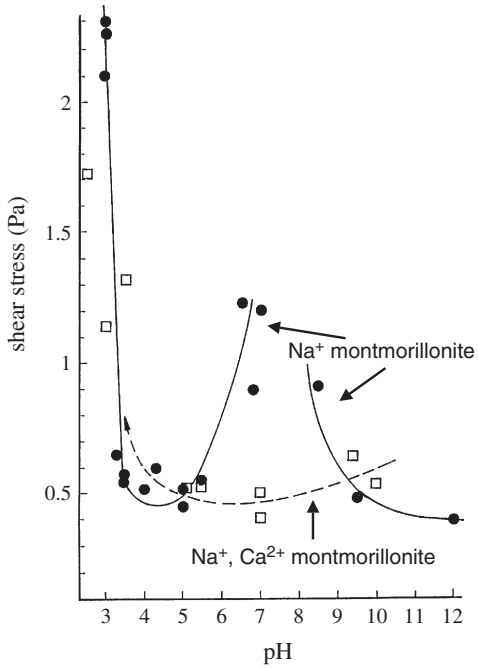

Fig. 5.26. Dependence of the shear stress (at a rate of shear of $94.5\,s^{-1}$) on the pH value for the dispersion of Na^+-montmorillonite (● —) and of the parent (Na^+, Ca^{2+})-bentonite (□ - - - -) (from Wyoming). The pH values were determined with indicator sticks just before the rheological measurements. From Permien and Lagaly (1995).

showed some elasticity in contrast to the more rigid card-house structure. Face/face aggregation and formation of band-type structures were clearly observed by TEM (Vali and Bachmann, 1988; Benna et al., 2001a, 2001b).

The effect of salt addition on the aggregation of clay mineral particles in dilute (<2% w/w) dispersions, and the resulting rheological properties are schematically shown in Fig. 5.27. Both the yield value and the viscosity are low when salt is absent. They decrease even further after the addition of modest amounts of salt (10^{-3}–10^{-2} mol/L NaCl) (Permien and Lagaly, 1995), then increase steeply. High salt concentrations can reduce viscosity and yield value again.

The minimum at low salt concentration is a consequence of the secondary electroviscous effect. In the absence of salt or at very low salt concentrations, single silicate layers, or packets of them, are surrounded by diffuse layers of cations, repelling each other by electrostatic forces (van Olphen, 1977; Güven and Pollastro, 1992; Jasmund and Lagaly, 1993; Lagaly et al., 1997; Quirk and Marčelja, 1997). When the particle concentration is sufficiently high (≥1% w/w for many Na^+-montmorillonite dispersions), the diffuse ionic layers around the silicate layers, or

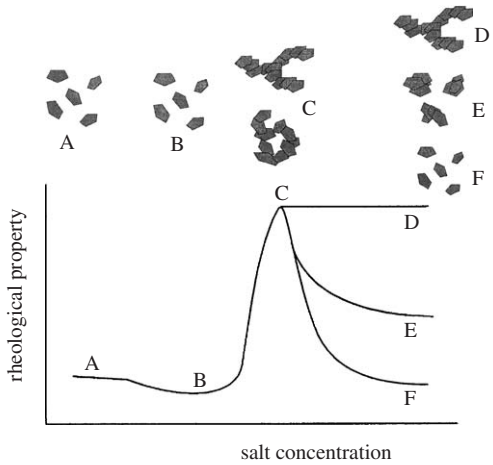

Fig. 5.27. Influence of 1:1 electrolytes on the flow behaviour of diluted clay dispersions. (A, B) isolated particles (B) minimum of rheological properties (viscosity, yield value) due to the electroviscous effect (C, D) aggregation in the form of networks (E, F) fragmentation of the networks at high salt concentrations.

particles restrict the translational and rotational motion of these units. As a result, the viscosity increases and a small yield value is observed (Norrish, 1954; Callaghan and Ottewill, 1974; Rand et al., 1980; Permien and Lagaly, 1994a). Addition of salt reduces the thickness of the diffuse ionic layer, increases the translational and rotational freedom of the particles, and reduces viscosity and yield value (Fig. 5.28). The thin shape together with the high aspect (diameter/thickness) ratio of these units are critical factors determining the appearance of the electroviscous effect (Adachi et al., 1998) which induces a certain parallel orientation of the platelets (Fukushima, 1984; Ramsay et al., 1990; Mourchid et al., 1995; Mongondry et al., 2005; Tateyama et al., 1997; Abend and Lagaly, 2000). As the repulsive force strongly decreases when the particle orientation deviates from the exact parallel position (Anandarajah, 1997), the particles arrange in a certain zig-zag structure as indicated in Fig. 5.28.

The sharp increase in rheological parameters at moderately high salt concentrations corresponds to the coagulation of the particles forming a volume-spanning network. This network may resist further salt addition but in most cases the influence of the van der Waals attraction at high salt concentrations contracts the bands into smaller aggregates (Fig. 5.27, E), or even to particle-like assemblages, disrupting the network structure (Fig. 5.27, F).

Addition of calcium ions has a pronounced effect on the type of aggregation. Small additions can strongly increase the yield value of Na^+-montmorillonite dispersions but high amounts of Ca^{2+} ions reduce this value considerably (Permien and

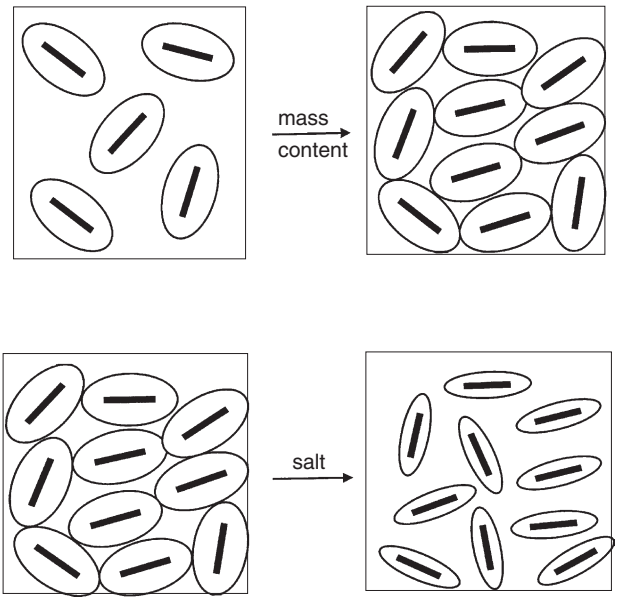

Fig. 5.28. The electroviscous effect: (above) Sufficiently high particle concentration reduces the mobility of the particles. (below) When the thickness of the diffuse ionic layers decreases at higher salt concentration, the particles again become more mobile. From Permien and Lagaly (1994a).

Lagaly, 1994b). The maximum of the shear stress at pH ~7 disappears in the presence of even small amounts of calcium ions (see also Permien and Lagaly, 1995; Benna et al., 1999). As discussed in Sections 5.2.1 and 5.4.10, calcium ions held together the silicate layers at a maximum distance of 1 nm (basal spacing 2 nm). Even small amounts of calcium ions nucleate face/face contacts and build up band-type networks. The flow behaviour of Ca^{2+}/Na^{+}-bentonite dispersions is therefore complex, and is sensitive to the ratio of Ca^{2+}/Na^{+} in the dispersion (Tombácz et al., 1989). Small amounts of calcium ions added to a Na^{+}-montmorillonite dispersion promote face/face contacts and stabilise band-type networks (Fig. 5.29b). At large amounts of calcium ions, the bands contract to form small aggregates, and eventually particle-like assemblages, and the network falls apart (Fig. 5.29c). Homoionic Ca^{2+}-smectites thus show only a modest tendency for forming band-type networks.

It may be assumed that calcium ions held between the negative charges at the edges and faces of two approaching particles act in a similar way as in the interlayer space and limit the particle distance to 2 nm. Stable edge (−)/Ca^{2+}/face (−) contacts would then be created that would build up a stable card-house network. However, this behaviour seems very unlikely. Calcium ions lying at the edges of particles with

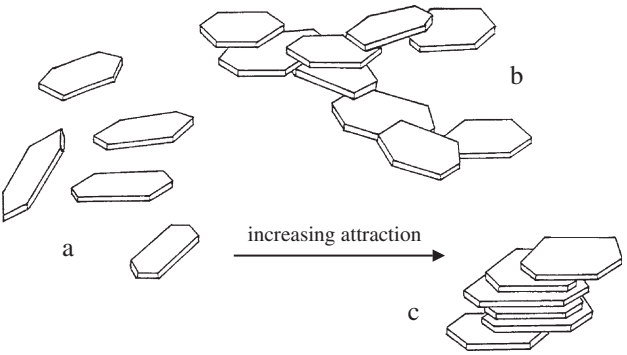

Fig. 5.29. Aggregation of the clay mineral layers with increasing attraction: (a) single layers, (b) band-type aggregates, (c) compact particles. From Permien and Lagaly (1994a).

very irregular contour lines are in a quite different force field than between the planar silicate layers in the interlayer space. The modest importance of the edge(−)/Ca^{2+}/face(−) contacts is expressed by the low shear stresses of the Ca^{2+}-montmorillonite dispersions in alkaline medium.

5.6.2. *Plasticity*

Plasticity is a very important property of ceramic masses (but also of metals, alloys, polymers, and plastics). "It may be defined as the property of a material which permits it to be deformed under stress without rupturing and to retain the shape produced after the stress is removed. It is the property that permits the material to be shaped by the application of a force. Clay materials in general develop plasticity when they are mixed with relatively small amounts of water" (cited from Grim, 1962). The plasticity of ceramic masses strongly depends on water content. The Atterberg method (Atterberg, 1911, 1912; Grim, 1962) determines the water content needed to develop optimum plasticity (see also Lagaly, 1989). Usually, there is a defined amount of water at which the clay is easily mouldable. With less moisture the mass cracks when moulded. The plastic limit is the lowest water content (expressed in percentage by weight of the clay dried at 120 °C) at which the mass can be rolled into threads without breaking. The Atterberg liquid limit is the water content at which the mass begins to flow. The difference between both values is called the 'plasticity index'. Table 5.11 shows these values for kaolinite, illite and montmorillonite. Different methods of shear-strain measurements of clay bodies as a function of the water content are also used to find optimum plasticity.

The plastic deformation of a given clay mass not only depends on the water content but also on the time needed for the clay to adjust so that shaping proceeds without rupturing. The rate of application of the stress is therefore important in the shaping process.

Table 5.11. Atterberg limits (percentage per mass of dried (120 °C) clays). Data from Müller-Vonmoos, see Lagaly (1989)

Clay	Cation	Liquid limit	Plastic limit	Plasticity index
Kaolin, KGa-2,	Na^+	69	31	38
Warren County,	Ca^{2+}	74	31	43
Georgia, USA	Na^+*	33	24	9
Illite, Bassin du	Na^+	76	29	47
Velay, Massif	Ca^{2+}	93	32	61
Central, France	Na^+*	54	29	25
Montmorillonite,	Na^+	431	48	383
SAz-1, Arizona, USA	Ca^{2+}	190	50	140

*In the presence of 0.5 g $Na_4P_2O_7 \cdot 10\ H_2O$/100 g clay.

Hofmann (1961, 1962) explained the cause of plasticity in terms of the card-house model (Fig. 5.30a).[10] When mechanical force is applied to the clay body, the T-type contacts between two particles may be broken but the particles can easily shift into neighbouring contact positions so cohesion between the particles is never lost as long as the water content is not too large. In the case of band-type structures, the particles may not only change positions, the network can also be deformed by rotation of the particles (Fig. 5.30b).

Bentonites are used very extensively in binding foundry-moulding sands (Grim, 1962; Odom, 1984), because the thin flexible layers of montmorillonite wrap up/envelop the quartz particles, and the band-type arrangement of the silicate layers provides the necessary plasticity to the sand (Fig. 5.31) (Hofmann, 1961, 1962).

5.6.3. Sedimentation and Filtration

In many practical applications, the process of sedimentation, the type of sediments, and conditions of destabilisation are important.

Two types of sedimentation may be distinguished (Fig. 5.32). If the solid content of the dispersion is low and the forces between the particles are not attractive, the particles settle independently from each other and accumulate at the bottom of the vessel forming a sediment the height of which increases with time (free or granular sedimentation). Usually, a sharp interface between the accumulated sediment and the dispersion is observed. The settling behaviour is described by Stokes' law (see

[10]The term "house-of-cards" was first used by Le Chatelier to explain the plasticity of clay masses. His idea was that the platy clay mineral particles adhere together as playing cards do when they are thrown on a table (Salmang, 1927). This picture describes band-type aggregates whereas Hofmann used this term for the 3-dimensional edge-face aggregation.

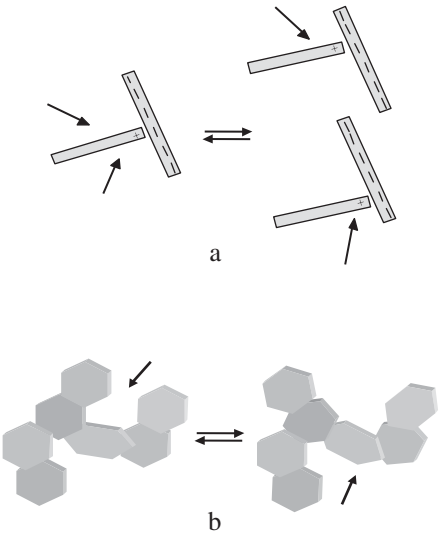

Fig. 5.30. Plasticity of ceramic masses is caused by particle movement from one contact into a neighbouring position (a) or by particle rotation (b).

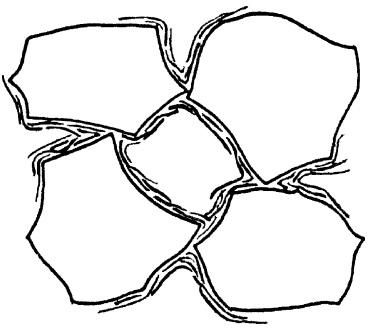

Fig. 5.31. Montmorillonite particles between quartz particles in foundry moulding sands Hofmann (1961). From Jasmund and Lagaly (1993).

Section 5.3.1). Free sedimentation is a pre-requisite for the size-fractionation of clays.

When attractive forces are operative, the particles no longer settle independently. At the upper end of the column the dispersion separates into a thin clear supernatant liquid and a sediment of apparently uniform visual characteristics. With time this interface slowly moves down. Structural sedimentation can also be observed when repulsive interparticle forces operating at high particle concentrations cause a certain ordering of the particles. This effect is pronounced for particles of anisotropic shape, which assume a preferred orientation (see Sections 5.6.1 and 5.6.4). Mixed types of

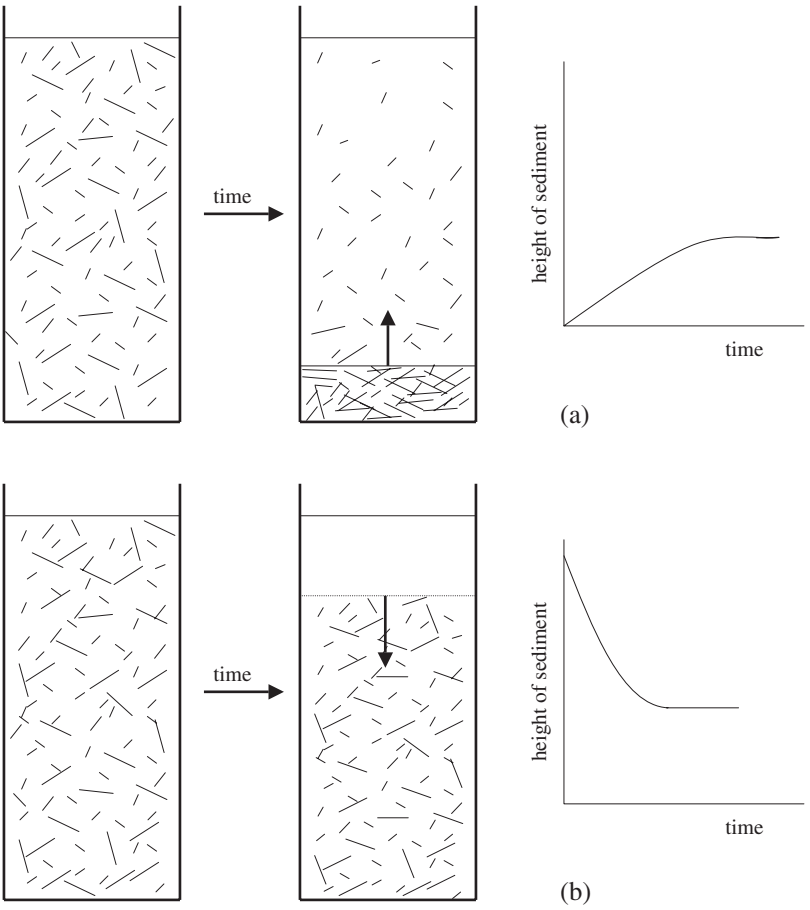

Fig. 5.32. Free (a) and structural (b) sedimentation.

sedimentation were also observed when a sediment grows on the bottom of the vessel and simultaneously a sediment separates at the top of the vessel.

Dispersions of Ca^{2+} and Mn^{2+} montmorillonite particles in the presence of 7 mmol/L $CaCl_2$ and 3 mmol/L $MnCl_2$ show a combination of free and structural sedimentation. In the first stage of an induction period, the dispersion occupies the entire volume of the column and only small amounts of particles settle. This is followed by a period of rapid sedimentation and finally by a stage of slow settling (Lapides and Heller-Kallai, 2002). The interaction between the particles causes several interesting phenomena including horizontal lenticular stratification during sedimentation, the dependence on the particle concentration, and the geometrical dimensions (diameter and height) of the columns. It seems that a weak interaction

between the particles stabilises the dispersion against sedimentation during the induction period. When the disturbance of the network of weakly connected particles during the induction period reaches a certain degree, the network falls apart, and the particles settle more rapidly.

Different types of sedimentation were observed with montmorillonite and kaolinite particles (treated with sodium diphosphate) in the presence of $FeCl_3$ solutions (newly prepared and aged solutions) and iron (hydr)oxide particles at different pHs (Pierre and Ma, 1997). The kaolinite dispersions showed a structural sedimentation at pH < 4 due to the formation of edge(+)/face(−) contacts and free sedimentation at higher pHs (Fig. 5.33). At $FeCl_3$ contents $\geqslant 3$ mmol/L the coagulated particles settled independently. At lower $FeCl_3$ concentrations structural sedimentation at pH < 4 changed into mixed-type sedimentation and free sedimentation with increasing pH. Ageing of the iron chloride solution changed the phase diagram, and the domain of structural sedimentation at $FeCl_3$ concentrations < 3 mmol/L was extended to high pH as a consequence of the formation of iron (hydr)oxide particles. A detailed discussion is difficult because even unaged $FeCl_3$ solutions form poly(hydroxo iron) species and colloidal iron (hydr)oxide particles such as goethite, α-FeO(OH), or akaganeite, β-FeO(OH) (Sections 5.4.8 and 5.4.9). The strong interaction between the iron ions and phosphate adsorbed at the edges should also be considered. In the presence of aluminium ions, structural sedimentation was observed at pH < 11 at all aluminium concentrations. No significant difference was found between aged and unaged aluminium salt solutions (Pierre and Ma, 1999).

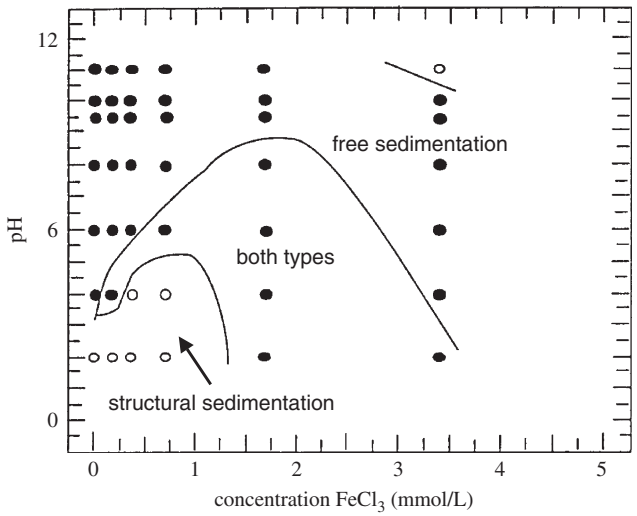

Fig. 5.33. Sedimentation behaviour of 0.5% dispersions of Na^+-kaolinite (Hydrite UF, Georgia Kaolin Comp., USA, treated with $Na_4P_2O_7$) in the presence of freshly prepared $FeCl_3$ solutions Pierre and Ma (1997).

The Na^+-montmorillonite particles of a 0.5% dispersion settled independently at $4 \leqslant pH \geqslant 10$ in the absence of $FeCl_3$. Structural sedimentation was observed at $pH < 4$ because of the formation of edge(+)/face(−) contacts between the particles. Addition of $FeCl_3$ or $AlCl_3$ solutions caused structural sedimentation at all pH values (Pierre and Ma, 1997, 1999).

The structure of the sediments was studied by SEM after supercritical drying with liquid CO_2 (Pierre, 1996). At low $FeCl_3$ concentrations some edge/face associations of kaolinite particles were observed but more typical was the agglomeration of small particles close to the edges of very larger particles. The montmorillonite particles looked like potato chips in a bag: while the accumulated sediments roughly maintained a uniform packing over longer distances, the other sediment types mostly comprised flocs with an increasingly open structure when going away from the centre of a floc. The accumulated sediments made at high $FeCl_3$ concentrations showed extensive face/face association so the sedimented particles had a preferred orientation.

The importance of sediment type to practical applications is illustrated in Fig. 5.34, which shows highly dispersed clay mineral layers and two types of aggregates. The sediments or filter cakes formed from these two types of dispersions are substantially different. Highly peptised dispersions of individual platelets (or silicate layers) form virtually impermeable filter cakes and compact, dense sediments that are difficult to stir. Formation of dense filter cakes finds applications in sealing operations, causes the plastering effect of drilling muds, and is of great importance to producing ceramic casts (see Chapter 10.1).

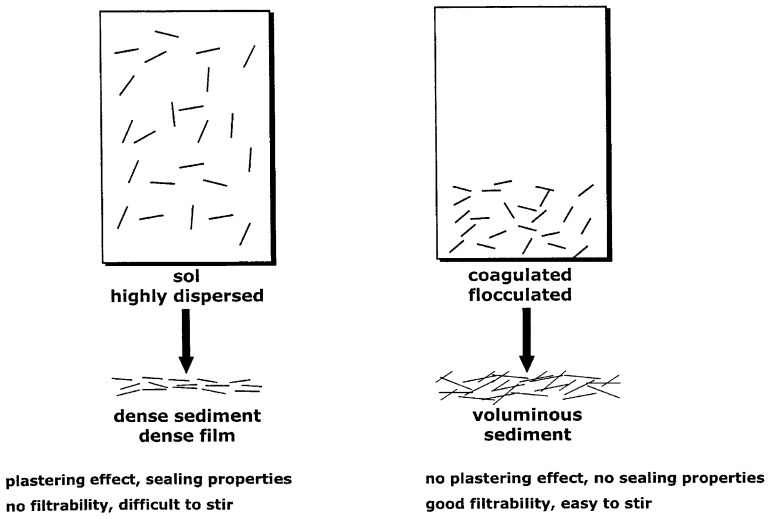

Fig. 5.34. Structure and properties of sediments formed from well dispersed (left) and aggregated (right) particles.

When the particle–particle interaction becomes attractive, the particles aggregate to some extent, and voluminous sediments are formed with large pores between the clay mineral plates. These sediments are easy to re-disperse by stirring and show no plastering effect. The simplest way of inducing the particles to settle, and changing the properties of the sediment, is to adjust the Na^+/Ca^{2+} ratio.

The influence of the different types of aggregation of montmorillonite particles (edge/face, face/face) on the filtration behaviour and the properties of the filter cakes obtained at two pressures (1.5 and 5.7 10^5 Pa) and three pH values was evaluated by Benna et al. (2001a, 2001b) (Fig. 5.35). At the lower applied pressure, the filter cake obtained from the acidic dispersion was thinner and less permeable than the filter

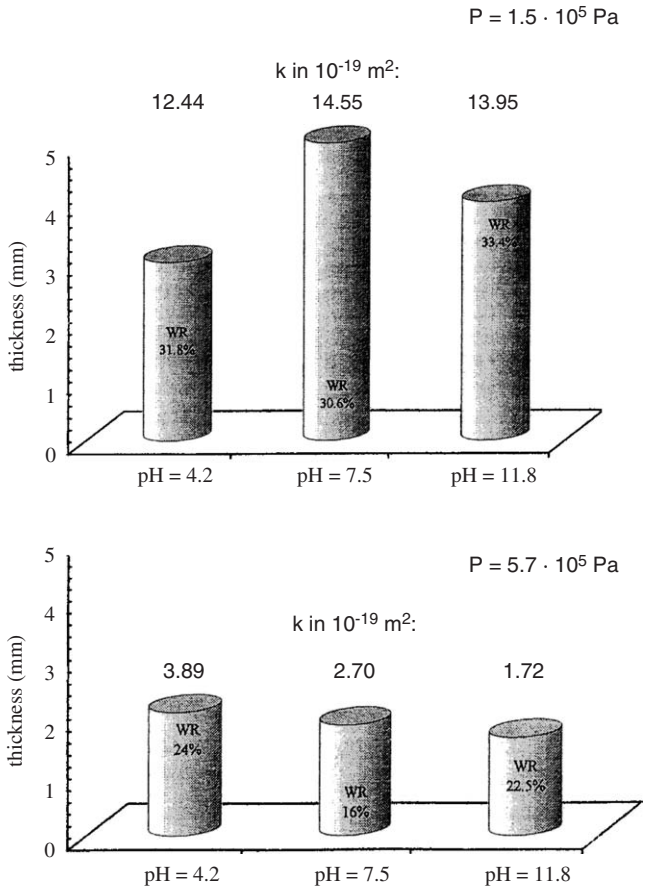

Fig. 5.35. Volume, water retention (WR in percentage of the water content before filtration), and permeability (Darcy's low) of filter cakes obtained from Na^+-bentonite (Wyoming) dispersions at three pH and two filtration pressures. From Benna et al. (2001b).

cakes from dispersions at pH 7.5 and 11.8. The largest cake volume and the highest permeability were observed at pH 7.5. In contrast to the edge(+)/face(−) network at acidic pH, the electrostatic repulsion between the faces increased cake volume and permeability. A certain degree of elasticity of the band-type structure in comparison with the card-house structure (Weiss and Frank, 1961; Weiss, 1962) may also contribute to the larger cake volume when band-type networks are formed at pH > 4.2. A somewhat stronger aggregation occurs at higher pH and electrolyte concentrations, reducing the volume and permeability. The higher applied pressure may overcome the double layer repulsion, and the cake volume and permeability at pH > 4.2 became smaller than for the acidic cake. The calculated and observed swelling pressure for plate–plate distances of 10 nm and 5 nm is 10^5 Pa and 5×10^5 Pa, respectively (Lubetkin et al., 1984; Huerta et al., 1992).

The settling behaviour of dispersed palygorskite is important in practical applications. Whereas the particles settle in dispersions with palygorskite contents $\leqslant 0.1\%$, settling is not observed at higher solid contents. Even if the force between the particles below c_K is repulsive, the highly anisometric particles form a network structure throughout the mass of the suspension. This is another example of repulsive gels (see Section 5.6.4).

The relation between polymer flocculation, sedimentation and filtration rate, and sediment volume was studied much earlier for kaolinite and neutral polyacrylamide (Dollimore and Horridge, 1973). The maximum sedimentation and filtration rates were always observed at pH ~5.8, irrespective of polymer concentration. The authors concluded that pH ~5.8 is the point of zero edge charge, and the kaolinite particles form card-house type aggregates. The sediment volume was high at pH < 5.8, and increased weakly with pH. At pH > 5.8 face(−)/face(−) aggregation began to form, and sediment volume decreased steeply with rising pH. Thus, sediment permeability was highest at pH ~5.8.

As montmorillonite is easily coagulated by salts or flocculated by polymers, this clay mineral can be used as a clarifying agent, especially when added to streams that naturally have a low concentration of dispersed particles.

5.6.4. Sol–Gel Transition

Transition from a sol into a gel and vice versa is very important in many practical applications because this phenomenon strongly influences flow behaviour, sedimentation, agitation, and filtration (Benna et al., 2001a), and lies behind time-dependent rheological behaviour. Gels are usually described as dispersed systems that show a degree of stiffness. That is, the vessel containing the dispersion can be upturned without the dispersion flowing out. Gels also show a degree of elasticity, and creeping measurements may be used to distinguish between sol and gel (Abend and Lagaly, 2000).

The experiment is briefly explained in Fig. 5.36. When a constant shear stress τ_0 is applied to the dispersion within time t_e, the strain increases as shown. At $t = t_e$ the

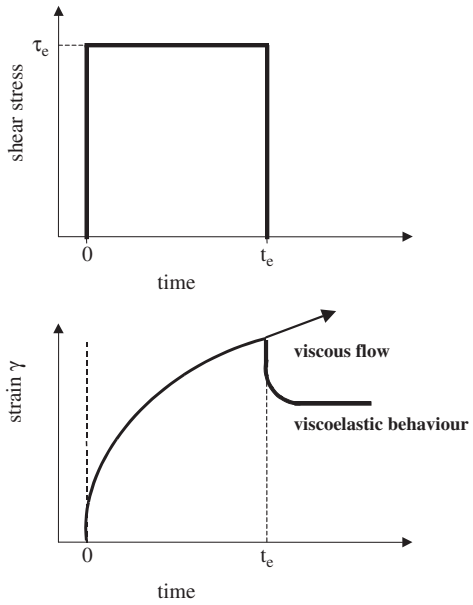

Fig. 5.36. Creeping experiments: The strain (relative deformation) γ is shown as a function of time t. During the time t_e the sample is deformed by applying the constant shear stress τ_e. At $t = t_e$ τ is set to zero and the sample relaxes (viscoelastic behaviour, full line) or flows further (viscous fluid, dotted line).

shear stress is set to zero, the sample relaxes, and in case of a viscoelastic behaviour, the strain decreases to a plateau. If the dispersion is a viscous fluid, the strain increases further. The reversible part of the compliance ($J = \gamma/\tau_0$) is $J_{rev} = 100\ (J_0 + J_R)/(J_0 + J_R + J_N)$. The position of the plateau gives the elastic ($J_0 + J_R$) and viscous (J_N) contributions to the compliance. A sol shows $J_{rev} = 0$, a gel $J_{rev} > 0$.

Fig. 5.37 shows the reversible compliance of Na^+-montmorillonite dispersion as a function of the NaCl concentration. $J_{rev} > 0$ indicates gel formation at low and high salt concentrations. Due to the electroviscous effect (Fig. 5.28), the dispersion stiffens at low salt concentrations and high montmorillonite contents (above 3–3.5% w/w). This type of gel is called a 'repulsive gel' although this is incorrect because it is not the gel but the interparticle force that is repulsive (Norrish, 1954; Callaghan and Ottewill, 1974; Rand et al., 1980; Ramsay, 1986; Sohm and Tadros, 1989; Ramsay and Lindner, 1993; Mourchid et al., 1995; Lott et al., 1996; Kroon et al., 1998; Mongondry et al., 2005). Addition of salt reduces the thickness of the diffuse ionic layer, the particles become more mobile again, and the gel turns into a sol. In a similar way, colloidal rod-like boehmite particles (γ-AlO(OH)) form repulsive gels at solid contents of 0.67% in solutions containing less than 10^{-4} mol/L NaCl. Despite

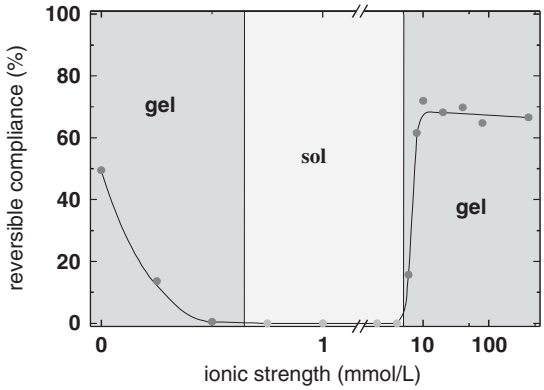

Fig. 5.37. Reversible compliance as a function of the NaCl concentration. 4% (w/w) dispersion of Na^+-montmorillonite (M 50, Ordu Turkey). From Abend and Lagaly (2000).

the repulsive forces, the particles are immobilised in a preferred orientation as indicated by birefringence measurements (Buining et al., 1994).

Temperature-dependent changes of Na^+-smectite gels were investigated using synchrotron-based small-angle scattering (Pons et al., 1981). A gel containing 17% (w/w) Na^+-montmorillonite (Wyoming) was studied before and after several cooling–heating cycles between –70 °C and room temperature. Below –10 °C the silicate layers were aggregated into 500–600 nm thick particles composed of domains of 4–5 silicate layers with two water layers between them. These domains were separated by zones of one or two silicate layers spaced less regularly by one, three or four layers of water. During heating to room temperature the interlayer spaces took up water molecules to form discrete hydrates with up to four water layers. This process proceeded slowly and could be followed by the changes in scattering patterns. Intercalation of more than four water layers was accompanied by a large expansion of the interlayer space, giving rise to a gel in which assemblages of (on average) 4–5 almost parallel silicate layers were still retained. Isolated and no longer parallel silicate layers filled the space between these units. About 25% of the layers were distributed as single layers. An interesting point is that the domains of 4–5 layers (in distances of about 8 nm) reflected the structure of the particle in the frozen gels. As the changes during cooling–heating cycles were nearly reversible, the deviation of the silicate layers from parallel orientation during heating must be modest, say, by no more than 15°. Several causes of this peculiar behaviour were mentioned (Pons et al., 1982). The influence of layer charge distribution was noted for beidellite gels where the layers constituting the domains remained at spacings of 1.54 nm and did not move in distances of 7–8 nm, as in montmorillonite, saponite, and hectorite (Pons et al., 1982). Organisation of the layers at different levels was also observed in TEM and SAXS studies (Hetzel et al., 1994; Faisander et al., 1998).

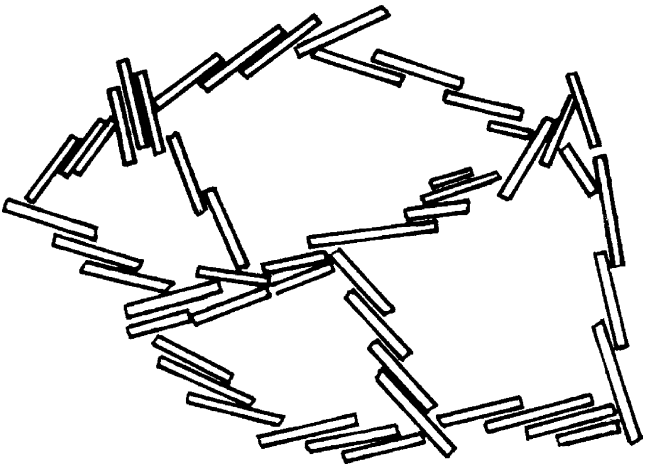

Fig. 5.38. Transition between band-type and card-house aggregation: formation of card-house contacts in band-type assemblages. Adapted from O'Brien (1971). From Lagaly et al. (1997).

Gel formation at salt concentrations above the critical coagulation concentration is caused by attractive forces between the particles when the van der Waals attraction dominates the electrostatic repulsion ('attractive gel'). At lower salt concentration the interaction is attractive between edges(−) and edges(−) and between edges(−) and faces(−); at higher salt concentrations it becomes attractive between the faces. It is likely there is a continuous transition from the edge(−)/face(−) (card-house) to the face(−)/face(−) aggregation (band-type structure) (Fig. 5.38). If the forces between the faces are strongly attractive at high salt concentration, the network contracts and disintegrates (Fig. 5.29b, c). Distinct particles form, the dispersion destabilises forming flocs that settle into a sediment.

The domains of sol, repulsive gel, attractive gel, and flocs are clearly seen in the phase diagrams (Fig. 5.39). The large domain of sol separates the two gel types. As expected, the repulsive gel forms only when the particle concentration is $> 3\%$ (w/w) and 3.5% (w/w), respectively. The salt concentration at which the gel liquefies into the sol increases with particle concentration because more densely packed particles require thinner diffuse ionic layers to become mobile again. If there is attraction between the particles, the attractive gel also has smaller solid contents because band-type aggregates can span a distinctly larger volume. Flocs are formed only at the highest salt concentration and moderately high particle concentrations. When Na^+ ions are replaced by K^+ and Cs^+ ions, the attraction between the particles becomes stronger because these cations are more strongly adsorbed in the Stern layer. The band-type aggregates are more stable resisting floc formation. A 2% (w/w) Na^+-montmorillonite dispersion does not coagulate into flocs, even at the highest KCl and

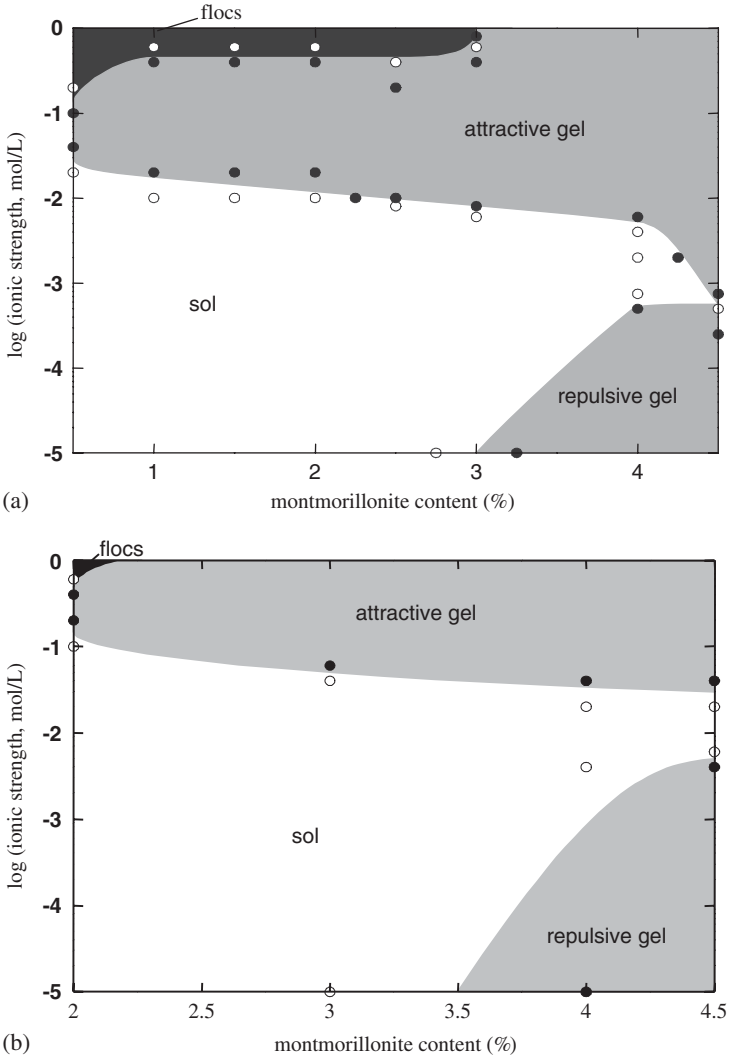

Fig. 5.39. Sol–gel diagram for Na^+-montmorillonite and NaCl. (a) Montmorillonite of Ordu, Turkey (M50); (b) montmorillonite of Wyoming (M 40A). From Abend and Lagaly (2000).

CsCl concentration, but remains in the gel state (Fig. 5.40). The liquefying action of phosphate addition (Penner and Lagaly, 2001) is also seen in the sol–gel diagram.

The difference between Laponite and montmorillonite is also seen in the phase diagram reported by (Mourchid et al., 1995; Mongondry et al., 2005). In Laponite

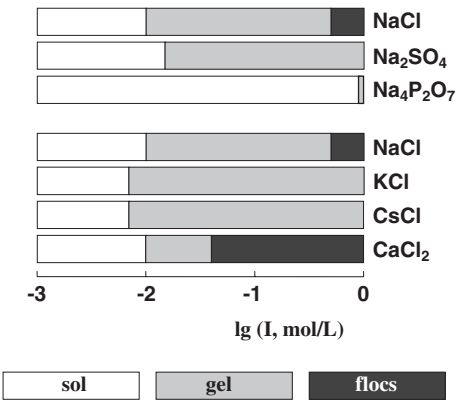

Fig. 5.40. Effect of salts on the transitions sol–gel and gel-flocs. 2% (w/w) Na^+-montmorillonite (Ordu, Turkey, M 50), I = ionic strength. From Abend and Lagaly (2000).

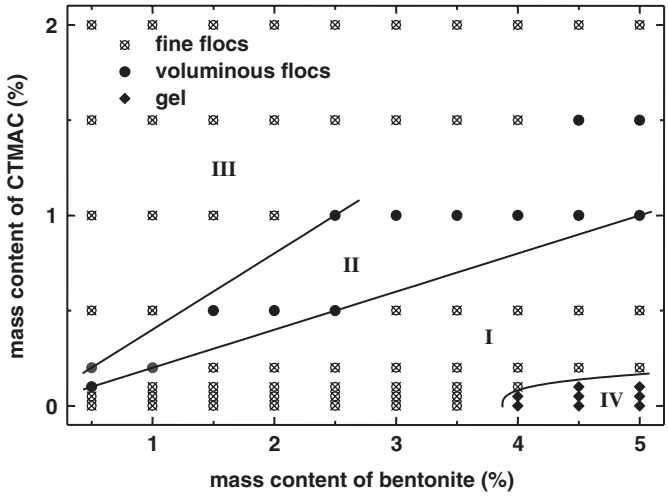

Fig. 5.41. Phase diagram of bentonite dispersions (Wyoming) in the presence of hexadecyl trimethylammonium chloride. From Janek and Lagaly (2002).

the gel domain extends to lower solid contents at higher salt concentrations, distinctly different from the sol–gel diagrams of montmorillonites (Fig. 5.39).

The addition of cationic surfactants impedes gel formation. Gels only form at low surfactant concentrations and high montmorillonite contents (Fig. 5.41). Outside the gel domain three types of dispersions were observed (Tahani et al., 1999; Janek and Lagaly, 2002; Kuwaharada et al., 2002). In domain I the dispersion consisted of fine flocs that separated into a voluminous sediment and a clear supernatant. When the

addition of the surfactant corresponded to the CEC of the bentonite, the particles showed maximum hydrophobicity, forming voluminous flocs that hardly settled (domain II), and the sediment volume reached its maximum value (Kuwaharada et al., 2002). At surfactant additions corresponding to twice the CEC, all particles were re-charged and again formed fine flocs (domain III). However, these fine flocs settled to distinctly thinner sediments than the fine flocs of domain I because the flocs were more densely packed, immobilising smaller volumes of water.

Different types of dispersions showed different flow behaviour: shear thinning flow and Bingham flow in domain I, plastic flow at the I/II transition, and Newtonian flow in domain III (Janek and Lagaly, 2002).

5.6.5. *Thixotropy*

Attractive gels often show thixotropic behaviour. In this case the gel is liquefied by shaking, stirring, or pouring but stiffens again with time. Stiffening and liquefaction are reversible. When mechanical energy is applied to a network of weakly adhering particles, contacts are broken, and the network disintegrates into fragments. During resting, the fragments driven by Brownian motion of the solvent molecules came into contact, an extended network reforms, and the liquefied dispersion becomes gel-like (Hofmann, 1952). This reversible process requires moderately attractive particle-particle interactions. Thixotropy is a very important property in many practical applications of clay, kaolin, and bentonite dispersions.

Thixotropic behaviour and the resting time required for gelation are highly dependent on the solid content of the dispersion. In simple experiments Hofmann (1952) determined the solid content required to form a gel that liquefied by shaking. The gel point was reached when the tubes could be turned without the dispersion flowing out. In modern viscometers, thixotropy (and antithixotropy) is indicated by the hysteresis between the up and down curves in shear stress-shear rate diagrams (see e.g., Lagaly, 1989). Dispersions of allophane show thixotropic behaviour (Wells and Theng, 1985).

Antithixotropic behaviour is not uncommon for clay dispersions. In this case the dispersions stiffen by (in most cases modest) shaking, inducing the particles to move into contact positions. It is therefore often observed that the up and down curves cross at a certain shear rate (Brandenburg and Lagaly, 1988).

Dispersions of Laponite, a synthetic hectorite-like mineral, often show an unusual thixotropic behaviour, limiting the practical uses of such materials. After cessation of shearing, the viscosity increases over a long period. Willenbacher (1996) observed a monotonic increase of the complex viscosity, $|\eta|^* = \varpi^{-1}(G'^2 + G''^2)^{1/2}$, of 1–3% (w/w) Laponite RD dispersions. An equilibrium value was not reached even after 16 days. The re-organisation is a co-operative, self-delaying process where the increasing rigidity of the network increasingly retards the mobility and orientation of the particles. This effect is probably related to the reduced anisotropy of the Laponite particles compared with montmorillonite, and hence the particles cannot align over

long distances as in montmorillonite gels. The sol–gel transition involves the formation of oriented micro-domains of particles (Mourchid et al., 1995).

5.6.6. Hydrogels of Organo-Clays

Garret and Walker (1962) described formation of gels of low-charge vermiculites in water after replacing the inorganic exchangeable cations by butylammonium ions. The gels are formed by delamination of the butylammonium vermiculite particles (Rausell-Colom, 1964; Smalley et al., 1989, 2001; Braganza et al., 1990; Hatharasinghe et al., 2000). This very peculiar behaviour seems to be related to the organisation of the water molecules between the alkyl chains (Lagaly, 1987b). The swelling of butylammonium vermiculites cannot be described by the DLVO theory because hydrophobic interactions have also to be considered. Smalley and co-workers (Smalley et al., 1989; Smalley, 1994a, 1994b) proposed a model for the swelling and gel formation of butylammonium vermiculite based on the Coulombic attraction theory (Sogami theory), postulating the existence of long-range attraction between the vermiculite layers.

Rausell-Colom and Salvador (1971a, 1971b) described gel formation of vermiculites in solutions of amino acids such as γ-aminobutyric acid, ω-aminocaproic acid, and ornithine. Repulsion between the carboxylate groups, accumulated in the interlayer space, promotes particle delamination. The gels are composed of independently diffracting large particles of silicate layers (19 layers spaced around $d = 13.5\,\text{nm}$; Santa Ollala vermiculite in the presence of $2 \times 10^{-2}\,\text{mol/L}$ ornithine, confined by a pressure of $99.4\,\text{g/cm}^2$). These particles have an average thickness of 260 nm and are completely separated from each other by the solution phase. Within the particles, ordered coherent domains (with about 6 silicate layers at equal distances of 13.1 nm) are separated by layers also in parallel orientation but less regularly spaced (Rausell-Colom et al., 1989).

Stable colloidal dispersions of fully delaminated montmorillonites were obtained by exchanging the inorganic interlayer cations by betaines $(CH_3)_3\,N^+\text{-}(CH_2)_n\text{-}CO_2^-$ Li^+ (Na^+). These dispersions were more stable against salts than Li^+ and Na^+ montmorillonites (Section 5.4.5).

5.6.7. Gelation in Organic Solvents

Thickening of organic solvents by hydrophobised bentonites (in a few cases also by hydrophobised clays and kaolins) is needed in many practical applications (Jones, 1983; Jasmund and Lagaly, 1993). Gelation of these dispersions often requires small amounts of polar additives (water, ethanol) to increase gel strength (Granquist and McAtee, 1963; Jasmund and Lagaly, 1993; Gherardi et al., 1996; Moraru, 2001).

The influence of small amounts of alkanols on gel formation of an industrial organo-bentonite in butyl acetate is shown in Fig. 5.42. A content of 11% (w/w) bentonite was required to form a gel. Addition of methanol reduced the solid content

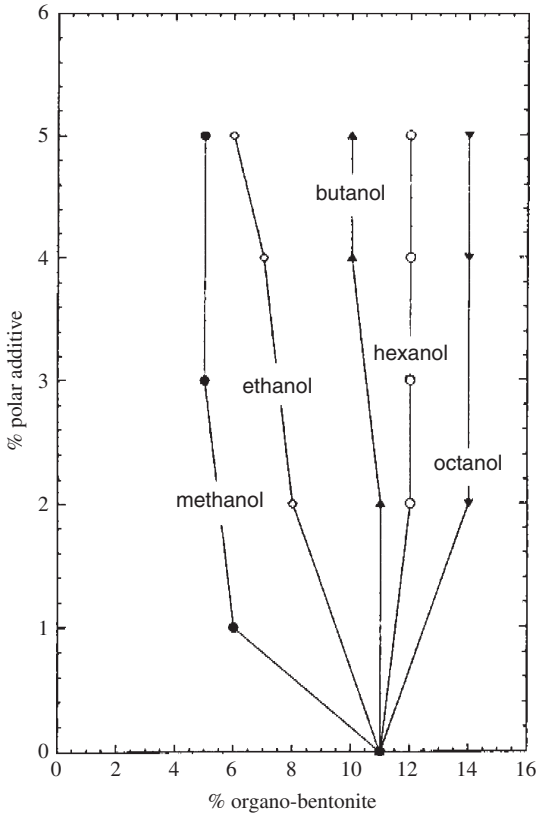

Fig. 5.42. Sol–gel diagram of an industrial organo-bentonite in butyl acetate in the presence of alcohols as polar additives. From Gherardi et al. (1996).

to about 5%. As the chain length of the alcohol increases, the phase boundary moved to higher solid contents, even above 11%. Hexanol and octanol no longer acted as stiffening agents but produced a liquefying effect (Gherardi et al., 1996).

The influence of polar additives was explained by the strong orientation of the adsorbed water molecules, giving rise to giant dipole moments on, and hydrogen bonding between, the particles (Moraru, 2001). Beyond a certain chain length alcohols evidently interfere with the formation of the network of hydrogen bonds between adjacent dispersed particles.

In referring to practical applications, the following effect is noted. Organophilic bentonites are usually prepared at an industrial scale by reacting the bentonite with quaternary alkylammonium ions without removing the excess cationic surfactants. The presence of excess alkylammonium ions can strongly influence the flow behaviour of dispersions in organic solvents (Fig. 5.43). A 1% dispersion of a technical

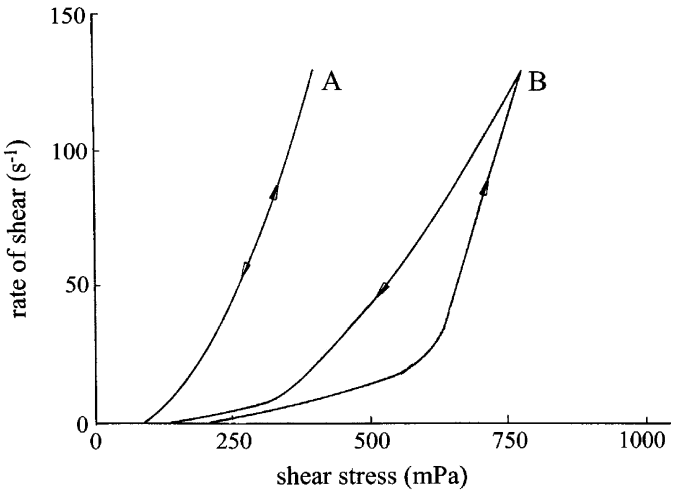

Fig. 5.43. Flow behaviour (rate of shear against shear stress) of 1% (w/w) dispersions of dioctadecyl dimethylammonium bentonite in xylene containing 0.2% ethanol and 0.02% water. (A) Organo bentonite as obtained with an excess of the alkylammonium salt (1.22 mmol N/g bentonite); (B) after washing out the excess of the alkylammonium salt (1.02 mmol N/g bentonite).

dioctadecyl dimethylammonium bentonite in xylene (activated with 0.2% ethanol and 0.02% water) showed low shear stress values. The excess surfactant cations i.e. the amount not bound by cation exchange but adsorbed together with the exchangeable cations, enhanced electrostatic repulsion by acting as a lubricant between the particles. When these cations were removed by washing, the dispersion stiffened and showed pronounced thixotropy. This example shows that even small changes in surfactant/bentonite ratio can markedly change flow properties and thixotropic (or antithixotropic) behaviour.

5.7. LAYER-BY-LAYER AGGREGATION: CLAY HYBRID FILMS

The formation and properties of hybrid films of clay minerals bridge clay colloid science and materials science. If appropriate conditions are selected, clay mineral platelets settle to form a sediment where the platelets preferentially adopt a parallel orientation (see Section 5.6.3). Drying produces oriented films that are often used in spectroscopic investigations and X-ray diffraction and are considered for possible new applications of clay minerals (Fitch et al., 1998; Fendler, 2001). Such films can also be prepared using the established methods of spin coating.

Possible applications require functionalisation of the films by introducing active compounds with the desired properties (optical, photochemical, electrochemical,

redox, acid/base properties). The diversity of designs is largely extended by building up hybrid films. Such films are constructed by the layer-by-layer techniques producing layers of clay mineral platelets that alternate with layers of organic materials, mainly long-chain compounds and polymers. Two methods were used.

Decher and co-workers (Decher and Schmitt, 1992; Lvov et al., 1993) studied the layer-by-layer superposition of polyanions and polycations on a substrate. These hybrid films are sometimes called "fuzzy assemblies" because of the lack of order in the film. Replacing the layers of the polyanions by layers of clay mineral platelets leads to clay-polymer hybrid films (Lvov et al., 1996; Kotov et al., 1997). The properties of these films, in particular their non-linear optical properties, are influenced by the textural organisation. AFM shows that these films never have a smooth surface (van Duffel et al., 1999, 2001; Schoonheydt, 2002).

The second method is based on the Langmuir–Blodgett technique. Kuhn and co-workers (Kuhn and Möbius, 1971; Kuhn, 1981; see also Möbius, 1978) studied the energy transfer between donor and acceptor molecules across layers of highly ordered alkyl chains. Langmuir–Blodgett films containing clay mineral particles can be prepared in two ways. The clay mineral is dispersed in the water subphase in the Langmuir trough and the water surface is covered with a chloroform solution of surfactant cations. The clay mineral platelets adsorb the cations and arrange in a floating film at the chloroform/water interface from where they can be picked up on to glass plates using the Langmuir-Blodgett technique (Umemura et al., 2001, 2002; Schoonheydt, 2002) (see Chapter 3). In a variant method, hydrophobised clay mineral platelets are dispersed in chloroform, spread over the water surface in the trough, and picked up on to hydrophobised glass plates (Kotov et al., 1994; Hotta et al., 1997).

Because of their optical and photochemical functionality the clay hybrid films so produced constitute interesting new materials for non-linear optics and sensors (Eckle and Decher, G., 2001; Fendler, 2001; van Duffel et al., 2001; Schoonheydt, 2002; Umemura et al., 2002) (see Chapter 3).

5.8. NANOPARTICLE GROWTH IN CLAYS[11]

Clay mineral particles provide confined volumes for the formation of colloidal particles, in particular of nano-size dimensions. The preparation of nanoparticles received a great deal of attention in the past few years because of their potential applications as nanostructured catalysts. As the growing nanoparticles have to be stabilised against aggregation, it is important to choose a suitable stabilising agent and process. The most commonly used stabilising agents are surfactants and polymers (Mayer and Antonietti, 1998). Colloid particles of controlled size were

[11]In co-operation with I. Dékány.

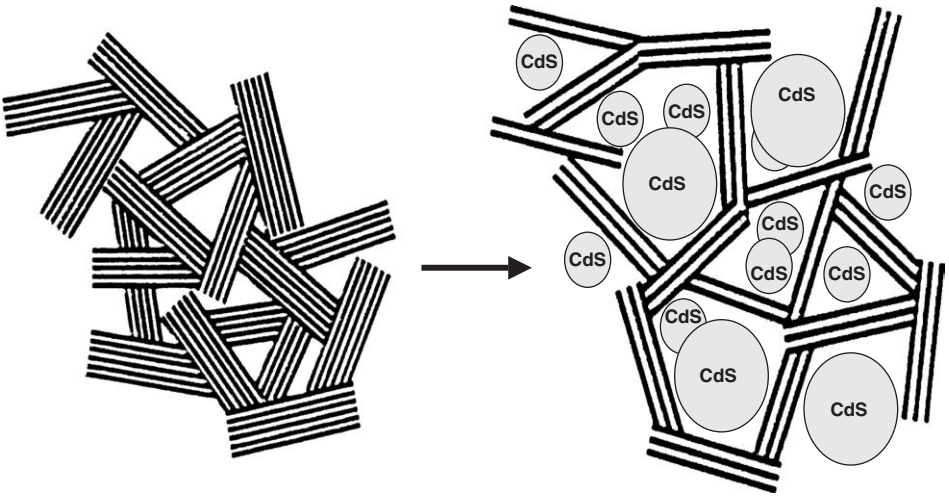

Fig. 5.44. Schematic illustration of nanophase reactors formed by aggregating clay mineral particles. CdS particles were nucleated in the methanol/cyclohexane adsorption layer around hexadecylpyridinium montmorillonite layers and particles Dékány et al. (1995).

generated within the internal space of micelles and microemulsions (Chen et al., 1999; Chiang, 2001; Ingelsten et al., 2001).

Another concept of recent development is to use the confined space between particles or layers of clay minerals as a nanoreactor, i.e. nanoparticle growth is limited by the clay mineral particles or layers surrounding the nanoparticles (Fig. 5.44).

Formation of colloidal metal particles was observed decades ago during the oxidation of octahedral Fe^{2+} ions in micas by interlayer silver cations. The silver atoms aggregated to Ag^0 particles outside the interlayer spaces (Sayin et al., 1979). Giannelis et al. (1988) described the diffusion of ruthenium atoms and clusters out of the interlayer space and aggregation between the clay mineral layers. Dékány and coworkers (Dékány, 1996; Király et al., 1996a; Szûcs et al., 1998; Dékány et al., 1999) reported the formation and properties of noble metal nanoparticles in great detail. Under appropriate experimental conditions metal particles are also observed between the silicate layers. The corresponding salts are usually dissolved in the confined volume of the interlayer space of intercalated clay minerals or between aggregated layers, and the absorbed metal ions are then reduced. In a typical experiment, montmorillonite modified by cationic surfactants (alkylammonium and alkylpyridinium ions) was first swollen in toluene. Palladium acetate (highly soluble in the aromatic solvent) was then adsorbed in the interlayer space of the organophilic montmorillonite and reduced to Pd^0 particles by ethanol at room temperature.

Nanosized palladium and silver particles were also prepared between kaolinite layers (Figs. 5.45 and 5.46). The large specific surface area necessary for the growth

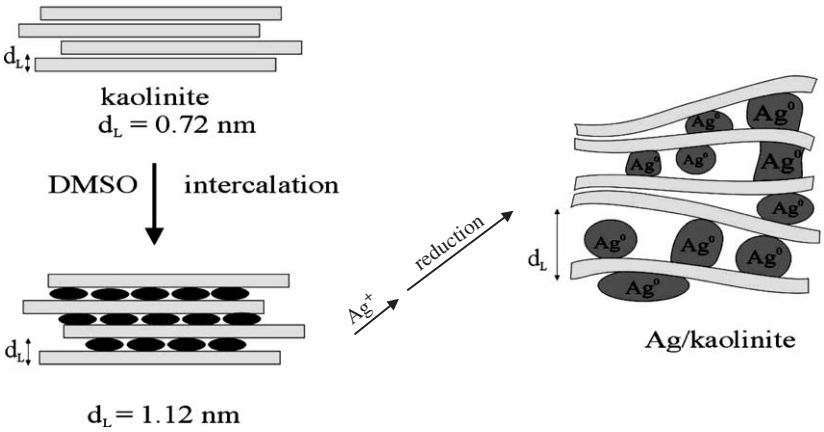

Fig. 5.45. Formation of silver nanoparticles between kaolinite particles.

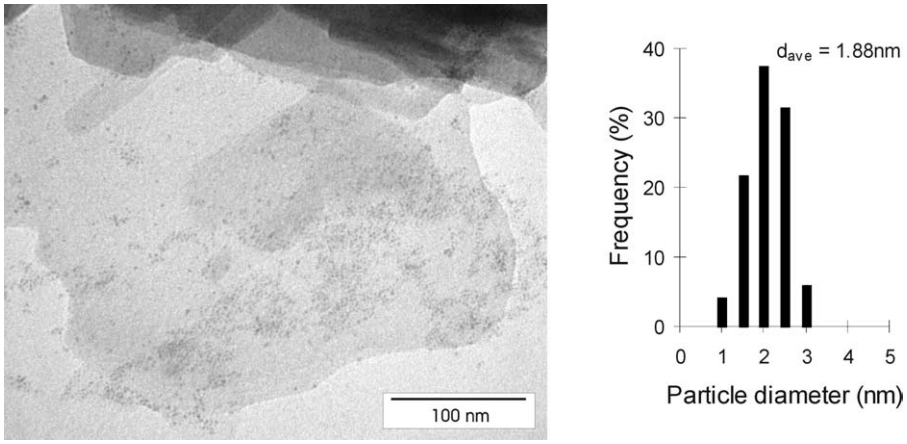

Fig. 5.46. Transmission electron micrograph of silver nanoparticles in kaolinite.

of the nanoparticles was created by intercalation of hydrazine, DMSO, and potassium acetate.

Several semiconductor and transition metal sulphides and oxides such as CdS, ZnS, FeS, Fe_2O_3, and TiO_2 were prepared by precipitation (e.g., Cd^{2+} and Zn^{2+} cations with H_2S), or hydrolysis in the limited volume between the layers of hydrophobised or pillared montmorillonite and layered double hydroxides (Fig. 5.44). These sulphide(oxide)/clay mineral nanocomposites provide new types of catalysts (Dékány, 1996; Dékány et al., 1995, 1996, 1999). Iron oxide nanoparticles on the

montmorillonite surface probably act as the nuclei for the formation of carbon nanotubes by decomposition of acetylene (Gournis et al., 2002).

In another procedure, the surface of the support is not hydrophobised by long alkyl chains before nanoparticle preparation, in contrast to the procedures described before. This simplifies the interpretation of catalytic processes because they are not influenced by the presence of alkyl chains. The preparation consists of two steps. First, the precursor ions are adsorbed on the surface of a dispersed clay mineral, e.g., on montmorillonite and saponite dispersed in toluene. Adsorption conditions have to be selected to ensure complete adsorption of the added precursor ions by the clay mineral. In the second step, the precursor ions in the adsorption layer are reduced. This is achieved by adding a reducing agent such as ethanol that is preferentially adsorbed by the clay mineral surface, as shown by test experiments. The important requirement is that no particles are formed in the bulk phase (dispersion medium). The size of such particles would significantly exceed the size of nanostructured materials (1–50 nm). Clay minerals are especially suitable because the adsorption of the precursor as well as the subsequent nanoparticle formation and growth proceed within the interlayer space (as nanophase reactor).

Polymers such as poly(vinyl pyrrolidone) and poly(diallyl dimethylammonium chloride) in combination with clay minerals were also used in the synthesis of nanoparticles (Papp and Dékány, 2003). For instance, Pd^0 particles were prepared in the presence of these polymers and well crystallised kaolinite intercalated with DMSO. The interlayer formation of nanoparticles is indicated by X-ray measurements. The presence of nanoparticles is also verified by TEM.

REFERENCES

Abend, S., Lagaly, G., 2000. Sol–gel transitions of sodium montmorillonite dispersions. Applied Clay Science 16, 201–227.

Adachi, Y., Nakaishi, K., Tamaki, M., 1998. Viscosity of a dilute suspension of sodium montmorillonite in an electrostatically stable condition. Journal of Colloid and Interface Science 198, 100–105.

Akari, S., Schrepp, W., Horn, D., 1996. Imaging of single polyethyleneimine polymers adsorbed on negatively charged latex spheres by chemical force microscopy. Langmuir 12, 857–860.

Alince, B., Bednar, F., van de Ven, T.G.M., 2001. Deposition of calcium carbonate particles on fiber surfaces induced by cationic polyelectrolyte and bentonite. Colloids and Surfaces A 190, 71–80.

Allen, T., 1997. Particle Size Measurement, vols. 1 and 2. Chapman & Hall, London.

Alperovitch, N., Shainberg, I., Keren, R., Singer, M.J., 1985. Effect of clay mineralogy and aluminum and iron oxides on the hydraulic conductivity of clay–sand mixtures. Clays and Clay Minerals 33, 443–450.

Anandarajah, A., 1997. Influence of particle orientation on one-dimensional compression of montmorillonite. Journal of Colloid and Interface Science 194, 44–52.

Andreasen, A.H.M., 1931. Einige Beiträge zur Erörterung der Feinheitsanalyse und ihrer Resultate. Archiv für Pflanzenbau. p. 245, see also Angewandte Chemie, 1935, p. 283.

Andreasen, A.H.M., 1935. Beispiele der Verwendung der Pipettenmethode bei der Feinheitsanalyse unter besonderer Berücksichtigung von Mineralfarben. Angewandte Chemie 48, 283–285.

Arias, M., Barral, M.T., Diaz-Fierros, F., 1995. Effects of iron and aluminium oxides on the colloidal and surface properties of kaolin. Clays and Clay Minerals 43, 406–416.

Atterberg, A., 1911. Die Plastizität der Tone. Internationale Mitteilungen der Bodenkunde I, 4–37.

Atterberg, A., 1912. Die Konsistenz und Bindigkeit der Boden. Interne Mitteilungen der Bodenkunde. II.

Avena, M.J., de Pauli, C.P., 1998. Proton adsorption and electrokinetics of an Argentinian montmorillonite. Journal of Colloid and Interface Science 202, 195–204.

Avery, R.G., Ramsay, J.D.F., 1986. Colloidal properties of synthetic hectorite clay dispersions. III. Light and small angle neutron scattering. Journal of Colloid and Interface Science 109, 448–454.

Bain, D.C., Smith, B.F.L., 1987. Chemical analysis. In: Wilson, M.J. (Ed.), A Handbook of Determinative Methods in Clay Mineralogy. Blackie, Glasgow, pp. 248–274.

Barclay, L.M., Ottewill, R.H., 1970. Measurement of forces between colloidal particles. Special Discussions of the Faraday Society, 138–147.

Barshad, I., 1969. Preparation of H saturated montmorillonite. Soil Science 108, 38–42.

Ben Brahim, J., Armağan, N., Besson, G., Tchoubar, C., 1986. Methode diffractometrique de characterisation des etats d′hydratation des smectites stabilité relative des couches eau inserées. Clay Minerals 21, 111–124.

Benna, M., Kbir-Ariguib, N., Clinard, C., Bergaya, F., 2001a. Static filtration of purified bentonite clay suspensions. Effect of clay content. Applied Clay Science 19, 103–120.

Benna, M., Kbir-Ariguib, N., Clinard, C., Bergaya, F., 2001b. Card-house microstructure of purified sodium montmorillonite gels evidenced by filtration properties at different pH. Progress in Colloid and Polymer Science 117, 204–210.

Benna, M., Kbir-Ariguib, N., Magnin, A., Bergaya, F., 1999. Effect of pH on rheological properties of purified sodium bentonite suspensions. Journal of Colloid and Interface Science 218, 442–455.

Bergman, R., Swenson, J., Börjesson, L., Jacobsson, P., 2000. Dielectric study of supercooled 2D water in a vermiculite clay. Journal of Chemical Physics 113, 357–363.

Bertram, R., Gessner, W., Müller, D., Görz, H., Schönherr, S., 1985. Zur Art der Al-Kationen in hochbasischen, hochkonzentrierten Aluminiumchloridlösungen. Zeitschrift für Anorganische und Allgemeine Chemie 525, 14–22.

Besson, G., Mifsud, C., Tchoubar, D.D., Mering, J., 1974. Order and disorder relations in the distribution of the substitutions in smectites, illites and vermiculites. Clays and Clay Minerals 22, 379–384.

Beyer, J., Graf von Reichenbach, H., 2002. An extended revision of the interlayer structures of one- and two-layer hydrates of Na-vermiculite. Clay Minerals 37, 157–168.

Billingham, J., Breen, C., Rawson, J.O., Yarwood, J., Mann, B.E., 1997. Adsorption of polycations on clays: a comparative in situ study using ^{133}CS and ^{23}Na solution phase NMR. Journal of Colloid and Interface Science 193, 183–189.

Blackmore, A.V., 1973. Aggregation of clay by the products of iron(III) hydrolysis. Australian Journal of Soil Research 11, 75–82.

Böhmer, M.R., Koopal, L.K., 1992. Adsorption of ionic surfactants on variable-charge surfaces. 1. Charge effects and structure of the adsorbed layer. Langmuir 8, 2649–2665.

Bolland, M.D.A., Posner, A.M., Quirk, J.P., 1980. pH-independent and pH-dependent surface charges on kaolinite. Clays and Clay Minerals 28, 412–418.

Borkovec, M., Wu, A., Degavics, G., Laggner, P., Sticher, H., 1993. Surface area and size distributions of soil particles. Colloids Surfaces A 73, 65–76.

Bottero, J.Y., Axelos, M., Tchoubar, D., Cases, J.M., Fripiat, J.J., Fiessinger, F., 1987. Mechanism of formation of aluminum trihydroxide from Keggin Al_{13} polymers. Journal of Colloid and Interface Science 117, 47–57.

Bottero, J.Y., Bruant, M., Cases, J.M., Canet, D., Fiessinger, F., 1988. Adsorption of non-ionic polyacrylate on sodium montmorillonite. Journal of Colloid and Interface Science 124, 515–527.

Bottero, J.Y., Cases, J.M., Fiessinger, F., Poirier, J.E., 1980. Studies of hydrolyzed aluminum chloride solutions. 1. Nature of aluminum species and composition of aqueous solutions. Journal of Physical Chemistry 84, 2933–2939.

Bottero, J.Y., Tchoubar, D., Arnaud, M., Quienne, P., 1991. Partial hydrolysis of ferric nitrate salt. Structural investigation by dynamic light scattering and small-angle X-ray scattering. Langmuir 7, 1365–1369.

Braganza, L.F., Crawford, R.J., Smalley, M.V., Thomas, R.K., 1990. Swelling of butylammonium vermiculite in water. Clays and Clay Minerals 38, 90–96.

Brandenburg, U., Lagaly, G., 1988. Rheological properties of sodium montmorillonite dispersions. Applied Clay Science 3, 263–279.

Breen, C., 1999. The characterisation and use of poly cation-exchanged bentonites. Applied Clay Science 15, 187–219.

Breen, C., Rawson, J.O., Mann, B.E., 1996. Adsorption of polycations on clays: an in situ study using ^{133}Cs solution-phase NMR. Journal of Materials Chemistry 6, 253–260.

Brindley, G.W., Brown, G. (Eds.), 1980. Crystal Structures of Clay Minerals and their X-ray Identification. Mineralogical Society, London.

Buining, P.A., Philipse, A.P., Lekkerkerker, H.N.W., 1994. Phase behavior of aqueous dispersions of colloidal boehmite rods. Langmuir 10, 2106–2114.

Cady, S.S., Pinnavaia, T.J., 1978. Porphyrin intercalation in mica-type silicates. Inorganic Chemistry 17, 1501–1507.

Callaghan, I.C., Ottewill, R.H., 1974. Interparticle forces in montmorillonite gels. Faraday Discussions 57, 110–118.

Cebula, J.D., Thomas, R.K., White, J.W., 1980. Small angle neutron scattering from dilute aqueous dispersions of clay. Journal of the Chemical Society, Faraday I 76, 314–321.

Chan, D.Y.C., Pashley, R.M., Quirk, J.P., 1984. Surface potentials derived from co-ion exclusion measurements on homoionic montmorillonite and illite. Clays and Clay Minerals 32, 131–138.

Chang, F.R.C., Skipper, N.T., Sposito, G., 1997. Monte Carlo and molecular dynamics simulations of interfacial structure in lithium-montmorillonite hydrates. Langmuir 13, 2074–2082.

Chang, F.R.C., Skipper, N.T., Sposito, G., 1995. Computer simulation of interlayer molecular structure in sodium montmorillonite hydrates. Langmuir 11, 2734–2741.

Chang, F.R.C., Skipper, N.T., Sposito, G., 1998. Monte Carlo and molecular dynamics simulations of electrical double-layer structures in potassium-montmorillonite hydrates. Langmuir 14, 1201–1207.

Chaplain, V., Janex, M.L., Lafuma, F., Graillat, C., Audebert, R., 1995. Coupling between polymer adsorption and colloidal particle aggregation. Colloid and Polymer Science 273, 984–993.

Chekin, S.S., 1992. Swelling of kaolinite crystals in polar organic liquids. Clays and Clay Minerals 40, 740–741.

Chen, D., Wang, C., Huang, T., 1999. Preparation of palladium ultrafine particles in reverse micelles. Journal of Colloid and Interface Science 210, 123–129.

Chenu, C., Jaunet, A.M., 1990. Modification de l′organisation texturale d′une montmorillonite calcique liées à l′adsorption d′un polysaccharide. Comptes Rendues de l′ Académie Française des Sciences, Paris, Series 2, 30, 975–980.

Chiang, C.L., 2001. Controlled growth of gold nanoparticles in AOT/C12E4/isooctane mixed reverse micelles. Journal of Colloid and Interface Science 239, 334–341.

Chou Chang, F.R., Sposito, G., 1994. The electrical double layer of a disk-shaped clay mineral particle: effect of particle size. Journal of Colloid and Interface Science 163, 19–27.

Chou Chang, F.R., Sposito, G., 1996. The electrical double layer of a disk-shaped clay mineral particle: effect of electrolyte properties and surface charge density. Journal of Colloid and Interface Science 178, 555–564.

Costanzo, P.M., Giese, R.F., Clemency, C.V., 1984. Synthesis of a 10-Å hydrated kaolinite. Clays and Clay Minerals 32, 29–35.

de Rooy, J.N., de Bruyn, P.L., Overbeek, J.T.G., 1980. Stability of dispersions in polar organic media. I. Electrostatic stabilization. Journal of Colloid and Interface Science 75, 542–554.

Decher, G., Schmitt, J., 1992. Fine-tuning of the film thickness of ultrathin multilayer films composed of consecutively alternating layers of anionic and cationic polyelectrolytes. Progress in Colloid and Polymer Science 89, 160–164.

Dékány, I., 1996. Preparation of nanoparticles in the interfacial layer of solid supports. In: Fendler, J.H., Dékány, I. (Eds.), Nanoparticles in Solids and Solutions. Nato ASI Series, High Technology, vol. 18. Kluwer Academic Publishers, Dordrecht, pp. 293–322.

Dékány, I., Túri, L., Galbács, Fendler, J.H., 1999. Cadmium ion adsorption controls the growth of CdS nanoparticles on layered montmorillonite and calumite surfaces. Applied Clay Science 15, 221–239.

Dékány, I., Turi, L., Tombácz, E., Fendler, J.H., 1995. Preparation of size-quantised CdS and ZnS particles in nanophase reactors provided by binary liquid adsorption at layered silicates. Langmuir 11, 2285–2292.

Dékány, I., Túri, L., Vankó, Gy., Juhász, G., Vérts, A., Burger, K., 1996. Preparation and characterisation of FeS and Fe_2O_3 nanoparticles. In: Fendler, J.H., Dékány, I. (Eds.), Nanoparticles in Solids and Solutions. Nato ASI Series, High Technology, vol. 18. Kluwer Academic Publishers, Dordrecht, pp. 555–568.

Delville, A., Laszlo, P., 1989. Simple results on cohesive energies of clays from a Monte Carlo calculation. New Journal of Chemistry 13, 481–491.

Derjaguin, B.V., Churaev, N.V., Müller, V.M., 1987. Surface Forces. Consultants Bureau, New York.

Deshpande, T.L., Greenland, D.J., Quirk, J.P., 1964. Role of iron oxides in the bonding of soil particles. Nature 201, 107–108.

Di Leo, P., Cuadros, J., 2003. ^{113}Cd, ^{1}H MAS and FTIR analysis of Cd^{2+} adsorption on dioctahedral and trioctahedral smectite. Clays and Clay Minerals 51, 403–414.

Dollimore, D., Horridge, T.A., 1973. The dependence of the flocculation behavior of China clay-polyacrylamide suspensions on the suspension pH. Journal of Colloid and Interface Science 42, 581–588.

Dousma, J., de Bruyn, P.L., 1976. Hydrolysis–precipitation studies of iron solutions I. Model for hydrolysis and precipitation from Fe(III) nitrate solutions. Journal of Colloid and Interface Science 56, 527–539.

Dudek, T., Środoń, J., Eberl, D.D., Elsass, F., Uhlik, P., 2002. Thickness distribution of illite crystals in shales. I: X-ray diffraction vs. high-resolution transmission electron microscopy measurements. Clays and Clay Minerals 50, 562–577.

Dufrêche, J.F., Marry, V., Bernard, O., Turq, P., 2001. Models for electrokinetic phenomena in montmorillonite. Colloids and Surfaces A 195, 171–180.

Durand-Piana, G., Lafuma, F., Audebert, R., 1987. Flocculation and adsorption properties of cationic polyelectrolytes toward Na-montmorillonite dilute suspensions. Journal of Colloid and Interface Science 119, 474–480.

Eckle, M., Decher, G., 2001. Tuning the performance of layer-by-layer assembled organic light emitting diodes by controlling the position of isolating clay barrier sheets. Nano Letters 1, 45–49.

El Rayah, H.M.E., Rowell, D.L., 1973. The influence of iron and aluminum hydroxides on the swelling of Na-montmorillonite and the permeability of a Na-soil. Journal of Soil Science 24, 137–144.

Faisander, K., Pons, C.H., Tchoubar, D., Thomas, F., 1998. Structural organization of Na- and K-montmorillonite suspensions in response to osmotic and thermal stresses. Clays and Clay Minerals 46, 636–648.

Fendler, J.H., 2001. Chemical self-assembly for electronic applications. Chemistry of Materials 13, 3196–3210.

Ferreiro, E.A., Helmy, A.K., de Bussetti, S.G., 1995. Interaction of Fe-oxyhydroxide colloidal particles with montmorillonite. Clay Minerals 30, 195–200.

Ferris, A.P., Jepson, W.B., 1975. The exchange capacities of kaolinite and the preparation of homoionic clays. Journal of Colloid and Interface Science 51, 245–259.

Fitch, A., Wang, Y., Park, S., Joo, P., 1998. Intelligent design of thin clay films: transport and tailoring. In: Yamagishi, A., Aramata, A., Taniguchi, M. (Eds.), The Latest Frontiers of Clay Chemistry. Proceedings of Sapporo Conference on the Chemistry of Clays and Clay Minerals, 1996. The Smectite Forum of Japan, Sendai, pp. 1–15.

Fitzsimmons, R.D., Posner, A.M., Quirk, J.P., 1970. Electron microscopic and kinetic study of the flocculation of calcium montmorillonite. Israel Journal of Chemistry 8, 301–314.

Frenkel, H., Shainberg, I., 1980. The effect of hydroxy-Al and hydroxy-Fe on montmorillonite particle size. Soil Science Society of America Journal 44, 626–629.

Frens, G., 1978. On coagulation in the primary minimum. Faraday Discussions of the Chemical Society 65, 146–155.

Frens, G., Overbeek, J.T.G., 1972. Repeptization and the theory of electrocratic colloids. Journal of Colloid and Interface Science 38, 376–387.

Frey, E., Lagaly, G., 1979a. Selective coagulation and mixed-layer formation from sodium smectite solutions. In: Mortland, M.M., Farmer, V.C. (Eds.), International Clay Conference 1978. Developments in Sedimentology 27. Elsevier, Amsterdam, pp. 131–140.

Frey, E., Lagaly, G., 1979b. Selective coagulation in mixed colloidal suspensions. Journal of Colloid and Interface Science 70, 46–55.

Fripiat, J.J., Cases, J., Francois, M., Letellier, M., 1982. Thermodynamic and microdynamic behavior of water in clay suspensions and gels. Journal of Colloid and Interface Science 89, 378–400.

Fripiat, J.J., Letellier, M., Levitz, P., 1984. Interactions of water with clay surfaces. Philosophical Transaction of the Royal Society, London, A 311, 287–299.

Fukushima, Y., 1984. X-ray diffraction study of aqueous montmorillonite emulsions. Clays and Clay Minerals 32, 320–326.

Galassi, C., Costa, A.L., Pozzi, P., 2001. Influence of ionic environment and pH on the electrokinetic properties of Ball Clays. Clays and Clay Minerals 49, 263–269.

Ganor, J., Cama, J., Metz, V., 2003. Surface protonation data of kaolinite-reevaluation based on dissolution experiments. Journal of Colloid and Interface Science 264, 67–75.

Garret, W.G., Walker, G.F., 1962. Swelling of some vermiculite-organic complexes in water. Clays and Clay Minerals 9, 557–567.

Garfinkel-Shweky, D., Yariv, S., 1997. The determination of surface basicity of the oxygen planes of expanding clay minerals by acridine orange. Journal of Colloid and Interface Science 188, 168–175.

Gherardi, B., Tahani, A., Levitz, P., Bergaya, F., 1996. Sol/gel phase diagrams of industrial organo-bentones in organic media. Applied Clay Science 11, 163–170.

Giannelis, E.P., Rightor, E.G., Pinnavaia, T.J., 1988. Reaction of metal-cluster carbonyls in pillared clay galleries: surface coordination chemistry and Fischer–Tropsch catalysis. Journal of the American Chemical Society 11, 3880–3885.

Giese, R.F., Fripiat, J.J., 1979. Water molecule positions, orientations, and motions in the dihydrates of Mg and Na vermiculites. Journal of Colloid and Interface Science 71, 441–450.

Gille, W., Koschel, B., Schwieger, W., 2002. The morphology of isomorphous substituted hectorites. Colloid and Polymer Science 280, 471–478.

Glaeser, R., Mantin, I., Mering, J., 1967. Observation sur la beidellite. Bulletin du Groupe Français des Argiles 19, 125–130.

Goldberg, S., 1992. Use of surface complexation models in soil chemical systems. Advances in Agronomy 47, 233–329.

Goldberg, S., Forster, H.S., 1990. Flocculation of reference clays and arid-zone soil clays. Soil Science Society of America Journal 54, 714–718.

Goldberg, S., Glaubig, R.A., 1987. Effect of saturating cation, pH, and aluminum and iron oxide on the flocculation of kaolinite and montmorillonite. Clays and Clay Minerals 35, 220–227.

Gournis, D., Karakassides, M.A., Baka, T., Boukos, N., Petridis, D., 2002. Catalytic synthesis of carbon nanotubes on clay minerals. Carbon 40, 2641–2646.

Grandjean, I., Laszlo, P., 1989. Deuterium nuclear magnetic resonance studies of water molecules restrained by their proximity to a clay surface. Clays and Clay Minerals 37, 403–408.

Granquist, W.T., McAtee, J., 1963. The gelation of hydrocarbons by montmorillonite organic complexes. Journal of Colloid Science 18, 409–420.
Greathouse, J.A., Refson, K., Sposito, G., 2000. Molecular dynamics simulation of water mobility in magnesium–smectite hydrates. Journal of the American Chemical Socity 122, 11459–11464.
Greathouse, J.A., Storm, E.W., 2002. Calcium hydration on montmorillonite clay surfaces studied by Monte Carlo simulations. Molecular Simulation 28, 633–647.
Greenland, D.J., 1975. Charge characteristics of some kaolinite-iron hydroxide complexes. Clay Minerals 10, 407–416.
Gregory, J., 1973. Rates of flocculation of latex particles by cationic polymers. Journal of Colloid and Interface Science 42, 448–456.
Gregory, J., 1975. Interaction of unequal double layers at constant charge. Journal of Colloid and Interface Science 51, 44–51.
Grim, R.E., 1962. Applied Clay Mineralogy. McGraw-Hill, New York.
Grim, R.E., 1968. Clay Mineralogy, 2nd edition. McGraw-Hill, New York.
Grim, R.E., Güven, N., 1978. Bentonites, Geology, Mineralogy and Uses. Elsevier, New York.
Güven, N., 1992a. Molecular aspects of clay-water interactions. In: Güven, N., Pollastro, R.M. (Eds.), Clay–Water Interface and its Rheological Implications. CMS Workshop Lectures, vol. 4. The Clay Minerals Society, Boulder, CO, pp. 2–79.
Güven, N., 1992b. Rheological aspects of aqueous smectite suspensions. In: Güven, N., Pollastro, R.M. (Eds.), Clay–Water Interface and its Rheological Implications. CMS Workshop Lectures, vol. 4. The Clay Minerals Society, Boulder, CO, pp. 82–125.
Güven, N., Pollastro, R.M. (Eds.), 1992. Clay–Water Interface and its Rheological Implications. CMS Workshop Lectures, vol. 4. The Clay Minerals Society, Boulder, CO.
Hagen, K.S., 1992. Modellverbindungen für die Eisen-Sauerstoff-Aggregation und die Biomineralisation. Angewandte Chemie 104, 1036.
Hatharasinghe, H.L.M., Smalley, M.V., Swenson, J., Hannon, A.C., King, S.M., 2000. Freezing experiments on clay gels. Langmuir 16, 5562–5567.
Healy, T.W., Wiese, G.R., Yates, D.E., Kavanagh, B.V., 1973. Heterocoagulation in mixed oxide colloidal dispersions. Journal Colloid Interface Science 42, 647–649.
Heller, H., Keren, R., 2001. Rheology of Na-rich montmorillonite suspension as affected by electrolyte concentration and shear rate. Clays and Clay Minerals 49, 286–291.
Heller, H., Keren, R., 2002. Anionic polyacrylamide polymers effect on rheological behavior of sodium montmorillonite suspensions. Soil Science Society of America Journal 66, 19–25.
Heller, H., Keren, R., 2003. Anionic polyacrylamide polymer adsorption by pyrophyllite and montmorillonite. Clays and Clay Minerals 51, 334–339.
Helmy, A.K., Ferreiro, E.A., 1974. Flocculation of NH_4-montmorillonite by electrolytes. Electroanalytical Chemistry and Interface Electrochemistry 57, 103–112.
Herrington, T.M., Clarke, A.Q., Watts, J.C., 1992. The surface charge of kaolin. Colloids and Surfaces 68, 161–169.
Hesterberg, D., Page, A.L., 1990a. Flocculation series test yielding time-invariant critical coagulation concentrations of sodium illite. Soil Science Society of America Journal 54, 729–735.
Hesterberg, D., Page, A.L., 1990b. Critical coagulation concentrations of sodium and potassium illite as affected by pH. Soil Science Society of America Journal 54, 735–739.

Hetzel, F., Doner, H.E., 1993. Some colloidal properties of beidellite: comparison with low and high charge montmorillonites. Clays and Clay Minerals 41, 453–460.

Hetzel, F., Tessier, D., Jaunet, A.M., Doner, H., 1994. The microstructure of three Na^+ smectites: the importance of particle geometry on dehydration and rehydration. Clays and Clay Minerals 42, 242–248.

Hinds, I.C., Ridler, P.J., Jennings, B.R., 1996. Electric birefringence for monotoring size changes in clay suspensions. Clay Minerals 31, 549–556.

Hirsch, D., Nir, S., Banin, A., 1989. Prediction of cadmium complexation in solution and adsorption to montmorillonite. Soil Science Society of America Journal 53, 716–721.

Hofmann, U., 1952. Neue Erkenntnisse auf dem Gebiete der Thixotropie, insbesondere bei tonhaltigen Gelen. Kolloid-Zeitschrift 125, 86–99.

Hofmann, U., 1961. Geheimnisse des Tons. Berichte der Deutschen Keramischen Gesellschaft 38, 201–207.

Hofmann, U., 1962. Die Tonminerale und die Plastizität des Tons. Keramische Zeitschrift 14, 14–19.

Hofmann, U., 1964. Oberflächenladung und Rheologie der Tonminerale. Berichte der Deutschen Keramischen Gesellschaft 41, 680–686.

Hollander, A.F., Somasundaran, P., Gryte, C.C., 1981. Adsorption of polyacrylamide and sulfonated polyacrylamide on Na-kaolinite. In: Tewari, P.H. (Ed.), Adsorption from Aqueous Solution. Plenum Press, New York, pp. 143–162.

Horn, D., 20012002. Vorstoß in die Nanowelt der Grenzflächen bei der Papierherstellung und –veredelung. Wochenblatt für Papierfabrikation 129/130, 3–15.

Hotta, Y., Taniguchi, M., Inukai, K., Yamagishi, A., 1997. Clay-modified electrodes prepared by the Langmuir-Blodgett method. Clay Minerals 32, 79–88.

Hougardy, J., Stone, W.E.E., Fripiat, J.J., 1976. NMR study of adsorbed water. I. Molecular orientation and protonic motions in the two-layer hydrate of a Na vermiculite. The Journal of Physical Chemistry 64, 3840–3851.

Hsi, H.R., Clifton, D.F., 1962. Flocculation of selected clays by various electrolytes. Clays and Clay Minerals 9, 269–275.

Huerta, M.M., Curry, J.E., McQuarrie, D.A., 1992. The effect of unequal ionic size on the swelling pressure in clays. Clays and Clay Minerals 40, 491–500.

Hunter, R.J., 1993. Introduction to Modern Colloid Science. Oxford University Press, Oxford.

Hunter, R.J., 1998. Recent developments in the electroacoustic characterisation of colloidal suspensions and emulsions. Colloids and Surfaces A 141, 37–65.

Hunter, R.J., James, M., 1992. Charge reversal of kaolinite by hydrolyzable metal ions: an electroacoustic study. Clays and Clay Minerals 40, 644–649.

Ingelsten, H.H., Bagve, R., Palmqvist, A., Skoglundh, M., Svanberg, C., Holmberg, K., Shah, D.O., 2001. Kinetics of formation of nano-sized platinum particles in water-in-oil microemulsions. Journal of Colloid and Interface Science 241, 104–111.

Israelachvili, J.N., 1994. Intermolecular and Surface Forces. Academic Press, London.

Janek, M., Komadel, P., Lagaly, G., 1997. Effect of autotransformation on the layer charge of smectites determined by the alkylammonium method. Clay Minerals 32, 623–632.

Janek, M., Lagaly, G., 2001. Proton saturation and rheological properties of smectite dispersions. Applied Clay Science 19, 121–130.

Janek, M., Lagaly, G., 2002. Interaction of a cationic surfactant with bentonite, a colloid chemistry study. Colloid and Polymer Science 281, 293–301.
Jasmund, K., Lagaly, G. (Eds.), 1993. Tonminerale und Tone, Struktur, Eigenschaften, Anwendung und Einsatz in Industrie und Umwelt. Steinkopff Verlag, Darmstadt.
Jennings, B.R., 1993. Size and thickness measurement of polydisperse clay samples. Clay Minerals 28, 485–494.
Jennings, B.R., Parslow, K., 1988. Particle size measurement: the equivalent spherical diameter. Proceedings of the Royal Society, London, A 419, 137–149.
Jenny, H., Reitemeier, R.F., 1935. Ionic exchange in relation to the stability of colloidal systems. Journal of Physical Chemistry 39, 593–604.
Jepson, W.B., 1984. Kaolins: their properties and uses. Philosophical Transactions of the Royal Society, London, A 311, 411–432.
Johnston, C.T., Sposito, G., Erickson, C., 1992. Vibrational probe studies of water interactions with montmorillonite. Clays and Clay Minerals 40, 722–730.
Jones, T.R., 1983. The properties and uses of clays which swell in organic solvents. Clay Minerals 18, 399–410.
Jozefaciuk, G., 2002. Effect of acid and alkali treatments on surface-charge properties of selected minerals. Clays and Clay Minerals 50, 647–656.
Kahn, A.J., 1958. The flocculation of sodium montmorillonite by electrolytes. Journal of Colloid Science 13, 51–60.
Karube, J., Nakaoshi, K., Sugimoto, H., Fujihira, M., 1992. Electrophoretic behavior of imogolite under alkaline conditions. Clays and Clay Minerals 40, 625–628.
Keller, W.D., 1985. The nascence of clay minerals. Clays and Clay Minerals 33, 161–172.
Keller, W.D., Reynolds, R.C., Inoue, A., 1986. Morphology of clay minerals in the smectite-to-illite conversion series by scanning electron microscopy. Clays and Clay Minerals 34, 187–197.
Keren, R., Shainberg, I., Klein, E., 1988. Settling and flocculation value of sodium–montmorillonite particles in aqueous media. Soil Science Society of America Journal 52, 76–80.
Keren, R., Sparks, D.L., 1995. The role of edge surfaces in flocculation of 2:1 clay minerals. Soil Science Society of America Journal 59, 430–435.
Khoe, G.H., Robins, R.G., 1989. Polymerization reactions in hydrolyzed iron (III) solutions. Journal of Colloid and Interface Science 133, 244–252.
Kim, H.S., Lamarche, C., Verdier, A., 1983. Étude des interactions entre une polyélectrolyte cationique de type ammonium tertiare et une suspension de bentonite aqueuse. Colloid and Polymer Science 261, 64–69.
Király, Z., Dékány, I., Mastalir, Á., Bartók, M., 1996a. In situ generation of palladium nanoparticles in smectite clays. Journal of Catalysis 161, 401–408.
Király, Z., Turi, L., Dékány, I., Bean, K., Vincent, B., 1996b. Van der Waals attraction between Stöber silica particles in a binary solvent system. Colloid and Polymer Science 274, 779–787.
Kjellander, R., 1996. Ion-ion correlations and effective charges in electrolyte and macroion systems. Berichte der Bunsengesellschaft für Physikalische Chemie 100, 894–904.
Kjellander, R., Marčelja, S., Quirk, J.P., 1988. Attractive double layer interactions between calcium clay particles. Journal of Colloid and Interface Science 126, 194–211.
Kleijn, W.B., Oster, J.D., 1982. A model of clay swelling and tactoid formation. Clays and Clay Minerals 30, 383–390.
Koschel, B., Gille, W., Schwieger, W., Janowski, F., 2000. Analysis of the morphology of hectorite by use of small-angle X-ray scattering. Colloid and Polymer Science 278, 805–809.

Kotov, N.A., Haraszti, T., Turi, L., Zavala, G., Geer, R.E., Dékány, I., Fendler, J.H., 1997. Mechanism of and defect formation in the self-assembly of polymeric polycation-montmorillonite ultrathin films. Journal of the American Chemical Society 119, 6821–6832.

Kotov, N.A., Meldrum, F.C., Fendler, J.H., Tombácz, E., Dékány, I., 1994. Spreading of clay organocomplexes on aqueous solutions: construction of Langmuir-Blodgett clay organo-complex multilayer films. Langmuir 10, 3797–3804.

Kraehenbuehl, F., Stoeckli, H.F., Brunner, F., Kahr, G., Müller-Vonmoos, M., 1987. Study of the water bentonite system by vapour adsorption, immersion calorimetry and X-ray techniques. Clay Minerals 22, 1–9.

Kretzschmar, R., Holthoff, H., Sticher, H., 1998. Influence of pH and humic acid on coagulation kinetics of kaolinite. A dynamic light scattering study. Journal of Colloid and Interface Science 202, 95–103.

Kroon, M., Vos, W.L., Wegdam, G.H., 1998. Structure and formation of a gel of colloidal disks. Physical Review E 57, 1962–1970.

Kuhn, H., 1981. Information, electron and energy transfer in surface layers. Pure and Applied Chemistry 53, 2105–2122.

Kuhn, H., Möbius, D., 1971. Systeme aus monomolekularen Schichten – Zusammenbau und physikalisch-chemisches Verhalten. Angewandte Chemie 83, 672–690.

Kuwaharada, S., Tateyama, H., Nishimura, S., Hirosue, H., 2002. Smectite quasicrystals in aqueous solutions as a function of cationic surfactant concentration. Clays and Clay Minerals 50, 18–24.

Lagaly, G., 1981. Characterization of clays by organic compounds. Clay Minerals 16, 1–21.

Lagaly, G., 1986. Colloids. Ullmann's Encyclopedia of Industrial Chemistry, vol. A7. VCH, Weinheim, pp. 341–367.

Lagaly, G., 1987a. Surface chemistry and catalysis. In: Pérez-Rodriguez, J.L., Galan, E. (Eds.), Lectures Conferencias. Euroclay '87. Sociedad Espanola de Arcillas, Sevilla, pp. 97–115.

Lagaly, G., 1987b. Water and solvents on surfaces bristling with alkyl chains. In: Kleeberg, H. (Ed.), Interaction of Water in Ionic and Nonionic Hydrates. Springer-Verlag, Berlin, pp. 229–240.

Lagaly, G., 1989. Principles of flow of kaolin and bentonite dispersions. Applied Clay Science 4, 105–123.

Lagaly, G., 1993. From clay mineral crystals to colloidal clay mineral dispersions. In: Dobiaś, B. (Ed.), Coagulation and Flocculation. Theory and Applications. Marcel Dekker, New York, pp. 427–494.

Lagaly, G., 1994. Layer charge determination by alkylammonium ions. In: Mermut, A. (Ed.), Charge Characteristics of 2:1 Clay Minerals. CMS Workshop Lectures, vol. 6. The Clay Minerals Society, Boulder, CO, pp. 1–46.

Lagaly, G., 2005. From clay minerals to clay mineral dispersions. In: Stechemesser, H., Dobiaš, B. (Eds.), Coagulation and Flocculation, 2nd edition. Taylor and Francis, Boca Raton, pp. 519–600.

Lagaly G., Fahn, R., 1983. Ton und Tonminerale. In: Ullmann's Encyclopedia of Technical Chemistry, 4th ed., vol. 23. Verlag Chemie, Weinheim, pp. 311–326.

Lagaly, G., Malberg, R., 1990. Disaggregation of alkylammonium montmorillonites in organic solvents. Colloids and Surfaces 49, 11–27.

Lagaly, G., Schön, G., Weiss, A., 1972. Über den Einfluß einer unsymmetrischen Ladungsverteilung auf die Wechselwirkung zwischen plättchenförmigen Kolloidteilchen. Kolloid-Zeitschrift und Zeitschrift für Polymere 250, 667–674.

Lagaly, G., Schulz, O., Zimehl, R., 1997. Dispersionen und Emulsionen. Eine Einführung in die Kolloidik feinverteilter Stoffe einschließlich der Tonminerale. Mit einem historischen Beitrag über Kolloidwissenschaftler von Klaus Beneke. Steinkopff Verlag, Darmstadt.

Lagaly, G., Witter, R., Sander, H., 1983. Water on hydrophobic surfaces. In: Ottewill, R.H., Rochester, C.H., Smith, A.L. (Eds.), Adsorption from Solution. Academic Press, London, pp. 65–77.

Lagaly, G., Ziesmer, S., 2003. Colloid chemistry of clay minerals: the coagulation of montmorillonite dispersions. Advances in Colloid and Interface Science 100–102, 105–128.

Lahav, N., 1990. Preparation of stable suspensions of delaminated kaolinite by combined dimethylsulfoxide–ammonium fluoride treatment. Clays and Clay Minerals 38, 219–222.

Lapides, I., Heller-Kallai, L., 2002. Novel features of smectite settling. Colloid and Polymer Science 280, 554–561.

Larsson, N., Siffert, B., 1983. Formation of lysozyme-containing crystals of montmorillonite. Journal of Colloid and Interface Science 93, 424–431.

Lee, L.T., Rahbari, R., Lecourtier, J., Chauveteau, G., 1991. Adsorption of polyacrylamides on the different faces of kaolinites. Journal of Colloid and Interface Science 147, 351–357.

Li, J., Tanguy, P.A., Carreau, P.J., Moan, M., 2001. Effect of thickener structure on paper-coating color properties. Colloid and Polymer Science 279, 865–871.

Li, H., Wei, S., Qing, C., Yang, J., 2003. Discussion on the position of the shear plane. Journal of Colloid and Interface science 258, 40–44.

Lott, M.P., Williams, D.J.A., Williams, P.R., 1996. The elastic properties of sodium montmorillonite suspensions. Colloid and Polymer Science 274, 43–48.

Low, P.F., 1987. The clay–water interface. In: Schultz, L.G., van Olphen, H., Mumpton, F.A. (Eds.), Proceedings of the International Clay Conference Denver 1985. The Clay Minerals Society, Bloomington, IN, pp. 247–256.

Lubetkin, S.D., Middleton, S.R., Ottewill, R.H., 1984. Some properties of clay water dispersions. Philosophical Transactions of the Royal Society, London, A 311, 353–368.

Lvov, Y., Ariga, K., Ichinose, I., Kunitake, T., 1996. Formation of ultrathin multilayer and hydrated gel from montmorillonite and linear polycations. Langmuir 12, 3038–3044.

Lvov, Y., Haas, H., Decher, G., Möhwald, H., Kalachev, A., 1993. Assembly of polyelectrolyte molecular films onto plasma-treated glass. Journal of Chemical Physics 97, 12835–12841.

Lyklema, J., 1984. Points of zero charge in the presence of specific adsorption. Journal of Colloid and Interface Science 99, 109–177.

Lyklema, J., 1989. Discrimination between physical and chemical adsorption of ions on oxides. Colloids and Surfaces 37, 197–204.

Lyklema, J., 1995. Fundamentals of Interface and Colloid Science. Volume II: Solid-Liquid Interfaces. Academic Press, London.

Mabire, F., Audebert, R., Quivoron, C., 1984. Flocculation properties of water-soluble cationic copolymers towards silica suspension: a semiquantitative interpretation of the role of molecular weight and cationicity through a "patchwork" model. Journal of Colloid and Interface Science 97, 120–136.

Machula, G., Dékány, I., Nagy, L.G., 1993. The properties of the adsorption layer and the stability of aerosil dispersions in binary liquids. Colloids and Surfaces A 71, 241–254.

Mackinnon, I.D.R., Uwins, P.J.R., Yago, A., Page, D., 1993. Kaolinite particle sizes in the $<2\,\mu m$ range using laser scattering. Clays and Clay Minerals 41, 613–623.

Madsen, F.T., Müller-Vonmoos, M., 1985. Swelling pressure calculated from mineralogical properties of a Jurassic Opalinum shale, Switzerland. Clays and Clay Minerals 33, 501–509.

Magdassi, S., Rodel, B.Z., 1996. Flocculation of montmorillonite dispersions based on surfactant-polymer interactions. Colloids and Surfaces A 119, 51–56.

Mamy, J., Gaultier, J.P., 1975. Étude de l′ évolution de l′ordre cristalline dans la montmorillonite en relation avec la diminution d′échangeabilité de potassium. In: Bailey, S.W. (Ed.), Proceedings of the International Clay Conference 1975. Applied Publishing Ltd., Wilmette, IL, pp. 149–155.

Manfredini, T., Pellacani, G.C., Pozzi, P., Corradi, A.B., 1990. Monomeric and oligomeric phosphates as deflocculants of concentrated aqueous clay suspensions. Applied Clay Science 5, 193–201.

Mangelsdorf, C.S., White, L.R., 1990. Effect of Stern-layer conductance on electrokinetic transport properties of colloidal particles. Journal of the Chemical Society Faraday Transactions 86, 2859–2870.

Manning, B.A., Goldberg, S., 1996. Modeling arsenate competitive adsorption on kaolinite, montmorillonite and illite. Clays and Clay Minerals 44, 609–623.

Marry, V., Turq, P., Cartailler, T., Levesque, D., 2002. Microscopic simulation of structure and dynamics of water and counterions in a monohydrated montmorillonite. Journal of Chemical Physics 117, 3454–3463.

Matijević, E., 1973. Colloid stability and complex chemistry. Journal of Colloid and Interface Science 43, 217–245.

Matijević, E., 1977. The role of chemical complexing in the formation and stability of colloidal dispersions. Journal of Colloid and Interface Science 58, 374–389.

Matijević, E., 1981. Interactions in mixed colloidal systems (heterocoagulation, adhesion, microflotation). Pure and Applied Chemistry 53, 2167–2179.

Mayer, A., Antonietti, M., 1998. Investigation of polymer-protected noble metal nanoparticles by transmission electron microscopy: control of particle morphology and shape. Colloid and Polymer Science 276, 769–779.

McAtee, J.L., Wells, L.M., 1967. Mutual adsorption of clay minerals and colloidal aluminum oxide—an electron microscopy investigation. Journal of Colloid and Interface Science 24, 203–210.

McBride, M.B., 1997. A critic of the diffuse double layer models applied to colloid and surface chemistry. Clays and Clay Minerals 45, 598–608.

McCormack, D., Carnie, S.L., Chan, D.Y.C., 1995. Calculation of electric double-layer force and interaction free energy between dissimilar surfaces. Journal of Colloid and Interface Science 169, 177–196.

Miller, N.P., Berg, J.C., O'Brien, R.W., 1992. The electrophoretic mobility of a porous aggregate. Journal of Colloid and Interface Science 153, 237–243.

Miller, S.E., Low, P.F., 1990. Characterization of the electrical double layer of montmorillonite. Langmuir 6, 572–578.

Möbius, D., 1978. Designed monolayer assemblies. Berichte der Bunsengesellschaft für Physikalische Chemie 82, 848–858.

Mongondry, P., Tassin, J.F., Nicolai, T., 2005. Revised state diagram of Laponite dispersions. Journal of Colloid and Interface Science 283, 397–405.

Moore, D.M., Reynolds, R.C. Jr., 1997. X-ray Diffraction and the Identification and Analysis of Clay Minerals, 2nd edition. Oxford University Press, Oxford.
Moraru, V.N., 2001. Structure formation of alkylammonium montmorillonites in organic media. Applied Clay Science 19, 11–26.
Mortland, M.M., Raman, K.V., 1968. Surface acidity of smectites in relation to hydration, exchangeable cation, and structure. Clays and Clay Minerals 16, 393–398.
Mourchid, A., Delville, A., Lambard, J., Lécolier, E., Levitz, P., 1995. Phase diagram of colloidal dispersions of anisotropic charged particles: equilibrium properties, structure, and rheology of Laponite suspensions. Langmuir 11, 1942–1950.
Muljadi, D., Posner, A.M., Quirk, J.P., 1966. The mechanism of phosphate adsorption by kaolinite, gibbsite and pseudoboehmite. Journal of Soil Science 17, 212–229.
Mulla, D.J., Low, P.F.J., 1983. The molar absorptivity of interparticle water in clay–water systems. Journal of Colloid and Interface Science 95, 51–60.
Nabzar, L., Pefferkorn, E., 1985. An experimental study of kaolinite crystal edge-polyacrylamide interactions in dilute suspensions. Journal of Colloid and Interface Science 108, 243–248.
Nabzar, L., Pefferkorn, E., Varoqui, R., 1984. Polyacrylamide-sodium kaolinite interactions: flocculation behavior of polymer clay suspensions. Journal of Colloid and Interface Science 102, 380–388.
Nadeau, P., 1985. The physical dimensions of fundamental particles. Clay Minerals 20, 499–514.
Nadeau, P., 1987. Clay particle engineering: a potential new technology with diverse applications. Applied Clay Science 2, 83–93.
Napper, D.H., 1983. Polymeric Stabilization of Colloidal Dispersions. Academic Press, London.
Neaman, A., Singer, A., 1999. Flocculation of homoionic sodium palygorskite, palygorskite-montmorillonite mixtures and palygorskite containing soil clays. Soil Science 164, 914–921.
Neumann, B.S., Sansom, K.G., 1971. The rheological properties of dispersions of Laponite, a synthetic hectorite-like clay, in electrolyte solutions. Clay Minerals 9, 231–243.
Nir, S., Hirsch, D., Navrot, J., Banin, A., 1986. Specific adsorption of lithium, sodium, potassium, and strontium to montmorillonite: observations and predictions. Soil Science Society of America Journal 50, 40–45.
Nir, S., Rytwo, G., Yermiyahu, U., Margulies, L., 1994. A model for cation adsorption to clays and membranes. Colloid and Polymer Science 272, 619–632.
Norris, J., Giese, R.F., Costanzo, P.M., van Oss, C., 1993. The surface energies of cation substituted laponite. Clay Minerals 28, 1–11.
Norrish, K., 1954. The swelling of montmorillonite. Discussions of the Faraday Society 18, 120–134.
Norrish, K., Rausell–Colom, J.A., 1963. Low-angle X-ray diffraction studies of the swelling of montmorillonite and vermiculite. In: Shineford, A., Franks, P.C. (Eds.), Clays and Clay Minerals, Proceedings of the 10th National Conference. Austin, Texas. Pergamon Press, New York, pp. 123–149.
Oades, J.M., 1984. Interactions of polycations of aluminum and iron with clays. Clays and Clay Minerals 32, 49–57.
Oakley, D.M., Jennings, B.R., 1982. Clay particle sizing by electrically induced birefringence. Clay Minerals 17, 313–325.

O'Brien, N.R., 1971. Fabric of kaolinite and illite floccules. Clays and Clay Minerals 19, 353–359.
O'Brien, R.W., Rowlands, W.N., 1993. Measuring the surface conductance of kaolinite particles. Journal of Colloid and Interface Science 159, 471–476.
O'Brien, R.W., White, L.R., 1978. Electrophoretic mobility of a spherical colloidal particle. Journal of the Chemical Society Faraday Transactions 2 (74), 1607–1626.
Odom, I.E., 1984. Smectite clay minerals: properties and uses. Philosophical Transactions of the Royal Society, London, A 311, 391–409.
Ohshima, H., 1995. Electrophoretic mobility of soft particles. Electrophoresis 16, 1360–1363.
Oster, J.D., Shainberg, I., Wood, J.D., 1980. Flocculation value and gel structure of sodium/calcium montmorillonite and illite suspensions. Soil Science Society of America Journal 44, 955–959.
Ottewill, R.H., 1977. Stability and instability in disperse systems. Journal of Colloid and Interface Science 58, 357–373.
Ottewill, R.H., Walker, T., 1968. The influence of nonionic surface active agents on the stability of polystyrene latex dispersions. Kolloid Zeitschrift und Zeitschrift für Polymere 227, 108–116.
Overbeek, J.T.G., 1977. Recent developments in the understanding of colloid stability. Journal of Colloid and Interface Science 58, 408–422.
Overbeek, J.T.G., 1980. The rule of Schulze and Hardy. Pure and Applied Chemistry 52, 1151–1161.
Overbeek, J.T.G., 1982. Strong and weak points in the interpretation of colloid stability. Advances in Colloid and Interface Science 16, 17–30.
Papp, S., Dékány, I., 2003. Stabilization of palladium nanoparticles by polymers and layer silicates. Colloid and Polymer Science 281, 727–737.
Parazak, D.P., Burkhardt, C.W., McCarthy, K.J., Stehlin, M.P., 1988. Hydrophobic flocculation. Journal of Colloid and Interface Science 123, 59–72.
Parfitt, R.L., 1978. Anion adsorption by soils and soil materials. Advances in Agronomy 30, 1–50.
Pashley, R.M., 1985. Electromobility of mica particles dispersed in aqueous solutions. Clays and Clay Minerals 33, 193–199.
Pashley, R.M., Quirk, J.P., 1984. The effect of cation valency on DLVO and hydration forces between macroscopic sheets of muscovite mica in relation to clay swelling. Colloids and Surfaces 9, 1–17.
Pefferkorn, E., Nabzar, I., Carroy, A., 1985. Adsorption of polyacrylamide to Na-kaolinite: correlation between clay structure and surface properties. Journal of Colloid and Interface Science 106, 94–103.
Pefferkorn, E., Nabzar, L., Varoqui, R., 1987. Polyacrylamide Na-kaolinite interactions: effect of electrolyte concentration on polymer adsorption. Colloid and Polymer Science 265, 889–896.
Penner, D., Lagaly, G., 2000. Influence of organic and inorganic salts on the aggregation of montmorillonite dispersions. Clays and Clay Minerals 48, 246–255.
Penner, D., Lagaly, G., 2001. Influence of anions on the rheological properties of clay mineral dispersions. Applied Clay Science 19, 131–142.
Pérez-Maqueda, L.A., Caneo, O.B., Poyato, J., Pérez-Rodriguez, J.L., 2001. Preparation and characterization of micron and submicron-sized vermiculite. Physical Chemistry of Minerals 28, 61–66.

Perkins, R., Brace, R., Matijević, E., 1974. Colloidal and surface properties of clay suspensions. I. Laponite CP. Journal of Colloid and Interface Science 48, 417–426.

Permien, T., Lagaly, G., 1994a. The rheological and colloidal properties of bentonite dispersions in the presence of organic compounds. I. Flow behaviour of sodium montmorillonite in water-alcohol. Clay Minerals 29, 751–760.

Permien, T., Lagaly, G., 1994b. The rheological and colloidal properties of bentonite dispersions in the presence of organic compounds. II. Flow behaviour of Wyoming bentonite in water-alcohol. Clay Minerals 29, 761–766.

Permien, T., Lagaly, G., 1994c. The rheological and colloidal properties of bentonite dispersions in the presence of organic compounds. III. The effect of alcohols on the coagulation of sodium montmorillonite. Colloid and Polymer Science 272, 1306–1312.

Permien, T., Lagaly, G., 1995. The rheological and colloidal properties of bentonite dispersions in the presence of organic compounds. V. Bentonite and sodium montmorillonite and surfactants. Clays and Clay Minerals 43, 229–236.

Pierre, A.C., 1992. The gelation of colloidal platelike particles. Journal of the Canadian Ceramic Society 61, 135–138.

Pierre, A.C., 1996. Structure of gels comprised of platelike particles. Case of boehmite, montmorillonite and kaolinite. Journal de Chimie et Physique 93, 1065–1079.

Pierre, A.C., Ma, K., 1997. Sedimentation behaviour of kaolinite and montmorillonite mixed with iron additives, as a function of their zeta potential. Journal of Materials Science 32, 2937–2947.

Pierre, A.C., Ma, K., 1999. DLVO theory and clay aggregate architectures formed with $AlCl_3$. Journal of the European Ceramic Society 19, 1615–1622.

Plançon, A., 2001. Order–disorder in clay mineral structures. Clay Minerals 36, 1–14.

Plaschke, M., Schäfer, T., Bundschuh, T., Ngo Manh, T., Knopp, R., Geckeis, H., Kim, J.I., 2001. Size characterization of bentonite colloids by different methods. Analytical Chemistry 73, 4338–4347.

Poinsignon, C., Cases, J.M., Fripiat, J.J., 1978. Electrical polarization of water molecules adsorbed by smectites. An infrared study. The Journal of Physical Chemistry 82, 1855–1860.

Pons, C.H., Rousseaux, E., Tchoubar, D., 1981. Utilisation du rayonnement synchroton en diffusion aux petits angles pour l'étude du gonflement des smectites: Étude du système eau–montmorillonite–Na en fonction de la température. Clay Minerals 16, 23–42.

Pons, C.H., Rousseaux, E., Tchoubar, D., 1982. Utilisation du rayonnement synchroton en diffusion aux petits angles pour l'étude du gonflement des smectites: II. Étude de différents systèmes eau–smectites en fonction de la température. Clay Minerals 17, 327–338.

Pugh, R.J., Kitchener, J.A., 1971. Theory of selective coagulation in mixed colloidal systems. Journal of Colloid and Interface Science 35, 656–664.

Quirk, J.P., Marčelja, S., 1997. Application of double-layer theories to the extensive crystalline swelling of Li-montmorillonite. Langmuir 13, 6241–6248.

Ramsay, J.D.F., 1986. Colloidal properties of synthetic hectorite clay dispersions. Journal of Colloid and Interface Science 109, 441–447.

Ramsay, J.D.F., Lindner, P., 1993. Small-angle neutron scattering investigations of the structure of thixotropic dispersions of smectite clay colloids. Journal of the Chemical Society Faraday Transactions 89, 4207–4217.

Ramsay, J.D.F., Swanton, S.W., Bunce, J., 1990. Swelling and dispersion of smectite clay colloids: determination of structure by neutron diffraction and small-angle neutron scattering. Journal of the Chemical Society Faraday Transactions 86, 3919–3926.

Rand, B., Pekenć, E., Goodwin, J.W., Smith, R.W., 1980. Investigation into the existence of edge-face coagulated structures in Na-montmorillonite suspensions. Journal of the Chemical Society Faraday I 76, 225–235.

Rasmusson, M., Rowlands, W., O'Brien, R.W., Hunter, R.J., 1997. The dynamic mobility and dielectric response of sodium bentonite. Journal of Colloid and Interface Science 189, 92–100.

Rausell-Colom, J.A., 1964. Small-angle X-ray diffraction study of the swelling of butylammonium-vermiculite. Transactions of the Faraday Society 60, 190–201.

Rausell-Colom, J.A., Saez-Auñón, J., Pons, C.H., 1989. Vermiculite gelation: structural and textural properties. Clay Minerals 24, 459–478.

Rausell-Colom, J.A., Salvador, P.S., 1971a. Complexes vermiculite-aminoacides. Clay Minerals 9, 139–149.

Rausell-Colom, J.A., Salvador, P.S., 1971b. Gélification de vermiculite dans des solutions d′acide γ-amino butyrique. Clay Minerals 9, 193–208.

Rowlands, W.N., O'Brien, R.W., 1995. The dynamic mobility and dielectric response of kaolinite particles. Journal of Colloid and Interface Science 175, 190–200.

Rupprecht, H., Gu, T., 1991. The structure of the adsorption layers of ionic surfactants at the solid/liquid interface. Colloid and Polymer Science 269, 506–522.

Rytwo, G., Nir, S., Margulies, L., 1995. Interactions of monovalent organic cations with montmorillonite: adsorption studies and model calculations. Soil Science Society of America Journal 59, 554–564.

Salmang, H., 1927. Die Ursachen der Bildsamkeit der Tone. Zeitschrift für Anorganische und Allgemeine Chemie 162, 115–126.

Sayin, M., Beyme, B., Graf von Reichenbach, H., 1979. Formation of metallic silver as related to iron oxidation in K-depleted micas. In: Mortland, M.M., Farmer, V.C. (Eds.), International Clay Conference 1978. Developments in Sedimentology 27. Elsevier, Amsterdam, pp. 177–186.

Schmidt, C.U., Lagaly, G., 1999. Surface modification of bentonites. I. Betaine montmorillonites and their rheological and colloidal properties. Clay Minerals 34, 447–458.

Schofield, R.K., Samson, H.R., 1954. Flocculation of kaolinite due to the attraction of oppositely charged crystal faces. Discussions of the Faraday Society 18, 135–145.

Schoonheydt, R.A., 2002. Smectite-type clay minerals as nanomaterials. Clays and Clay Minerals 50, 411–420.

Schramm, L.L., Kwak, J.C.T., 1982a. Influence of exchangeable cation composition on the size and shape of montmorillonite particles in dilute suspension. Clays and Clay Minerals 30, 40–48.

Schramm, L.L., Kwak, J.C.T., 1982b. Interactions in clay suspensions: the distribution of ions in suspension and the influence of tactoid formation. Colloids and Surfaces 3, 43–60.

Schramm, L.L., Yariv, S., Ghosh, D.K., Hepler, L.G., 1997. Electrokinetic study of the adsorption of ethyl violet and crystal violet by montmorillonite clay particles. Canadian Journal of Chemistry 75, 1868–1877.

Schroth, B.K., Sposito, G., 1997. Surface charge properties of kaolinite. Clays and Clay Minerals 45, 85–91.

Schwertmann, U., 1969. Aggregation of aged hydrogen clays. In: Heller, L. (Ed.), Proceedings of the International Clay Conference, Tokyo, 1969. Israel University Press, Jerusalem, pp. 683–690.

Secor, R.B., Radke, C.J., 1985. Spillover of the diffuse double layer on montmorillonite particles. Journal of Colloid and Interface Science 103, 237–244.

Séquaris, J.M., Camara Decimavilla, S., Correales Ortega, J.A., 2002. Polyvinylpyrrolidone adsorption and structural studies on homoionic Li-, Na-, K-, and Cs-montmorillonite colloidal solutions. Journal of Colloid and Interface Science 252, 93–101.

Siffert, B., Espinasse, P., 1980. Adsorption of organic diacids and sodium polyacrylate onto montmorillonite. Clays and Clay Minerals 28, 381–387.

Siffert, B., Kim, K.B., 1992. Study of surface ionization of kaolinite in water by zetametry – influence on the rheological properties of kaolinite suspension. Applied Clay Science 6, 369–382.

Skipper, N.T., Sposito, G., Chang, F.R.C., 1995. Monte Carlo simulation of interlayer molecular structure in swelling clay minerals. 2. Monolayer hydrates. Clays and Clay Minerals 43, 294–303.

Slade, P.G., Quirk, J.P., Norrish, K., 1991. Crystalline swelling of smectite samples in concentrated NaCl solutions in relation to layer charge. Clays and Clay Minerals 39, 234–238.

Slepetys, R.A., Cleland, A.J., 1993. Determination of shape of kaolin pigment particles. Clay Minerals 28, 495–508.

Smalley, M.V., 1994a. Electrical theory of clay swelling. Langmuir 10, 2884–2891.

Smalley, M.V., 1994b. One-phase and two-phase regions of colloid stability. Progress in Colloid and Polymer Science 97, 59–64.

Smalley, M.V., Hathrasinghe, H.L.M., Osborne, I., Swenson, J., King, S.M., 2001. Bridging flocculation in vermiculite-PEO mixtures. Langmuir 17, 3800–3812.

Smalley, M.V., Thomas, R.K., Braganza, L.F., Matsuo, T., 1989. Effects of hydrostatic pressure on the swelling of butylammonium vermiculite. Clays and Clay Minerals 37, 474–478.

Sohm, R., Tadros, T.F., 1989. Viscoelastic properties of sodium montmorillonite (gelwhite H) suspensions. Journal of Colloid and Interface Science 132, 62–71.

Sposito, G., 1992. The diffuse-ion swarm near smectitic particles suspended in 1:1 electrolyte solutions: modified Gouy-Chapman theory and quasicrystal formation. In: Güven, N., Pollastro, R.M. (Eds.), Clay-Water Interface and its Rheological Implications. CMS Workshop Lectures, vol. 4. The Clay Minerals Society, Boulder, CO, pp. 128–155.

Sposito, G., Grasso, D., 1999. Electrical double layer structure, forces, and fields at the clay water interface. In: Hsu, J.P. (Ed.), Interfacial Forces and Fields: Theory and Applications. Marcel Dekker, New York, pp. 207–249.

Sridharan, A., Satayamurty, P.V., 1996. Potential-distance relationships of clay–water systems considering the Stern theory. Clays and Clay Minerals 44, 479–484.

Środoń, J., Eberl, D.D., Drits, V.A., 2000. Evolution of fundamental-particle size during illitization of smectite and implications for reaction mechanism. Clays and Clay Minerals 48, 446–458.

Stenius, P., Järnström, L., Rigdahl, M., 1990. Aggregation in concentrated kaolin suspensions stabilized by polyacrylate. Colloids and Surfaces 51, 219–238.

Stul, M.S., van Leemput, L., 1982. Particle-size distribution, cation exchange capacity and charge density of deferrated montmorillonites. Clay Minerals 17, 209–215.

Stumm, W., Huang, C.P., Jenkins, S.R., 1970. Specific chemical interaction affecting the stability of dispersed systems. Croatica Chemica Acta 42, 233–244.

Stutzmann, T., Siffert, B., 1977. Contribution to the adsorption mechanism of acetamide and polyacrylamide onto clays. Clays and Clay Minerals 25, 392–406.

Sun, Y., Lin, H., Low, P.F., 1986. The nonspecific interaction of water with the surfaces of clay minerals. Journal of Colloid and Interface Science 112, 556–564.

Suquet, H., de la Calle, C., Pézérat, H., 1975. Swelling and structural organization of saponite. Clays and Clay Minerals 23, 1–9.

Suquet, H., Pézérat, H., 1987. Parameters influencing layer stacking types in saponite and vermiculite: a review. Clays and Clay Minerals 35, 353–362.

Swartzen-Allen, L.S., Matijević, E., 1976. Colloid and surface properties of clay suspensions. III. Stability of montmorillonite and kaolinite. Journal of Colloid and Interface Science 56, 159–167.

Swenson, J., Bergman, R., Bowron, D.T., Longeville, S., 2002. Water structure and dynamics in a fully hydrated sodium vermiculite clay. Philosophical Magazine B 82, 497–506.

Swenson, J., Bergman, R., Longeville, S., 2001. A neutron spin-echo study of confined water. Journal of Chemical Physics 115, 11299–11305.

Szûcs, A., Király, Z., Berger, F., Dékány, I., 1998. Preparation and hydrogen sorption of Pd nanoparticles on Al_2O_3-pillared clays. Colloids and Surfaces A 139, 109–118.

Tahani, A., Karroua, M., Van Damme, H., Levitz, P., Bergaya, F., 1999. Adsorption of a cationic surface on Na-montmorillonite: inspection of adsorption layer by X-ray and fluorescence spectroscopies. Journal of Colloid and Interface Science 216, 242–249.

Tateyama, H., Hirosue, H., Nishimura, S., Tsunematsu, K., Jinnai, K., Imagawa, K., 1988. Theoretical aspects of interaction between colloidal particles with various shapes in liquid. In: Mackenzie, J.D., Ulrich, D.R. (Eds.), Ultrastructure Processing of Advanced Ceramics. John Wiley & Sons, New York, pp. 453–461.

Tateyama, H., Scales, P.J., Ooi, M., Nishimura, S., Rees, K., Healy, T.W., 1997. X-ray diffraction and rheology study of highly ordered clay platelet alignement in aqueous solutions of sodium tripolyphosphate. Langmuir 13, 2440–2446.

Tchoubar, D., Bottero, J.Y., Quienne, P., Arnaud, M., 1991. Partial hydrolysis of ferric chloride salt. Structural investigation by photon-correlation spectroscopy and small-angle X-ray scattering. Langmuir 7, 398–402.

Theng, B.K.G., 1979. Formation and Properties of Clay-Polymer Complexes. Elsevier, Amsterdam.

Thomas, F., Michot, L.J., Vantelon, D., Montargès, E., Prélot, B., Cruchaudet, M., Delon, J.F., 1999. Layer charge and electrophoretic mobility of smectites. Colloids and Surfaces A 159, 351–358.

Tombácz, E., Ábrahám, I., Gilde, M., Szántó, F., 1990. The pH-dependent colloidal stability of aqueous montmorillonite suspensions. Colloids and Surfaces 49, 71–80.

Tombácz, E., Balázs, I., Lakatos, J., Szántó, F., 1989. Influence of exchangeable cations on stability and rheological properties of montmorillonite suspensions. Colloid and Polymer Science 267, 1016–1025.

Touillaux, P., Salvador, P., Vandermeersche, C., Fripiat, J.J., 1968. Study of water layers adsorbed on Na- and Ca-montmorillonite by the pulsed nuclear magnetic resonance technique. Israel Journal of Chemistry 6, 337–348.

Touret, O., Pons, C.H., Tessier, D., Tardy, Y., 1990. Étude de la repartition de l'eau dans des argiles saturées Mg^{2+} aux fortes teneurs en eau. Clay Minerals 25, 217–233.

Tournassat, C., Greneche, J-M., Tisserant, D., Charlet, L., 2003a. The titration of clay minerals. I. Discontinuous backtitration technique combined with CEC measurements. Journal of Colloid and Interface Science 273, 224–233.

Tournassat, C., Ferrage, E., Poinsignon, C., Charlet, L., 2003b. The titration of clay minerals. II. Structure-based model and implications for clay reactivity. Journal of Colloid and Interface Science 273, 234–246.

Tributh, H., Lagaly, G., 1986. Aufbereitung und Identifizierung von Boden– und Lagerstättentonen. GIT–Fachzeitschrift für das Laboratorium 30, 524–529, 771–776.

Umemura, Y., Yamagishi, A., Schoonheydt, R.A., Persoons, A., de Schryver, F., 2001. Fabrication of hybrid films of alkylammonium cations ($C_nH_{2n+1}NH_3^+$; $n = 4$–18) and a smectite clay by the Langmuir-Blodgett method. Langmuir 17, 449–455.

Umemura, Y., Yamagishi, A., Schoonheydt, R.A., Persoons, A., de Schryver, F., 2002. Langmuir-Blodgett films of a clay mineral and ruthenium(II) complexes with a noncentrosymmetric structure. Journal of the American Chemical Society 124, 992–997.

Usui, S., 1973. Interaction of electrical double layers at constant surface charge. Journal of Colloid and Interface Science 44, 107–113.

Vali, H., Bachmann, L., 1988. Ultrastructure and flow behavior of colloidal smectite dispersions. Journal of Colloid and Interface Science 126, 278–291.

Vali, H., Köster, H.M., 1986. Expanding behaviour, structural disorder, regular and random irregular interstratification of 2:1 layer–silicates studied by high-resolution images of transmission electron microscopy. Clay Minerals 21, 827–859.

van Bruggen, M.P.B., Donker, M., Lekkerkerker, H.N.W., Hughes, T.L., 1999. Anomalous stability of aqueous boehmite dispersions induced by hydrolyzed aluminium poly cations. Colloids and Surfaces A 150, 115–128.

van Duffel, B., Schoonheydt, R.A., Grim, C.P.M., de Schryver, F.C., 1999. Multilayered clay films: atomic force microscopy study and modeling. Langmuir 15, 7520–7529.

van Duffel, B., Verbies, T., Elshocht, S.V., Persoons, A., De Schryver, F.C., Schoonheydt, R.A., 2001. Fuzzy assembly and second harmonic generation of clay/polymer/dye monolayer films. Langmuir 17, 1243–1249.

van Olphen, H., 1977. An Introduction to Clay Colloid Chemistry, 2nd edition. Wiley, New York.

van Olphen, H., Fripiat, J.J., 1979. Data Handbook for Clay Materials and other Non-Metallic Minerals. Pergamon Press, Oxford.

van Oss, C.J., Giese, R.F., Costanzo, P.M., 1990. DLVO and non-DLVO interactions in hectorite. Clays and Clay Minerals 38, 151–159.

Verwey, E.J.W., Overbeek, J.T.G., 1948. Theory of the Stability of Lyophobic Colloids. Elsevier, Amsterdam.

Vincent, B., 1973. The van der Waals attraction between colloid particles having adsorbed layers. II. Calculation of interaction curves. Journal of Colloid and Interface Science 42, 270–285.

Vincent, B., 1990. The calculation of depletion layer thickness as a function of bulk polymer concentration. Colloids and Surfaces 50, 241–249.

von Hahn, F-V., 1928, Dispersoidanalyse. Die Methoden der Teilchengrössenbestimmung und ihre theoretischen Grundlagen. Ostwald, Wolfgang (Ed.) Handbuch der Kolloidwissenschaft, Band III. Verlag Theodor Steinkopff, Dresden und Leipzig.

Wanner, H., Albinsson, Y., Karnland, O., Wieland, E., Wersin, P., Charlet, L., 1994. The acid/base chemistry of montmorillonite. Radiochimica Acta 66/67, 157–162.

Weiss, A., 1962. Neuere Untersuchungen über die Struktur thixotroper Gele. Rheologica Acta 2, 292–304.

Weiss, A., 1963. Ein Geheimnis des chinesischen Porzellans. Angewandte Chemie 72, 755–762.

Weiss, A., Frank, R., 1961. Über den Bau der Gerüste in thixotropen Gelen. Zeitschrift für Naturforschung 16b, 141–142.

Weiss, A., Häbisch, A., Weiss, A., 1964. Einige Eigenschaften der 1. bis 4. Wasserschicht in quellungsfähigen Schichtsilicaten. Berichte der Deutschen Keramischen Geselllschaft 41, 687–690.

Weiss A., Russow, J., 1963. Über die Lage der austauschbaren Kationen bei Kaolinit. In: Proceedings of the International Clay Conference Stockholm, vol. 1, pp. 203–213.

Wendelbo, R., Rosenqvist, I.T., 1987. Effects of anion adsorption on mechanical properties of clay–water systems. In: Schultz, L.G., van Olphen, H., Mumpton, F.A. (Eds.), Proceedings of the International Clay Conference Denver 1985. The Clay Minerals Society, Bloomington, IN, pp. 422–426.

Wells, N., Theng, B.K.G., 1985. Factors affecting the flow behaviour of soil allophane suspensions under low shear rates. Journal of Colloid and Interface Science 104, 398–408.

Wierenga, A.M., Lenstra, T.A.J., Philipse, A.P., 1998. Aqueous dispersions of colloidal gibbsite platelets: synthesis, characterisation and intrinsic viscosity measurements. Colloids and Surfaces A 134, 359–371.

Wiewiora, A., Pérez-Rodriguez, J.L., Pérez-Maqueda, L.A., Drapala, J., 2003. Particle size distribution in sonicated high- and low-charge vermiculites. Applied Clay Science 24, 51–58.

Willenbacher, N., 1996. Unusual thixotropic properties of aqueous dispersions of Laponite RD. Journal of Colloid and Interface Science 182, 501–510.

Williams, B.G., Drover, S.P., 1967. Factors in gel formation in soil suspensions. Soil Science 104, 326–331.

Xiao, H., Lui, Z., Wiseman, N., 1999. Synergetic effect of cationic polymer microparticles and anionic polymer on fine clay flocculation. Journal of Colloid and Interface Science 216, 409–417.

Yariv, S., 1992. The effect of tetrahedral substitution of Si by Al on the surface acidity of the oxygen plane of clay minerals. International Reviews on Physical Chemistry 11, 345–375.

Yong, R.N., Ohtsubo, M., 1987. Interparticle action and rheology of kaolinite–amorphous iron hydroxide (ferrihydrite) complexes. Applied Clay Science 2, 63–81.

Zerwer, A., Santamarina, J.C., 1994. Double layers in pyrometamorphosed bentonite: index properties and complex permittivity. Applied Clay Science 9, 283–291.

Zimehl, R., Lagaly, G., 1986. Coagulation of latex dispersions by inorganic salts: structural effects. Progress in Colloid and Polymer Science 72, 28–36.